Modulation of Growth and Differentiation of Mesenchymal Cells for Cartilage and Bone Tissue Engineering

Inauguraldissertation

zur

Erlangung der Würde eines Dr. sc. med.

vorgelegt der

Medizinischen Fakultät

der Universität Basel

von

Ralph Duhr

aus Mertzig, Luxemburg

Basel, 2015

Genehmigt von der Medizinischen Fakultät

auf Antrag von

Prof. Dr. Ivan Martin (Dissertationsleiter und Fakultätsverantwortlicher)

PD Dr. Dr. Claude Jaquiéry (Korreferent)

Dr. David Wendt (Korreferent)

PD Dr. Dobrila Nesic (Externe Expertin)

Basel, den ……..

……..

Prof. Dr. Thomas Gasser

Dekan der medizinischen Fakultät

Table of contents

Acknowledgements

Many people have contributed to my thesis in many different ways. I would like to express my gratitude to

Prof. Ivan Martin for giving me the opportunity to do my PhD in his lab, for the excellent supervision, and for his great support during the last years

Dr. Dobrila Nesic and Dr. Claude Jaquiéry for accepting to be members of my PhD committee

Dr. David Wendt for his helpful support and patient guidance during the entire period of my PhD

The National Research Fund, Luxembourg (AFR Reference: 4090751) for the financial support

Adelaide Asnaghi and Atanas Todorov for the superb collaboration and invaluable advices in many projects

Rosaria Santoro for the introduction to the subject

All my colleagues contributing to the different projects for the fruitful cooperation and insightful discussions, especially Andrea Barbero, Sergio Sesia, Allison Hoch, Nunzia Di Maggio, Helen Quasnichka, Lucas Eichenberger, Karoliina Pelttari, Benjamin Pippenger, Manuele Muraro, and Jeroen Geurts

All the cooperation partners of the BIOCOMET project

The members of the animal facility and of the core facilities for microscopy, flow cytometry, and scanning electron microscopy for their technical help

All the present and former members of the groups of Tissue Engineering, Cardiac Surgery and Engineering, Oncology Surgery, and Cell and Gene Therapy, for the great working atmosphere, the good discussions and the helpful feedback

Prof. Michael Heberer for his tireless support to all of us

Sandra and Francine for providing us a perfect working environment

Anke, Hilary, Denise, and Gökhan for their support in all administrative and financial questions

Marcus, Tarek, Rik, Max, Alex, Amir, and Lukas for providing a clinical perspective

Conradin, Riaz, and Thomas for the discussions on bioreactor design and automation

My former 422 office mates, Waldi, Elia, Alex, Sasan, and Flurina for the good times we had

My fellow sportsmen and sportswomen for the nice distractions during numerous hours of football, table football and fitness training

All my dear friends for staying in contact during the last years

Anna and Stefano, Adam and Stefania, Bea and Matteo for welcoming me and making me feel at home in Basel

My entire family for their support during all these years

Danielle for your encouragement and your love

Abstract

Tissue engineering is a highly promising technology for the treatment of challenging cartilage and bone lesions for which no adequate therapeutic options are available yet. However for their widespread use, engineered tissues will first have to prove a predictable clinical success. To reach this objective, a reproducibly high product quality will be required, which can be achieved by a better knowledge and a continuous control of the cell phenotype during all phases of the tissue engineering process. The aim of this thesis is therefore to demonstrate how two types of mesenchymal cells, chondrocytes and bone marrow-derived mesenchymal/stromal cells (BMSC), can be modulated during growth and differentiation in order to conserve and fully exploit their potential. The present work is divided into 4 chapters. Chapter I will reveal how different chondrocyte subpopulations change their phenotype during *in vitro* proliferation and how this can lead to the detection of cells with increased differentiation capacity. In chapter II, the parameters governing the maintenance of osteogenic potential of BMSC during expansion will be analyzed. Chapter III will demonstrate how the coculture of BMSC with macrophages can result in a better cartilage-forming capacity. Finally in chapter IV, the effect of ascorbic acid on chondrogenic differentiation will be established.

Chapter I: The De-differentiation of Human Chondrocytes is Linked to Individual Cell Divisions

The relationship between proliferation and de-differentiation of chondrocytes during *in vitro* culture remains poorly understood. It was hypothesized here that cell proliferation tracking could reveal differences in the progression of de-differentiation and chondrogenic potential among subpopulations proliferating at different rates. Results showed that changes in the expression of cell surface markers and extracellular matrix genes were linked to individual cell divisions. Different culture conditions influenced cell doubling rates but not the relationship between cell divisions and phenotypic alterations, which indicated a strong coupling between both phenomena. Interestingly the highest chondrogenic potential was measured for slowly growing chondrocytes, even after a same number of total doublings was reached for all subpopulations. The increased understanding of the link between proliferation, de-differentiation and re-differentiation capacity will lead to innovative ways to maintain chondrogenic differentiation potential during chondrocyte

expansion. It will also facilitate the identification of progenitor populations with intrinsically superior capacity for the generation of enhanced engineered cartilage grafts.

Chapter II: Perfused 3D Scaffolds and Hydroxyapatite Substrate Maintain the Osteogenic Potential of Human Bone Marrow-Derived Mesenchymal Stromal Cells during Expansion

In previous studies it was repeatedly shown that the expansion of bone marrow-derived mesenchymal/stromal cells (BMSC) on 3D ceramic scaffolds resulted in increased maintenance of osteogenic potential as compared to culture on 2D polystyrene (PS). Since several culture parameters completely differ between 3D ceramic and 2D PS culture, the individual influences of the 3D scaffold and the ceramic material, as well as of the extracellular matrix deposition were investigated here. Results revealed that BMSC expanded on 2D PS only yielded bone matrix if the culture time was not longer than 2 weeks. Cells cultured for 3 weeks on both 3D PS and 3D ceramic scaffolds produced a dense bone matrix. The number of explants containing bone was higher with cells expanded on 3D ceramic compared to 3D PS. However there were no significant differences between cells extracted from 3D ceramic and directly implanted constructs. These findings suggest that the bone-forming capacity of BMSC can be maintained by a 3D environment and further improved by a ceramic substrate material, but that a preexisting 3D niche is not required for bone formation. The preservation of BMSC with osteogenic potential during 3D expansion in bioreactors opens the perspective for a streamlined production of large-scale bone grafts for clinical use.

Chapter III: Anti-Inflammatory/Tissue Repair Macrophages Enhance the Cartilage-Forming Capacity of Human Bone Marrow-Derived Mesenchymal Stromal Cells

Macrophages play a key role in healing processes, by regulating inflammation and stimulating tissue repair. However their influence on the tissue formation potential of BMSC is unknown. The effect of the coculture of macrophages with either pro-inflammatory or tissue-remodeling traits on the chondrogenic differentiation capacity of BMSC was therefore tested here. Results showed that the coculture of BMSC with tissue-repair but not with pro-inflammatory macrophages resulted in significantly higher glycosaminoglycan content and type II collagen expression, while type X collagen expression was unaffected. This chondro-inductive effect was found to be

caused by an increased survival and higher clonogenic and chondrogenic capacity of BMSC that were cocultured with tissue-repair macrophages. No difference was detected however in the cartilage tissue maturation in nude mice, as evidenced by similar accumulation of type X collagen and calcified tissue. These results demonstrated that a coculture with tissue-repair macrophages can improve the chondrogenic differentiation capacity of BMSC. This increased knowledge can lead to new coculture strategies for the manufacturing of cartilage grafts with enhanced quality.

Chapter IV: Chondrogenic Differentiation and Collagen Synthesis of Human Chondrocytes in the Absence of Ascorbic Acid

Ascorbic acid is considered to be an important supplement for cartilage tissue engineering because of its role in collagen hydroxylation *in vivo*. Due to its instability, ascorbic acid requires specific liquid handling conditions, which poses significant challenges to the automation of cartilage graft manufacturing. The aim of this study was to investigate the effect of ascorbic acid on chondrogenesis *in vitro*, with special regard to collagen synthesis and hydroxylation. Results showed that cartilage gene expression, tissue formation, and production of glycosaminoglycans were indistinguishable whether chondrocyte micromass pellets were cultured with or without ascorbic acid. Not adding ascorbic acid caused a reduction of collagen deposition, but collagen hydroxylation was not significantly different. Collagen secretion was unaffected and collagens showed a similar fibril structure in the absence of ascorbic acid. In conclusion, ascorbic acid did not influence chondrogenesis except for a small effect on collagen quantity, and can thus be omitted to simplify automation for a more cost-efficient cartilage graft manufacturing.

Conclusion

In this work, four different approaches to modulate the growth and differentiation of chondrocytes and BMSC were presented. With the gained knowledge the cell phenotype can be better controlled during manufacturing processes, which will be required for the production of engineered tissue grafts with reproducibly high quality for clinical translation.

General Introduction

In this first section, the main topics covered by my thesis will be introduced. An overview of articular cartilage and bone tissue composition and biology will be given, which will be completed with a summary of therapeutic options for common cartilage and bone lesions. Next, I will explain how the emerging field of tissue engineering can deal with current limitations in tissue regeneration. I will particularly enlarge upon current approaches in cartilage and bone tissue engineering, highlight the remaining challenges and indicate which role bioreactors could play for the widespread clinical use of engineered tissue grafts. In the thesis outline, I will state the specific aims and scientific questions answered by my thesis. The following chapters will then demonstrate how the mentioned challenges in cartilage and bone tissue engineering can be overcome by the modulation of growth and differentiation of mesenchymal cells. I will finish with a general conclusion and future perspectives.

A. Articular cartilage

1. Structure and properties

Articular cartilage is the connective tissue layer that covers the surface of synovial joints. This tissue has unique biomechanical features, providing at the same time resilience to compression, dampening of loads, and lubrication of the gliding surface. The unmatched properties of articular cartilage emanate from its highly organized structural and molecular composition and are essential for stable movement with low friction (Fig. 1) (Buckwalter and Mankin, 1998a). Only a few millimeters in thickness, articular cartilage contains a low density of a single cell type, the chondrocyte, but neither blood vessels, nor lymphatic vessels, nor nerves. During development, articular cartilage arises from a dense population of mesenchymal cells in the cartilage anlage that are expressing specific transcription factors and signaling molecules at the prospective joint site and differentiate into articular chondrocytes (Decker et al., 2014). The chondrocytes are embedded in small cavities called lacunae, which offer protection, and are specialized in synthesizing a dense extracellular matrix (ECM) that consists mainly of collagen proteins, proteoglycans, and interstitial fluid (Mow et al., 1992). The principal collagen of articular cartilage is collagen type II which is structured in a fibrillary meshwork and gives the tensile strength. Whereas collagens type IX and type XI are thought to further stabilize the

collagen network, collagen type IV surrounds and shelters the chondrocytes in the lacunae. Aggrecan as the core protein and the attached glycosaminoglycans such as chondroitin sulfate and keratin sulfate constitute most proteoglycans. The proteoglycans themselves are bound via link protein to a hyaluronan backbone; hence articular cartilage is also referred to as hyaline cartilage. The aqueous interstitial fluid contains a high concentration of cations to counterbalance the negatively charged proteoglycans, which together contribute to the tissue stiffness through the occurrence of swelling pressures (Buckwalter and Mankin, 1998a). Articular cartilage is arranged into different zones according to the depth from the joint surface. The superficial zone consists of a thin sheet of densely packed collagen fibrils oriented parallel to the surface and flattened chondrocytes secreting lubricin and other anti-adhesive factors to ensure friction-less movement. The chondrocytes in the middle/transitional zone are round and produce randomly arranged ECM fibers that contribute to the resilience of cartilage. In the deep/radial zone chondrocytes and fibers are aligned perpendicular to the surface. This cartilage layer is adjacent to the tide mark, which serves as a boundary to the deeper subchondral bone (Decker et al., 2014). The cartilage ECM is slowly but continuously remodeled throughout lifetime to maintain its composition, organization, and functionality, however alterations may appear with age and injury (Buckwalter and Mankin, 1998b).

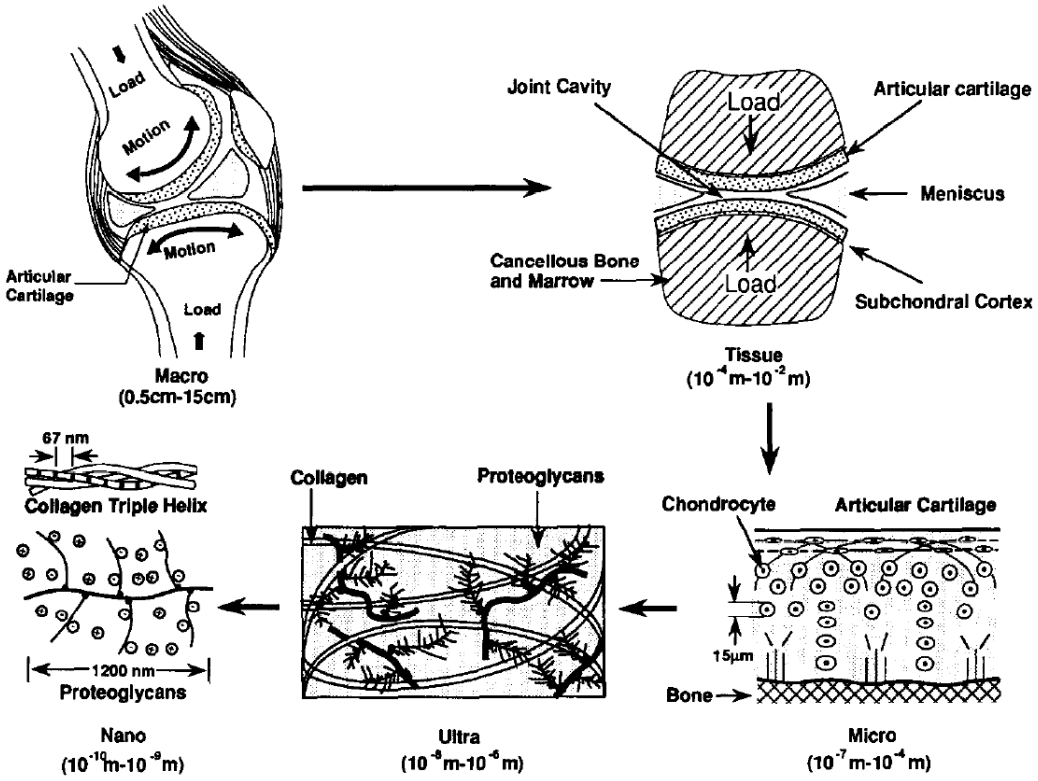

Figure 1: The structural and molecular composition of articular cartilage at different scales (illustration reprinted from Biomaterials 13, 67–97. Mow, V. C., Ratcliffe, A. and Poole, A. R. Cartilage and diarthrodial joints as paradigms for hierarchical materials and structures, copyright 1992, with permission from Elsevier).

2. Cartilage lesions and treatments

Cartilage lesions mainly result from trauma or a progressive degeneration with age known as osteoarthritis (OA). Since cartilage is avascular and chondrocytes have a low metabolism, self-repair of damaged cartilage is very limited. After a mechanical insult or age-related deterioration, the ECM structure and chondrocyte activity further decline over time, finally leading to a loss of joint function, associated with strong pain (Buckwalter and Mankin, 1998b; Gelber, 2000). To treat damaged articular cartilage, a wide range of surgical procedures has been developed. For end-stage OA, total knee arthroplasty, during which the entire joint is replaced by an artificial prosthesis, is the most common treatment. However due to the limited durability of these synthetic devices and the complications associated with revision surgery, this technique is only suitable for elderly patients. An alternative treatment for localized cartilage defects in the younger population is a technique called microfracture which consists of drilling holes into the underlying subchondral bone to stimulate the regeneration by resident progenitor cells from the marrow. Another surgical method named mosaicplasty comprises the transplantation of pieces of healthy cartilage from non-weight bearing regions to the defect area. However the disadvantage of this procedure is the resulting donor site morbidity (Bhosale and Richardson, 2008). Autologous chondrocyte implantation (ACI) and the more recent matrix-assisted ACI (MACI) are two cell-based techniques that consist of an *in vitro* expansion of isolated autologous chondrocytes and their reinjection in the defect site as a suspension or in combination with a supportive matrix (Bartlett et al., 2005; Brittberg et al., 1994). The clinical outcome of the above techniques is highly variable because the newly generated tissue is mostly fibrocartilage with biomechanical properties that are inferior to those of native articular cartilage (Bhosale and Richardson, 2008). The clinical need for cartilage repair thus persists and requires innovative treatments with better long-term outcomes. The emerging field of tissue engineering could remedy to this problem by providing mechanically functional grafts of hyaline cartilage tissue made from autologous cells.

B. Bone

1. Structure and properties

Bone, the principal component of the skeleton, is a vascularized connective tissue that provides structural stability, enables mobility and protects the organs of the human body. Moreover bone is a site of hematopoiesis and serves as a calcium and phosphate reservoir. Bone is composed of different cell types and has an extracellular matrix made of an organic part, mainly collagen, and an inorganic mineralized component. Bone formation occurs during development by either of two distinct processes: intramembranous ossification or endochondral ossification. The bones of the skull are formed by intramembranous ossification when mesenchymal cells condensate and differentiate directly into osteoblasts. The osteoblasts secrete an extracellular matrix rich in collagen type I and generate thereby the so-called osteoid that starts to be calcified by the deposition of minerals. The osteoblasts in the osteoid become osteocytes and produce the spongy/trabecular bone tissue around emerging blood vessels. The osteoblasts on the outside of the osteoid give rise to the periosteum which forms a surrounding solid layer of compact/cortical bone (Gilbert, 2000). During endochondral ossification, which is the process by which the other bones of the body are created, condensed mesenchymal cells first differentiate into chondrocytes and produce a cartilaginous template. The chondrocytes become hypertrophic and attract blood vessels, while the matrix starts to be mineralized. The hypertrophic chondrocytes subsequently undergo apoptosis. The surrounding cells of the perichondrium differentiate into osteoblasts and produce the compact bone collar. Osteoblasts invading with the blood vessels generate the primary ossification center of spongy bone, where also the bone marrow develops. At the end of the bones, a secondary ossification center forms by the same process of chondrocyte hypertrophy and osteoblast invasion. During childhood bones are further growing in length due to proliferating and differentiating chondrocytes in the growth plate adjacent to this secondary ossification center (Fig. 2) (Kronenberg, 2003). Throughout life bone undergoes a constant process of remodeling during which, in a very coordinated manner, old bone is resorbed by osteoclasts that have differentiated from monocytes and new bone is produced by osteoblasts. This whole process is thought to be orchestrated by mechanosensing osteocytes (Raggatt and Partridge, 2010).

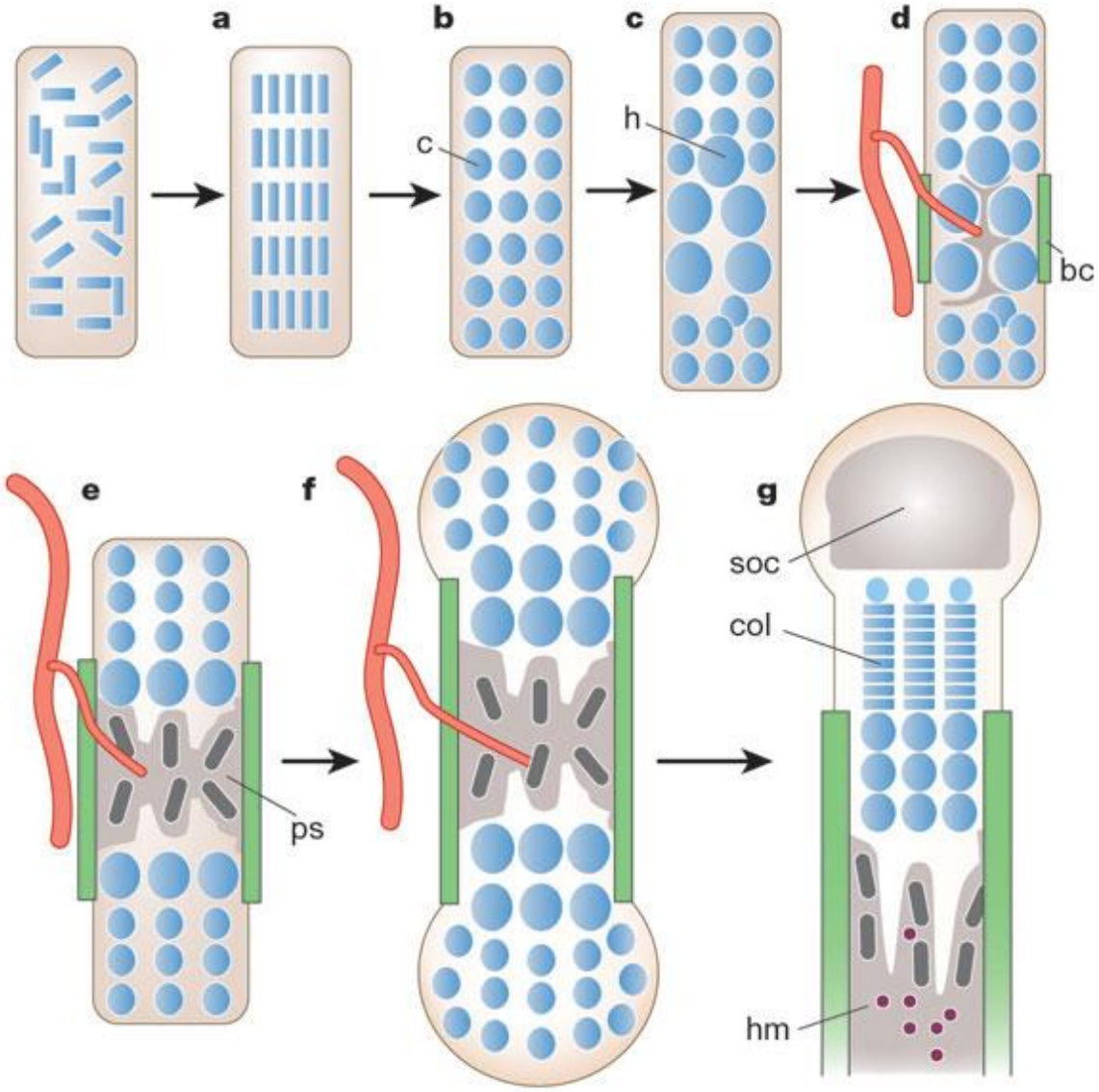

Figure 2: Steps of endochondral ossification. **a.** Condensation of mesenchymal cells. **b.** Differentiation into chondrocytes (c). **c.** Chondrocytes become hypertrophic (h). **d.** Hypertrophic chondrocytes produce mineralized extracellular matrix, attract blood vessels, and undergo apoptosis. Surrounding cells of the perichondrium become osteoblasts and form the bone collar (bc). **e.** Osteoblasts invading with the blood vessels generate the primary ossification center of spongy bone (ps). **f.** and **g.** The secondary ossification center (soc) forms at the end of the bones. Bones are further growing in length due to proliferating and differentiating chondrocytes (col). The bone marrow (hm) develops in the spongy bone (illustration reprinted by permission from Macmillan Publishers Ltd: Nature, 423, 332–336. Kronenberg, H. M. Developmental regulation of the growth plate, copyright 2003).

2. Bone lesions and treatments

Fractures are the most common bone lesions and heal under normal circumstances in an efficient physiological process. Bone fracture healing occurs by either of two distinct processes, which resemble developmental bone formation: primary or secondary healing. The majority of fractures heal via secondary healing, an indirect process that resembles the route of endochondral ossification, involving the formation of a cartilaginous soft callus by invading mesenchymal progenitor cells, which is then mineralized and remodeled by osteoclasts and osteoblasts (Schindeler et al., 2008).

Very stable fractures restore through primary fracture healing, which proceeds by resorption of bone fragments by osteoclasts and deposition of new bone by osteoblasts (Sfeir et al., 2005). To improve bone fracture healing, partial stabilization by internal or external fixation can be applied to unite the fracture (Perren, 2002). However, bone regeneration can be severely impaired by several factors, as in the case of large segmental defects, absence of vascularization, and osteoporotic or inflammatory environments, which need additional treatment. More advanced therapies are also applied in other conditions that require the formation of new bone such as spinal fusion, maxillary sinus elevation, or craniofacial reconstruction due to congenital defects or after tumor excision. In these challenging cases, therapeutic options include autografts with substitute material harvested from the patient's iliac crest, allografts of demineralized bone, and synthetic biomaterials. Additionally autologous bone marrow or growth factors such as bone morphogenetic proteins (BMP) can be administered. Although these treatments can provide good clinical outcomes, several shortcomings such as insufficient osteogenesis, donor site morbidity, or therapeutic side-effects have been reported (De Long et al., 2007; Dimitriou et al., 2011). Bone tissue engineering offers the possibility to overcome these current issues by generating large functional bone grafts that closely mimic the physiological bone formation process and support the body's self-healing capacity (Amini et al., 2012).

C. Tissue Engineering

The aim of tissue engineering is to generate functional biological grafts in order to repair damaged tissues, improve organ functions or regenerate entire body parts. These artificial living substitutes are generated from cells cultured *in vitro* on a supportive material and being instructed with specific physico-chemical signals. To achieve these complex interactions between human cells, materials, and molecules, an interdisciplinary approach combining methods and principles of engineering, medical, and life sciences is required (Langer and Vacanti, 1993; Lanza et al., 2011). In the standard tissue engineering paradigm, a tissue biopsy is harvested, from which cells are isolated and expanded *in vitro* in 2D dishes. When a sufficient number of cells have been reached, the cell suspension is seeded on a scaffold material. Most commonly porous materials – a plethora of different biomaterials and architectures exist – or hydrogels are used as scaffolds. The role of the scaffold on the one hand is to give the necessary structural support to the cells and to the produced ECM. On the

other hand the scaffold provides further biomechanical and biochemical signals that instruct the cells to differentiate and produce the wanted distinctive ECM (Chen et al., 1997; Engler et al., 2006). After the construct culture phase that allows the tissue to mature, the generated graft is then transplanted into the patient (Fig. 3). Besides being used in therapeutic applications, tissue engineered constructs can also serve as *in vitro* model systems to study tissue development and disease, or to perform drug testing under more physiological conditions (Hirt et al., 2014; Martin et al., 2004).

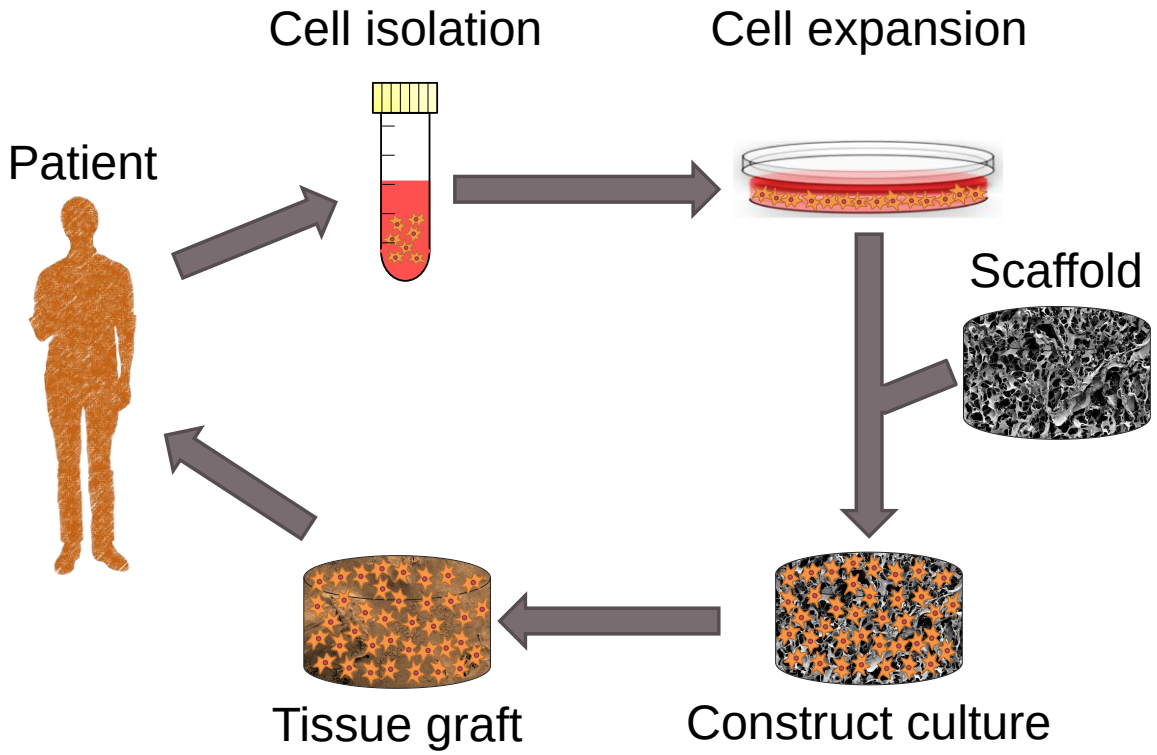

Figure 3: The standard tissue engineering paradigm. Cells are isolated from a tissue biopsy and expanded in 2D. Expanded cells are seeded on a 3D scaffold material and instructed to secrete the specific extracellular matrix. The mature tissue graft is then implanted into the patient.

1. **Cartilage tissue engineering**

Since cartilage consists of only one cell type and is avascular, the production of newly engineered cartilage grafts seems straightforward. Still the neocartilage needs to perfectly mimic the complex and unique properties of native cartilage, i.e. withstand considerable external forces and at the same time allow a smooth movement of the joints. The successful treatment of cartilage lesions by joint resurfacing with engineered cartilage still has to be verified in clinical trials involving large patient numbers. However, a better long-term outcome is generally expected when the cells accumulate high amounts of collagen type II and aggrecan, because these grafts have better biomechanical properties (Vunjak-Novakovic et al., 1999). In

order to produce cartilage *in vitro*, typically autologous chondrocytes are harvested from a non-weight-bearing region of the joint. Alternatively, chondrocytes can be obtained from the nasal septum, the ribs or the ear. From all these tissues, only low cell numbers can be isolated, due to the limited size of biopsies. The different chondrocyte sources have advantages and disadvantages related to their accessibility and donor site morbidity on the one hand, and the biological performance of the cells on the other hand (Candrian et al., 2008; Kafienah et al., 2002; Pelttari et al., 2014; Scotti et al., 2011; Tay et al., 2004). More engineered extracellular matrix (ECM) can be achieved from higher cell densities, but increased cell numbers are only beneficial if the cells still have the capacity to produce the right protein composition (Francioli et al., 2010; Moretti et al., 2005; Woods et al., 2007). In fact, in contrast to terminally differentiated chondrocytes that almost never divide *in vivo*, isolated chondrocytes quickly proliferate *in vitro*, but also start altering their gene expression, from mainly collagen type II and aggrecan to mostly collagen type I and versican (Benya and Shaffer, 1982; Binette et al., 1998). This process is called de-differentiation and progresses with cell passages. Since de-differentiation is only partially reversible, overly expanded chondrocytes have lost their potential to produce a hyaline-like cartilaginous matrix (Giovannini et al., 2010; Schulze-Tanzil et al., 2004). The fibrous matrix that de-differentiated chondrocytes produce instead has poor biomechanical properties and cannot be used anymore for tissue engineering applications. In order to better maintain the chondrogenic potential during proliferation and to increase the deposition of extracellular matrix when cells are supposed to re-differentiate, different growth factor cocktails are commonly added (Jakob et al., 2001; Yaeger et al., 1997). *Nevertheless current engineered cartilage tissues still lack the reproducibly high quality required for a broader use in the clinic, partially due to the insufficient knowledge and control over the chondrocyte phenotype during proliferation and differentiation processes*. Moreover, chondrocytes are known to have a substantial intra- and inter-donor variability (Barbero et al., 2003; Barbero et al., 2004). Different approaches have been proposed to identify chondrocytes with an increased intrinsic chondrogenic potential (Candela et al., 2014; Dowthwaite et al., 2004; Grogan et al., 2007; Pretzel et al., 2011; Williams et al., 2010). *However, a defined set of distinctive markers to prospectively isolate and better characterize these cell populations is still missing.*

Mesenchymal stem/stromal cells derived from the bone marrow (BMSC) or other tissues, as well as induced pluripotent stem cells (iPSC) have been proposed as

alternative cell sources for cartilage tissue engineering. All these cell types theoretically have the capacity to differentiate into chondrocytes. However their potential can be variable, leading to an unpredictable composition of extracellular matrix that is unsuitable for engineered cartilage grafts. Moreover, to date, phenotypic stability of these cells can still not be completely ensured. This can result in unwanted side-effects such as the further differentiation of BMSC into hypertrophic chondrocytes, which will cause the cartilaginous extracellular matrix to turn into bone in a process similar to endochondral ossification (Bhattacharjee et al., 2015; Centola et al., 2013; Craft et al., 2015; Diekman et al., 2012; Hellingman et al., 2012). *Innovative approaches are therefore required to increase the cartilage-forming capacity of BMSC and to possibly stabilize their phenotype for use in cartilage tissue engineering applications.*

2. **Bone tissue engineering**

Engineered bone grafts could become an attractive therapeutic alternative considering the limitations of current clinical treatments of bone lesions. However for an adequate repair, bone grafts need not only to have the right biomechanical features, but also to allow for a fast integration into the surrounding bone tissue and vasculature. Ideally, tissue engineered bone should thus have high osteoinductive and angiogenic potential and it should be available in different sizes, of-the-shelf and at reasonable cost (Amini et al., 2012). Similar to its developmental formation, bone can be engineered via direct osteogenesis, a process resembling intramembranous ossification, or via a hypertrophic cartilage template which is inspired by endochondral ossification. Besides giving rise to a functional bone marrow, the latter procedure is also considered to be biologically more reproducible (Scotti et al., 2010; Scotti et al., 2013). Amongst others, mesenchymal stem/stromal cells from bone marrow (BMSC), adipose tissue and other sources, or iPSC can be used to generate bone (Szpalski et al., 2012). The advantage of certain cell sources is that through their chondrogenic potential, it is easier to induce them to an endochondral ossification process. On the other hand, cell sources containing progenitors for blood vessels, such as the stromal vascular fraction of fat tissue, can help in ensuring a fast vascularization of engineered bone grafts (Güven et al., 2011). BMSC can be harvested from bone marrow aspirates, however they account for less than 0.01% of the total number of isolated cells and therefore need an enormous amount of cell doublings before the required number of cells for a tissue engineering application is reached (Pittenger et al., 1999). The differentiation potential of BMSC decreases with

increasing passages in monolayer culture, probably due to a number of factors that are inherently different to their native environment. (Banfi et al., 2000; Hoch and Leach, 2014). In case BMSC cannot differentiate anymore into to osteoblasts or chondrocytes, they produce a fibrous matrix that is not osteoinductive and will not turn into bone upon implantation, resulting into poor bone healing and graft failure. A number of protocols have been developed to better preserve the BMSC differentiation potential for bone tissue engineering, such as the expansion in bioreactors on ceramic scaffolds (Braccini et al., 2005; Papadimitropoulos et al., 2014). *Nevertheless, further research efforts are required to better understand and also learn how to control the phenotype of BMSC in order to exploit their full potency for the clinical translation of engineered bone grafts.*

3. **Bioreactors for tissue engineering**

Bioreactors are systems that allow carrying out biological processes under defined and controlled conditions. By ensuring a closed environment with stable temperature, pH, and gas supply and by providing a constant provision of nutrients and removal of waste products, bioreactors can help in tissue engineering applications to increase process and product standardization, safety and quality. Bioreactors also offer the possibility for automation and scale-up, which can further improve reproducibility and cost-effectiveness. Moreover bioreactors cannot only be used to generate engineered tissues, but also as 3D culture model systems mimicking aspects of the *in vivo* environment (Martin et al., 2004; Martin et al., 2009; Martin et al., 2014; Wendt et al., 2009). Mechanical bioreactors are used for example to provide physical stimuli in order to activate mechanobiological cell pathways or to test the performance of the engineered constructs (Démarteau et al., 2003; Grad et al., 2011). Since manual procedures of cell seeding usually result in irregular cell patterns and poor cell penetration, bioreactor systems have been designed to ensure the perfusion of the 3D scaffold for homogeneous cell and tissue distribution (Wendt et al., 2003; Wendt et al., 2006). The advantage of higher mass transfer rates of such a perfusion culture also enables the generation of large cartilage grafts (Santoro et al., 2010). From a regulatory perspective, bioreactors allow a simple integration of in-process controls (Santoro et al., 2011). Merging these engineering principles, tissue engineering production processes can be streamlined by combining cell expansion and the following graft maturation in perfusion bioreactors, eliminating the need for numerous costly and labor-intensive manual steps (Fig. 4) (Wendt et al., 2011).

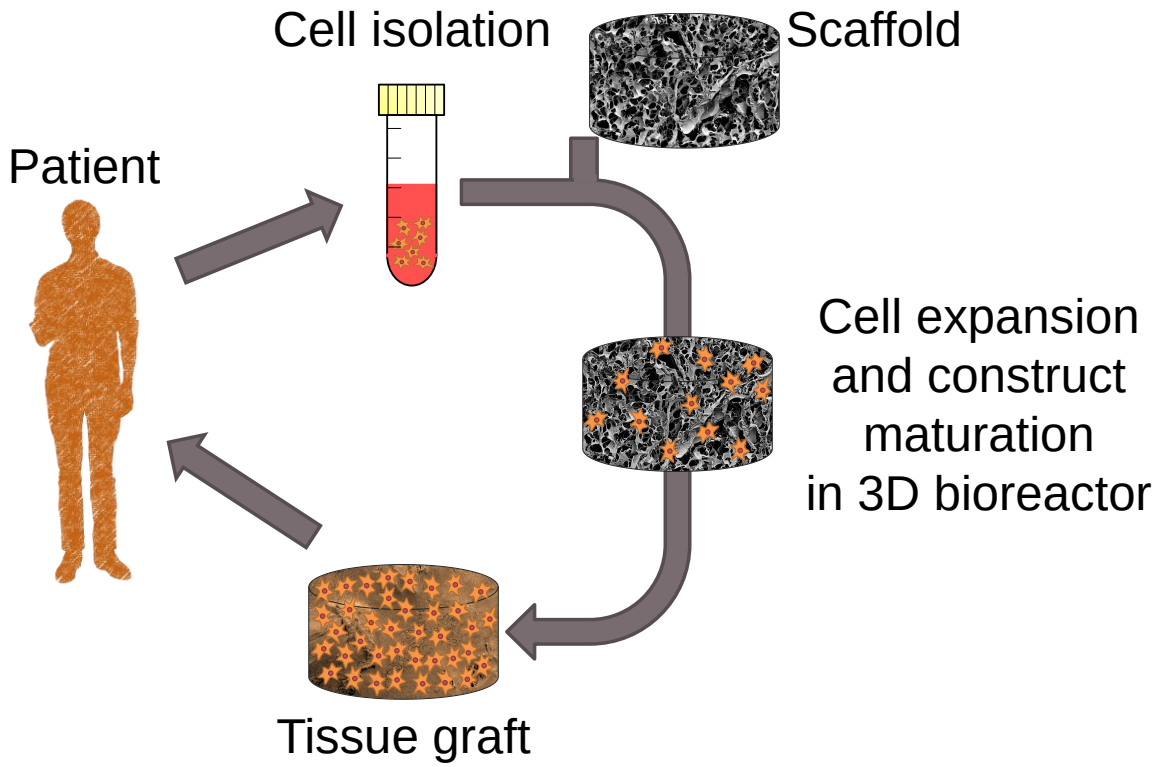

Figure 4: In the streamlined tissue engineering paradigm, the cell seeding, cell expansion and construct maturation phases are performed consecutively in the same perfused 3D bioreactor. In this way, several costly and labor-intensive manual steps can be eliminated.

In this way the use of bioreactors could, together with the mentioned increased reproducibility and quality, be key for the widespread clinical translation of tissue engineered products (Wendt et al., 2009). In order to also achieve a fully automated workflow, the time-consuming exchange of culture medium can be replaced in bioreactors with a completely automated system (Asnaghi et al., 2009). However, complex process requirements such as the handling of many different liquids often hinder the automation of tissue manufacturing. *Before being implemented in bioreactors, the frequently inefficient manual processes thus need to be reconsidered and simplified by applying novel concepts originating from new insights in cell biology.*

Thesis Outline

Aim

Despite many advances in the field of cartilage and bone tissue engineering during the last years, translation to the clinic could be observed only in some cases (Fulco et al., 2014; Liebergall et al., 2013; Pelttari et al., 2014; Saris et al., 2008). Current problems include low standardization and high manufacturing costs (Martin et al., 2014), but also a lack of reproducibility due to incomplete control over the cell behavior, leading to an insufficient tissue maturation and quality *in vitro* with unpredictable clinical outcome. For a widespread use of engineered tissues in the treatment of cartilage and bone lesions, a better knowledge and ideally a continuous control of the cell phenotype during all phases of the tissue engineering process are therefore essential. The aim of this thesis is to demonstrate how the phenotype of two types of mesenchymal cells, chondrocytes and bone marrow derived mesenchymal/stromal cells (BMSC), can be modulated during growth and differentiation to conserve and fully exploit their potential (Fig. 5).

Since tissue engineering is highly multidisciplinary, all the studies presented here were done in collaboration with other researchers. The individual contributions are highlighted on the first page of each chapter.

Chapter I: The De-differentiation of Human Chondrocytes is Linked to Individual Cell Divisions

During *in vitro* expansion, the phenotype of articular chondrocytes quickly changes and their chondrogenic potential is progressively lost. However the interrelation between chondrocyte proliferation and concurrent de-differentiation remains poorly understood. In order to investigate how phenotypic changes relate to cell divisions and to study how this possible link is influenced by different culture environments, cell division tracking of freshly isolated chondrocytes was performed. It was hypothesized that selecting chondrocytes based on their number of cell divisions reveals differences among subpopulations in the progression of de-differentiation and in their chondrogenic potential. With an improved understanding of the interplay between chondrocyte proliferation and de-differentiation, innovative ways of cell expansion and/or selection can be developed that preserve the full chondrogenic potential for the manufacturing of enhanced cartilage grafts.

Chapter II: Perfused 3D Scaffolds and Hydroxyapatite Substrate Maintain the Osteogenic Potential of Human Bone Marrow-Derived Mesenchymal Stromal Cells during Expansion

The expansion of BMSC on perfused 3D ceramic scaffolds leads to more extensive and more reproducible *in vivo* bone formation than BMSC cultured in monolayer on 2D polystyrene (PS). Given that the bioreactor-based culture of BMSC on 3D ceramic inherently encompasses several aspects that are completely different than in 2D PS and could substantially affect the in vivo osteogenic potential, the aim of this work was to investigate the individual roles of i) the 3D scaffold vs 2D surface and of ii) the ceramic vs PS substrate material during expansion, as well as of iii) the extracellular matrix deposited before implantation. An enhanced control over the culture parameters responsible for the preservation of the osteogenic capacity of BMSC during expansion will allow the further use of these cells in clinical applications.

Chapter III: Anti-Inflammatory/Tissue Repair Macrophages Enhance the Cartilage-Forming Capacity of Human Bone Marrow-Derived Mesenchymal Stromal Cells

Macrophages exerting different functions have been identified as key players in healing processes due to their capacity to secrete growth factors and cytokines (Brown et al., 2014; Park and Barbul, 2004). However the direct influence of macrophages on the tissue forming capacity of BMSC is unknown. The aim of this study was therefore to investigate whether macrophages with pro-inflammatory or tissue-remodeling traits could modulate the chondrogenic differentiation of BMSC *in vitro* and if this would have consequences for the cartilage tissue maturation *in vivo*. Moreover, the cellular mechanisms possibly accounting for this phenomenon were assessed. An increased understanding of their interactions with BMSC can help in developing strategies to selectively recruit and polarize macrophages for improved chondrogenic differentiation or phenotypic stabilization.

Chapter IV: Chondrogenic Differentiation and Collagen Synthesis of Human Chondrocytes in the Absence of Ascorbic Acid

The introduction of automation for the manufacturing of engineered cartilage is essential for a broad clinical adoption in the long-term, but unstable medium supplements pose significant challenges to automation due to their special requirements for liquid handling. Ascorbic acid is such an unstable compound that is

added to chondrogenic medium because of its role in collagen hydroxylation. The aim of this part of the work was to investigate the effect of ascorbic acid on the chondrogenesis of human nasal chondrocytes, with special regard to collagen synthesis and hydroxylation. The knowledge of the precise requirements for ascorbic acid during chondrogenic differentiation will help to develop appropriate automation strategies that ensure the manufacturing of high quality engineered cartilage grafts.

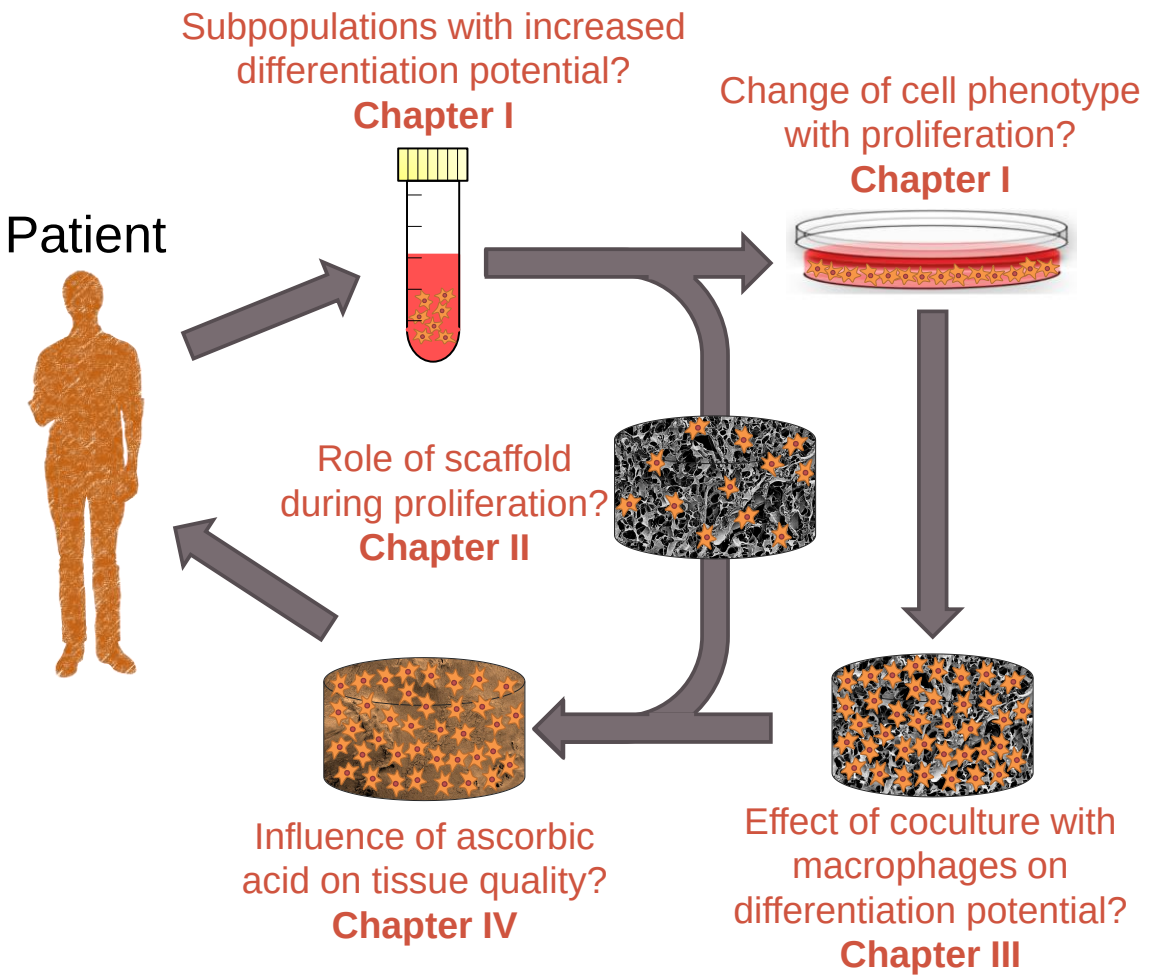

Figure 5: Outline of the scientific questions addressed in this thesis. Chondrocytes will be selected based on their number of cell divisions to assess differences among subpopulations in the progression of phenotypic changes and in their chondrogenic potential (**Chapter I**). In the streamlined tissue engineering paradigm, the influence of the 3D scaffold, the scaffold material and the matrix formation on the osteogenic potential of BMSC will be investigated (**Chapter II**). The effect of tissue-repair and pro-inflammatory macrophages on the chondrogenic capacity of BMSC will be tested (**Chapter III**). The influence of ascorbic acid on the chondrogenesis of chondrocytes will be studied, with special regard to collagen synthesis and hydroxylation (**Chapter IV**).

REFERENCES

Amini, A. R., Laurencin, C. T. and Nukavarapu, S. P. (2012). Bone tissue engineering: recent advances and challenges. *Crit. Rev. Biomed. Eng.* **40**, 363–408.

Asnaghi, M. A., Jungebluth, P., Raimondi, M. T., Dickinson, S. C., Rees, L. E. N., Go, T., Cogan, T. A., Dodson, A., Parnigotto, P. P., Hollander, A. P., et al. (2009). A double-chamber rotating bioreactor for the development of tissue-engineered hollow organs: from concept to clinical trial. *Biomaterials* **30**, 5260–5269.

Banfi, A., Muraglia, A., Dozin, B., Mastrogiacomo, M., Cancedda, R. and Quarto, R. (2000). Proliferation kinetics and differentiation potential of ex vivo expanded human bone marrow stromal cells: Implications for their use in cell therapy. *Exp. Hematol.* **28**, 707–715.

Barbero, A., Ploegert, S., Heberer, M. and Martin, I. (2003). Plasticity of clonal populations of dedifferentiated adult human articular chondrocytes. *Arthritis Rheum.* **48**, 1315–1325.

Barbero, A., Grogan, S., Schäfer, D., Heberer, M., Mainil-Varlet, P. and Martin, I. (2004). Age related changes in human articular chondrocyte yield, proliferation and post-expansion chondrogenic capacity. *Osteoarthritis Cartilage* **12**, 476–484.

Bartlett, W., Skinner, J. A., Gooding, C. R., Carrington, R. W. J., Flanagan, A. M., Briggs, T. W. R. and Bentley, G. (2005). Autologous chondrocyte implantation versus matrix-induced autologous chondrocyte implantation for osteochondral defects of the knee: a prospective, randomised study. *J. Bone Joint Surg. Br.* **87**, 640–645.

Benya, P. D. and Shaffer, J. D. (1982). Dedifferentiated chondrocytes reexpress the differentiated collagen phenotype when cultured in agarose gels. *Cell* **30**, 215–224.

Bhattacharjee, M., Coburn, J., Centola, M., Murab, S., Barbero, A., Kaplan, D. L., Martin, I. and Ghosh, S. (2015). Tissue engineering strategies to study cartilage development, degeneration and regeneration. *Adv. Drug Deliv. Rev.* **84**, 107–122.

Bhosale, A. M. and Richardson, J. B. (2008). Articular cartilage: structure, injuries and review of management. *Br. Med. Bull.* **87**, 77–95.

Binette, F., McQuaid, D. P., Haudenschild, D. R., Yaeger, P. C., McPherson, J. M. and Tubo, R. (1998). Expression of a stable articular cartilage phenotype without evidence of hypertrophy by adult human articular chondrocytes in vitro. *J. Orthop. Res.* **16**, 207–216.

Braccini, A., Wendt, D., Jaquiery, C., Jakob, M., Heberer, M., Kenins, L., Wodnar-Filipowicz, A., Quarto, R. and Martin, I. (2005). Three-dimensional perfusion culture of human bone marrow cells and generation of osteoinductive grafts. *Stem Cells* **23**, 1066–1072.

Brittberg, M., Lindahl, A., Nilsson, A., Ohlsson, C., Isaksson, O. and Peterson, L. (1994). Treatment of Deep Cartilage Defects in the Knee with Autologous Chondrocyte Transplantation. *N. Engl. J. Med.* **331**, 889–895.

Brown, B. N., Sicari, B. M. and Badylak, S. F. (2014). Rethinking Regenerative Medicine: A Macrophage-Centered Approach. *Front. Immunol.* **5**,.

Buckwalter, J. A. and Mankin, H. J. (1998a). Articular cartilage: tissue design and chondrocyte-matrix interactions. *Instr. Course Lect.* **47**, 477–486.

Buckwalter, J. A. and Mankin, H. J. (1998b). Articular cartilage: degeneration and osteoarthritis, repair, regeneration, and transplantation. *Instr. Course Lect.* **47**, 487–504.

Candela, M. E., Yasuhara, R., Iwamoto, M. and Enomoto-Iwamoto, M. (2014). Resident mesenchymal progenitors of articular cartilage. *Matrix Biol.* **39**, 44–49.

Candrian, C., Vonwil, D., Barbero, A., Bonacina, E., Miot, S., Farhadi, J., Wirz, D., Dickinson, S., Hollander, A., Jakob, M., et al. (2008). Engineered cartilage generated by nasal chondrocytes is responsive to physical forces resembling joint loading. *Arthritis Rheum.* **58**, 197–208.

Centola, M., Tonnarelli, B., Schären, S., Glaser, N., Barbero, A. and Martin, I. (2013). Priming 3D cultures of human mesenchymal stromal cells toward cartilage formation via developmental pathways. *Stem Cells Dev.* **22**, 2849–2858.

Chen, C. S., Mrksich, M., Huang, S., Whitesides, G. M. and Ingber, D. E. (1997). Geometric control of cell life and death. *Science* **276**, 1425–1428.

Craft, A. M., Rockel, J. S., Nartiss, Y., Kandel, R. A., Alman, B. A. and Keller, G. M. (2015). Generation of articular chondrocytes from human pluripotent stem cells. *Nat. Biotechnol.* **33**, 638–645.

Decker, R. S., Koyama, E. and Pacifici, M. (2014). Genesis and morphogenesis of limb synovial joints and articular cartilage. *Matrix Biol.* **39C**, 5–10.

De Long, W. G., Einhorn, T. A., Koval, K., McKee, M., Smith, W., Sanders, R. and Watson, T. (2007). Bone grafts and bone graft substitutes in orthopaedic trauma surgery. A critical analysis. *J. Bone Joint Surg. Am.* **89**, 649–658.

Démarteau, O., Jakob, M., Schäfer, D., Heberer, M. and Martin, I. (2003). Development and validation of a bioreactor for physical stimulation of engineered cartilage. *Biorheology* **40**, 331–336.

Diekman, B. O., Christoforou, N., Willard, V. P., Sun, H., Sanchez-Adams, J., Leong, K. W. and Guilak, F. (2012). Cartilage tissue engineering using differentiated and purified induced pluripotent stem cells. *Proc. Natl. Acad. Sci.*

Dimitriou, R., Jones, E., McGonagle, D. and Giannoudis, P. V. (2011). Bone regeneration: current concepts and future directions. *BMC Med.* **9**, 66.

Dowthwaite, G. P., Bishop, J. C., Redman, S. N., Khan, I. M., Rooney, P., Evans, D. J. R., Haughton, L., Bayram, Z., Boyer, S., Thomson, B., et al. (2004).

The surface of articular cartilage contains a progenitor cell population. *J. Cell Sci.* **117**, 889–897.

Engler, A. J., Sen, S., Sweeney, H. L. and Discher, D. E. (2006). Matrix elasticity directs stem cell lineage specification. *Cell* **126**, 677–689.

Francioli, S. E., Candrian, C., Martin, K., Heberer, M., Martin, I. and Barbero, A. (2010). Effect of three-dimensional expansion and cell seeding density on the cartilage-forming capacity of human articular chondrocytes in type II collagen sponges. *J. Biomed. Mater. Res. A* **95**, 924–931.

Fulco, I., Miot, S., Haug, M. D., Barbero, A., Wixmerten, A., Feliciano, S., Wolf, F., Jundt, G., Marsano, A., Farhadi, J., et al. (2014). Engineered autologous cartilage tissue for nasal reconstruction after tumour resection: an observational first-in-human trial. *Lancet* **384**, 337–346.

Gelber, A. C. (2000). Joint Injury in Young Adults and Risk for Subsequent Knee and Hip Osteoarthritis. *Ann. Intern. Med.* **133**, 321.

Gilbert, S. F. (2000). Osteogenesis: The Development of Bones. *Dev. Biol.* **6th edition**,.

Giovannini, S., Diaz-Romero, J., Aigner, T., Mainil-Varlet, P. and Nesic, D. (2010). Population doublings and percentage of S100-positive cells as predictors of in vitro chondrogenicity of expanded human articular chondrocytes. *J. Cell. Physiol.* **222**, 411–420.

Grad, S., Eglin, D., Alini, M. and Stoddart, M. J. (2011). Physical stimulation of chondrogenic cells in vitro: a review. *Clin. Orthop.* **469**, 2764–2772.

Grogan, S. P., Barbero, A., Diaz-Romero, J., Cleton-Jansen, A.-M., Soeder, S., Whiteside, R., Hogendoorn, P. C. W., Farhadi, J., Aigner, T., Martin, I., et al. (2007). Identification of markers to characterize and sort human articular chondrocytes with enhanced in vitro chondrogenic capacity. *Arthritis Rheum.* **56**, 586–595.

Güven, S., Mehrkens, A., Saxer, F., Schaefer, D. J., Martinetti, R., Martin, I. and Scherberich, A. (2011). Engineering of large osteogenic grafts with rapid engraftment capacity using mesenchymal and endothelial progenitors from human adipose tissue. *Biomaterials* **32**, 5801–5809.

Hellingman, C. A., Koevoet, W. and van Osch, G. J. V. M. (2012). Can one generate stable hyaline cartilage from adult mesenchymal stem cells? A developmental approach. *J. Tissue Eng. Regen. Med.* **6**, e1–e11.

Hirt, C., Papadimitropoulos, A., Mele, V., Muraro, M. G., Mengus, C., Iezzi, G., Terracciano, L., Martin, I. and Spagnoli, G. C. (2014). “In vitro” 3D models of tumor-immune system interaction. *Adv. Drug Deliv. Rev.* **79-80**, 145–154.

Hoch, A. I. and Leach, J. K. (2014). Concise review: optimizing expansion of bone marrow mesenchymal stem/stromal cells for clinical applications. *Stem Cells Transl. Med.* **3**, 643–652.

Jakob, M., Démarteau, O., Schäfer, D., Hintermann, B., Dick, W., Heberer, M. and Martin, I. (2001). Specific growth factors during the expansion and

redifferentiation of adult human articular chondrocytes enhance chondrogenesis and cartilaginous tissue formation in vitro. *J. Cell. Biochem.* **81**, 368–377.

Kafienah, W. 'el, Jakob, M., Démarteau, O., Frazer, A., Barker, M. D., Martin, I. and Hollander, A. P. (2002). Three-dimensional tissue engineering of hyaline cartilage: comparison of adult nasal and articular chondrocytes. *Tissue Eng.* **8**, 817–826.

Kronenberg, H. M. (2003). Developmental regulation of the growth plate. *Nature* **423**, 332–336.

Langer, R. and Vacanti, J. P. (1993). Tissue engineering. *Science* **260**, 920–926.

Lanza, R., Langer, R. and Vacanti, J. P. (2011). *Principles of Tissue Engineering*. Academic Press.

Liebergall, M., Schroeder, J., Mosheiff, R., Gazit, Z., Yoram, Z., Rasooly, L., Daskal, A., Khoury, A., Weil, Y. and Beyth, S. (2013). Stem Cell–based Therapy for Prevention of Delayed Fracture Union: A Randomized and Prospective Preliminary Study. *Mol. Ther.* **21**, 1631–1638.

Martin, I., Wendt, D. and Heberer, M. (2004). The role of bioreactors in tissue engineering. *Trends Biotechnol.* **22**, 80–86.

Martin, I., Smith, T. and Wendt, D. (2009). Bioreactor-based roadmap for the translation of tissue engineering strategies into clinical products. *Trends Biotechnol.* **27**, 495–502.

Martin, I., Simmons, P. J. and Williams, D. F. (2014). Manufacturing challenges in regenerative medicine. *Sci. Transl. Med.* **6**, 232fs16.

Moretti, M., Wendt, D., Dickinson, S. C., Sims, T. J., Hollander, A. P., Kelly, D. J., Prendergast, P. J., Heberer, M. and Martin, I. (2005). Effects of in vitro preculture on in vivo development of human engineered cartilage in an ectopic model. *Tissue Eng.* **11**, 1421–1428.

Mow, V. C., Ratcliffe, A. and Poole, A. R. (1992). Cartilage and diarthrodial joints as paradigms for hierarchical materials and structures. *Biomaterials* **13**, 67–97.

Papadimitropoulos, A., Piccinini, E., Brachat, S., Braccini, A., Wendt, D., Barbero, A., Jacobi, C. and Martin, I. (2014). Expansion of Human Mesenchymal Stromal Cells from Fresh Bone Marrow in a 3D Scaffold-Based System under Direct Perfusion. *PloS One* **9**, e102359.

Park, J. E. and Barbul, A. (2004). Understanding the role of immune regulation in wound healing. *Am. J. Surg.* **187**, S11–S16.

Pelttari, K., Pippenger, B., Mumme, M., Feliciano, S., Scotti, C., Mainil-Varlet, P., Procino, A., von Rechenberg, B., Schwamborn, T., Jakob, M., et al. (2014). Adult human neural crest-derived cells for articular cartilage repair. *Sci. Transl. Med.* **6**, 251ra119.

Perren, S. M. (2002). Evolution of the internal fixation of long bone fractures. The scientific basis of biological internal fixation: choosing a new balance between stability and biology. *J. Bone Joint Surg. Br.* **84**, 1093–1110.

Pittenger, M. F., Mackay, A. M., Beck, S. C., Jaiswal, R. K., Douglas, R., Mosca, J. D., Moorman, M. A., Simonetti, D. W., Craig, S. and Marshak, D. R. (1999). Multilineage potential of adult human mesenchymal stem cells. *Science* **284**, 143–147.

Pretzel, D., Linss, S., Rochler, S., Endres, M., Kaps, C., Alsalameh, S. and Kinne, R. W. (2011). Relative percentage and zonal distribution of mesenchymal progenitor cells in human osteoarthritic and normal cartilage. *Arthritis Res. Ther.* **13**, R64.

Raggatt, L. J. and Partridge, N. C. (2010). Cellular and Molecular Mechanisms of Bone Remodeling. *J. Biol. Chem.* **285**, 25103–25108.

Santoro, R., Olivares, A. L., Brans, G., Wirz, D., Longinotti, C., Lacroix, D., Martin, I. and Wendt, D. (2010). Bioreactor based engineering of large-scale human cartilage grafts for joint resurfacing. *Biomaterials* **31**, 8946–8952.

Santoro, R., Krause, C., Martin, I. and Wendt, D. (2011). On-line monitoring of oxygen as a non-destructive method to quantify cells in engineered 3D tissue constructs. *J. Tissue Eng. Regen. Med.*

Saris, D. B. F., Vanlauwe, J., Victor, J., Haspl, M., Bohnsack, M., Fortems, Y., Vandekerckhove, B., Almqvist, K. F., Claes, T., Handelberg, F., et al. (2008). Characterized chondrocyte implantation results in better structural repair when treating symptomatic cartilage defects of the knee in a randomized controlled trial versus microfracture. *Am. J. Sports Med.* **36**, 235–246.

Schindeler, A., McDonald, M. M., Bokko, P. and Little, D. G. (2008). Bone remodeling during fracture repair: The cellular picture. *Semin. Cell Dev. Biol.* **19**, 459–466.

Schulze-Tanzil, G., Mobasheri, A., de Souza, P., John, T. and Shakibaei, M. (2004). Loss of chondrogenic potential in dedifferentiated chondrocytes correlates with deficient Shc-Erk interaction and apoptosis. *Osteoarthr. Cartil.* **12**, 448–458.

Scotti, C., Tonnarelli, B., Papadimitropoulos, A., Scherberich, A., Schaeren, S., Schauerte, A., Lopez-Rios, J., Zeller, R., Barbero, A. and Martin, I. (2010). Recapitulation of endochondral bone formation using human adult mesenchymal stem cells as a paradigm for developmental engineering. *Proc. Natl. Acad. Sci. U. S. A.* **107**, 7251–7256.

Scotti, C., Osmokrovic, A., Wolf, F., Miot, S., Peretti, G. M., Barbero, A. and Martin, I. (2011). Response of Human Engineered Cartilage Based on Articular or Nasal Chondrocytes to Interleukin-1β and Low Oxygen. *Tissue Eng. Part A*.

Scotti, C., Piccinini, E., Takizawa, H., Todorov, A., Bourgine, P., Papadimitropoulos, A., Barbero, A., Manz, M. G. and Martin, I. (2013).

Engineering of a functional bone organ through endochondral ossification. *Proc. Natl. Acad. Sci. U. S. A.* **110**, 3997–4002.

Sfeir, C., Ho, L., Doll, B. A., Azari, K. and Hollinger, J. O. (2005). Fracture Repair. In *Bone Regeneration and Repair* (ed. MD, J. R. L.) and MD, G. E. F.), pp. 21–44. Humana Press.

Szpalski, C., Barbaro, M., Sagebin, F. and Warren, S. M. (2012). Bone tissue engineering: current strategies and techniques--part II: Cell types. *Tissue Eng. Part B Rev.* **18**, 258–269.

Tay, A. G., Farhadi, J., Suetterlin, R., Pierer, G., Heberer, M. and Martin, I. (2004). Cell yield, proliferation, and postexpansion differentiation capacity of human ear, nasal, and rib chondrocytes. *Tissue Eng.* **10**, 762–770.

Vunjak-Novakovic, G., Martin, I., Obradovic, B., Treppo, S., Grodzinsky, A. J., Langer, R. and Freed, L. E. (1999). Bioreactor cultivation conditions modulate the composition and mechanical properties of tissue-engineered cartilage. *J. Orthop. Res.* **17**, 130–138.

Wendt, D., Marsano, A., Jakob, M., Heberer, M. and Martin, I. (2003). Oscillating perfusion of cell suspensions through three-dimensional scaffolds enhances cell seeding efficiency and uniformity. *Biotechnol. Bioeng.* **84**, 205–214.

Wendt, D., Stroebel, S., Jakob, M., John, G. T. and Martin, I. (2006). Uniform tissues engineered by seeding and culturing cells in 3D scaffolds under perfusion at defined oxygen tensions. *Biorheology* **43**, 481–488.

Wendt, D., Riboldi, S. A., Cioffi, M. and Martin, I. (2009). Bioreactors in tissue engineering: scientific challenges and clinical perspectives. *Adv. Biochem. Eng. Biotechnol.* **112**, 1–27.

Wendt, D. J., Santoro, R., Tonnarelli, B. and Martin, I. (2011). Streamlined engineering of large-scale human cartilage grafts. *Trans. Orthop. Res. Soc.* **36**, 124.

Williams, R., Khan, I. M., Richardson, K., Nelson, L., McCarthy, H. E., Analbelsi, T., Singhrao, S. K., Dowthwaite, G. P., Jones, R. E., Baird, D. M., et al. (2010). Identification and clonal characterisation of a progenitor cell sub-population in normal human articular cartilage. *PloS One* **5**, e13246.

Woods, A., Wang, G. and Beier, F. (2007). Regulation of chondrocyte differentiation by the actin cytoskeleton and adhesive interactions. *J. Cell. Physiol.* **213**, 1–8.

Yaeger, P. C., Masi, T. L., de Ortiz, J. L., Binette, F., Tubo, R. and McPherson, J. M. (1997). Synergistic action of transforming growth factor-beta and insulin-like growth factor-I induces expression of type II collagen and aggrecan genes in adult human articular chondrocytes. *Exp. Cell Res.* **237**, 318–325.

Chapter I.

The De-differentiation of Human Chondrocytes is Linked to Individual Cell Divisions

The De-differentiation of Human Chondrocytes is Linked to Individual Cell Divisions

Ralph Duhr, David Wendt, Ivan Martin

Departments of Surgery and of Biomedicine, University Hospital Basel, University of Basel, Basel, Switzerland

Ralph Duhr: Conception and design, collection and/or assembly of data, data analysis and interpretation, manuscript writing

David Wendt: Conception and design, data analysis and interpretation, final approval of manuscript

Ivan Martin: Conception and design, data analysis and interpretation, final approval of manuscript

ABSTRACT

The production of engineered cartilage using primary chondrocytes typically requires an initial *in vitro* expansion phase, during which cells lose their native phenotype and chondrogenic potential. The relationship between chondrocyte proliferation and de-differentiation remains however poorly understood. We hypothesized that cell proliferation tracking reveals differences in the progression of de-differentiation and chondrogenic potential among subpopulations. Following the doublings of freshly isolated human chondrocytes allowed the distinction of cells dividing at heterogeneous rates during culture. Changes in the expression of cell surface markers CD54, CD90 and CD166 as well as of extracellular matrix genes collagen type I, collagen type II, aggrecan and versican were linked to individual cell divisions. Different culture conditions influenced cell doubling rates but not the relation to phenotypic alterations indicating a strong coupling between both phenomena. Interestingly the highest chondrogenic potential was measured for slowly growing chondrocytes, even after a same number of total doublings was reached. This increased understanding of the interrelation between proliferation, de-differentiation and re-differentiation capacity will help in finding innovative ways to maintain chondrogenic differentiation potential during chondrocyte expansion and in identifying progenitor populations with intrinsically superior capacity for the generation of enhanced engineered cartilage grafts.

INTRODUCTION

Biological joint resurfacing with grafts engineered from autologous chondrocytes has been reported to hold great promise for the treatment of damaged articular cartilage (Pelttari et al., 2014; Santoro et al., 2010). In order to obtain a sufficient number of cells for the production of these large-size grafts, considerable cell expansion from a small cartilage biopsy is required. During the expansion phase chondrocytes start to de-differentiate by changing the expression of characteristic genes and cell surface markers (Benya and Shaffer, 1982; Binette et al., 1998; Diaz-Romero et al., 2005). Since de-differentiation is only partially reversible, chondrogenic potential is progressively lost with cell proliferation and overly expanded chondrocytes hardly produce any hyaline cartilage matrix (Schulze-Tanzil, 2009). The onset of proliferation and de-differentiation of terminally differentiated chondrocytes in culture is presumably caused by the imposed culture environment. The provision of 3D environments, matched substrate stiffness, extracellular matrix components or growth factors have thus been proposed to better maintain the chondrocyte phenotype during proliferation (Barbero et al., 2006; Jakob et al., 2001; Mhanna et al., 2014; Schrobback et al., 2011; Schuh et al., 2010). Nevertheless these methods only delay the decline of cartilage formation capacity and the connection between proliferation and concurrent de-differentiation of articular chondrocytes in *in vitro* culture remains poorly understood.

The progressive phenotypic changes and loss of chondrogenic differentiation potential with cell passages and cumulative population doublings suggests that proliferation and de-differentiation are coupled (Giovannini et al., 2010; Schulze-Tanzil et al., 2004). However the assessment of cell populations after expansion rather than single cells results in an averaging of possible subsets, dominated by rapidly dividing cells and masking slower growing subpopulations. For chondrocytes

this could be particularly of an issue since clonal studies have shown that primary cells from a same cartilage biopsy proliferate with very heterogeneous growth kinetics and have variable re-differentiation potential (Barbero et al., 2003; Barbero et al., 2005).

The fluorescent proliferation tracking dye carboxyfluorescein succinimidyl ester (CFSE) has been widely used *in vitro* and *in vivo* to analyze cell populations with heterogeneous growth rates such as lymphocytes or hematopoietic stem cells on a single cell level (Parish, 1999; Takizawa and Manz, 2012). When CFSE-labeled cells divide, their fluorescence is halved among the two daughter cells, which allows the determination of the number of prior divisions of each individual cell over multiple generations. From the fluorescence profiles, proliferation kinetics in response to extracellular signals and the link between phenotypical changes and cell divisions can then be established (Hasbold et al., 1999; Hawkins et al., 2007).

Proliferation tracking of freshly isolated chondrocytes was performed here to investigate the connection between single cell divisions and phenotypic changes and to study how this possible link is influenced by different culture environments. We hypothesized that selecting chondrocytes based on their number of cell divisions reveals differences among subpopulations in the progression of de-differentiation and in their chondrogenic potential. With an improved understanding of the interplay between chondrocyte proliferation and de-differentiation, innovative ways of cell expansion and/or selection can be developed that preserve the full chondrogenic potential for the manufacturing of enhanced cartilage grafts.

MATERIALS AND METHODS

Cell isolation and CFSE labeling

Full-thickness samples of human articular cartilage were collected from the tibial plateaus of 2 cadavers and 9 patients undergoing total knee replacement (mean age 68 years, range 56 – 84 years) after informed consent by relatives or patients respectively and in accordance to the local ethical commissions (University Hospital Basel). Only the macroscopically healthy cartilage parts were considered for this study. Cells were isolated during 22 h at 37°C using 0.15% collagenase II (Worthington, USA), as previously described (Jakob et al., 2003). After digestion, cells were resuspended at a concentration of $1x10^6$ cells/ml in phosphate buffered saline (PBS; Gibco, Life Technologies, Switzerland). Carboxyfluorescein diacetate succinimidyl ester (Sigma, Switzerland) diluted in PBS was immediately added to the cell suspension at a final concentration of 1 µM to yield the fluorescent intracellular division tracking dye carboxyfluorescein succinimidyl ester (CFSE). After 5 minutes of incubation in the dark at room temperature, the reaction was quenched by addition of a large excess of cold complete medium (CM) consisting of Dulbecco's modified Eagle's medium containing 4.5 mg/ml D-glucose and 0.1 mM nonessential amino acids, supplemented with 10% fetal bovine serum, 1 mM sodium pyruvate, 100 mM HEPES buffer, 100 U/ml penicillin, 100 µg/ml streptomycin, and 0.29 mg/ml L-glutamine (all from Life Technologies). Since CFSE staining of chondrocytes lead to a wide distribution of initial fluorescence (Chawla et al., 2010), where indicated, cells were sorted 24 h after labeling using a FACSAria III cell sorter (BD Biosciences, USA) to obtain a lower coefficient of variation of fluorescence. These chondrocytes with a narrow CFSE fluorescence distribution were used to generate visually distinctive peaks of generations of proliferating cells (Nordon et al., 1999).

Cell culture

Cells were plated in tissue culture flasks at a density of $1x10^4$ cells/cm^2 and cultured in CM with or without (no GF) growth factors consisting of 1 ng/ml transforming growth factor beta 1 and 5 ng/ml fibroblast growth factor 2 (both from R&D Systems, UK) at 37°C and 5% CO_2 in a humidified incubator (Heraeus, Thermo Scientific, USA) with medium exchange every 3 days (Barbero et al., 2005). A control of undivided CFSE labeled cells was generated by addition of colchicine (Sigma) at a concentration of 100 ng/ml. To inhibit Rho small GTPases, a modified C3 transferase (CT04, Cytoskeleton, USA) was added at a final concentration of 0.5 µg/ml. Cell culture in tissue culture flasks was monitored on an IX50 inverted microscope with phase contrast (Olympus, Japan). At the indicated time points, cells were detached using 0.05% trypsin-EDTA (Gibco) and further processed. In case of re-plating after FACS sorting, cells were seeded at a density of $5x10^3$ cells/cm^2 and grown in CM with growth factors until reaching 90% confluence.

Flow cytometry and fluorescence-activated cell sorting

The expression of cell surface markers was measured by staining chondrocytes with saturating concentrations of mouse antibodies conjugated to phycoerythrin (PE) or allophycocyanin (APC) against human CD49c, CD54, CD90 and CD166 (all from BD Biosciences) diluted in PBS supplemented with 0.1% bovine serum albumin and 2 mM EDTA (both from Sigma). Matched isotype controls (BD Biosciences) were used to set negative gates. A final concentration of 2 µg/ml of 4',6-diamidino-2-phenylindole (DAPI; Sigma) was added shortly before analysis to gate out dead cells. Flow cytometric measurements of CFSE and stained cell surface markers were performed on an LSRFortessa (BD Biosciences). Data were analyzed using FlowJo v10.0.7 (Tree Star Inc., USA) and modeled by series of equally spaced Gaussian curves cells with ModFit LT v4 (Verity Software House, USA) to determine the

number of cells in each generation, using the peak position and standard deviation of CFSE-labeled colchicine-treated (Hawkins et al., 2007). From the number of cells in each generation *i*, precursor numbers were calculated as

$$precursor\ number\ of\ generation\ i = number\ of\ cells\ in\ generation\ i/2^{i-1}$$

Precursor frequencies were then determined by dividing for each generation the calculated precursor number by the sum of precursors from all generations (Nordon et al., 1999). Additionally, chondrocytes were sorted after 6 days of proliferation into 4 groups according to their number of cell divisions derived from their retention of CFSE-associated fluorescence, to be assessed by RT-PCR, chondrogenically re-differentiated in micromass pellets, or further expanded.

Quantitative RT-PCR

mRNA of chondrocytes was extracted using Quick-RNA Miniprep (Zymo Research, Germany), according to the manufacturer's protocol. DNaseI (Zymo Research) was used to remove trace DNA. Isolated RNA was quantified using a NanoDrop spectrophotometer (Thermo Fischer Scientific, USA). Reverse transcription into cDNA was done from 3 µg of RNA by using 500 µg/ml random hexamers (Promega, USA) and 0.5 µl of 200 UI/ml SuperScript III reverse transcriptase (Invitrogen), in the presence of dNTPs. Quantitative real-time PCR was carried out on an ABI Prism 7700 Sequence Detection System (Perkin-Elmer/Applied Biosystems, Switzerland). After an initial denaturation at 95°C for 10 min, cDNA was amplified for 40 cycles, each consisting of a denaturation step at 95°C for 15 s and an annealing/extension step at 60°C for 60 s. Primers and probes for aggrecan, versican, collagen type I, collagen type II and GAPDH were used as previously described (Martin et al., 2001). Assay on-Demand (Applied Biosystems) was used to measure the expression of SOX9 (Hs00165814_m1). For each sample, the threshold cycle (Ct) value of the

reference gene GAPDH was subtracted from the Ct value of the gene of interest, to derive ΔCt. The relative gene expression of each group normalized to the unsorted whole cell population was calculated as $2^{-\Delta\Delta Ct}$. Each sample was assessed at least in duplicate for each gene of interest.

Bioreactors and alginate encapsulation

For culture in perfusion bioreactors, $5x10^4$ freshly isolated CFSE-stained chondrocytes were seeded on Hyalofast scaffolds (6 mm diameter, 2 mm thick; Anika Therapeutics, Italy) coated with 50 µg/ml fibronectin (Sigma). A superficial velocity of 1 mm/s was applied for 16 h, then cells were cultured for 6 additional days at a superficial velocity of 100 mm/s in CM with growth factors and medium exchange after 3 days (Santoro et al., 2011).

Alternatively $5x10^4$ labeled chondrocytes were re-suspended in 1 ml of 1.25% alginate solution (Sigma) and encapsulated in 102 mM $CaCl_2$ (Sigma) solution as previously described (De Ceuninck et al., 2004). Beads were cultured for 7 days in CM with growth factors, with medium exchange after 3 days, and afterwards dissolved using 50 mM EDTA.

Chondrogenic differentiation

Chondrocytes were re-differentiated as spherical pellets of $1x10^5$ cells/well, formed by centrifugation at 300x*g* in 96-well plates with V-shaped bottom (Sarstedt, Germany), in serum-free D-MEM medium (Gibco) containing 1 mM sodium pyruvate, 100 mM HEPES buffer, 100 U/ml penicillin, 100 µg/ml streptomycin, and 0.29 mg/ml L-glutamine, ITS+1 (10 µg/ml insulin, 5.5 µg/ml transferrin, 5 ng/ml selenium, 0.5 mg/ml bovine serum albumin, 4.7 µg/ml linoleic acid; Sigma, Switzerland), 100 µM ascorbic acid 2-phosphate, 1.25 mg/ml human serum albumin, 100 nM dexamethasone (Sigma), and 10 ng/ml TGF-β1 (R&D Systems), with medium

changed twice weekly. After 3 weeks of culture, pellets were processed biochemically for glycosaminoglycan (GAG) and DNA content and histologically for Safranin-O staining.

Biochemical and histological analyses

Cartilaginous pellets were digested in 250 µl of proteinase K solution containing 1 mg/ml proteinase K in 50 mM Tris with 1 mM EDTA, 1 mM iodoacetamide, and 10 mg/ml pepstatin A (all from Sigma) for 16 h at 56°C. The glycosaminoglycan content of pellets was determined by spectrophotometry using dimethylmethylene blue, with chondroitin sulphate as a standard (Barbosa et al., 2003). The DNA content of pellets was measured using the CyQuant cell proliferation assay kit (Invitrogen), with calf thymus DNA as a standard. The amount of GAG in pellets was then normalized to the DNA content (Barbero, 2004).

For histology, micromass pellets were fixed overnight in 4% formalin, encapsulated in HistoGel (Thermo Scientific) and embedded in paraffin. 5 µm thick sections were stained with Safranin-O (Barbero, 2004).

Statistical analysis

Data are presented as mean and standard deviation of the indicated number of independent experiments. Statistical analysis was performed using two-tailed unpaired t-test or one-way ANOVA followed by Tukey's post hoc test for multiple comparisons with Prism software (GraphPad Software, USA). Values of $p < 0.05$ were considered statistically significant.

RESULTS

Division tracking reveals differentially proliferating chondrocyte subpopulations

We labeled articular chondrocytes immediately after isolation with the cell proliferation tracking dye CFSE in order to identify possible subpopulations based on differential growth rates. Analysis of chondrocytes with narrow fluorescence distribution revealed distinct peaks of cell divisions after 4 days in culture whereas colchicine treated cells did not divide and were concentrated in one single peak of uniformly high fluorescence, marking the undivided population (Fig. 1A). The modeling of growth kinetics with the help of fluorescence data allowed the attribution of generation numbers to the peaks, the quantification of subpopulations and the calculation of the frequency of precursor cells. In the proliferating population, the fraction of cells that had undergone 0 or 1 division was drastically decreased compared to the percentage of their corresponding precursors in the original population. Meanwhile the subpopulations with 3 or more divisions had increased relatively to the fraction of their precursors (Fig. 1B). Chondrocytes that were not sorted for a low coefficient of variation of initial fluorescence showed broad CFSE distributions after several days in culture and cells with 6 or more divisions approached autofluorescence. Even if no visually distinctive peaks could be observed, CFSE profiles of these cells could be still be modeled with Gaussian curves showing an overlap between neighboring subpopulations (Fig. 1C).

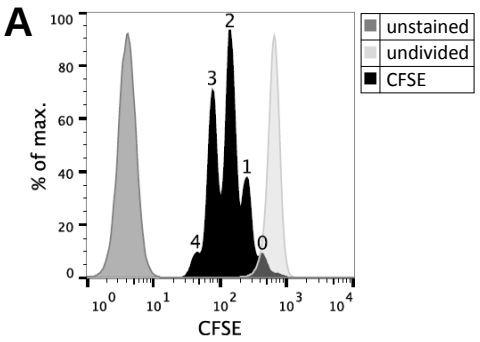

B

subpopulations on day 4		
cell divisions	fraction measured	calculated precursors
0	4.43%	16.02%
1	16.96%	30.67%
2	41.76%	37.76%
3	31.88%	14.41%
4	4.97%	1.12%

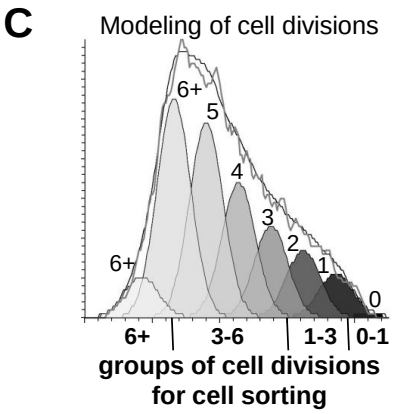

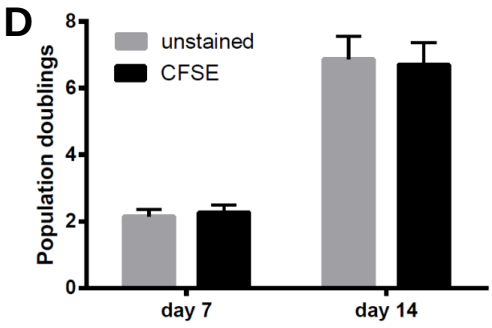

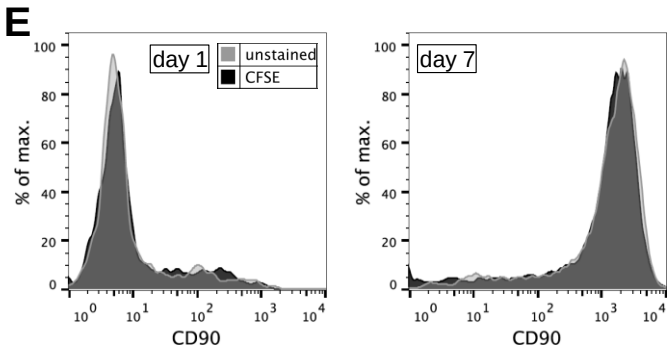

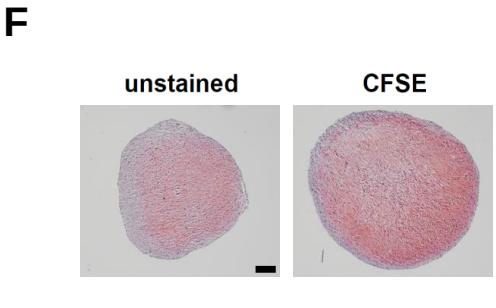

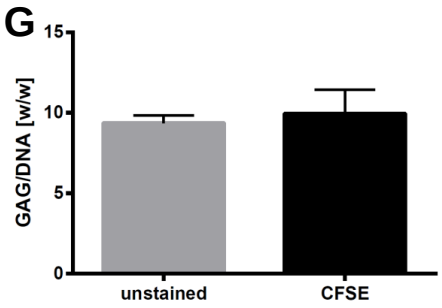

Figure 1: **CFSE staining reveals subpopulations of chondrocytes proliferating at different rates.** (A) Fluorescence profile measured by flow cytometry of CFSE-stained freshly isolated chondrocytes, initially sorted for uniform fluorescence, after 4 days in culture. Proliferation was inhibited with colchicine to determine the position of the peak of undivided cells and the coefficient of variation for modeling. Numbers of cell divisions are indicated. (B) From the fluorescence profile, the subpopulations of different chondrocyte generations were quantified, which then allowed the calculation of precursor frequencies in the original population, indicating a rapid overgrowth by faster proliferating cells. (C) Fluorescence profile of CFSE-labeled chondrocytes with broad distribution of initial fluorescence. Subpopulations were identified based a model (black lines) using equally spaced Gaussian curves, showing good fit of the fluorescence measurements (grey line) and partial overlapping between successive groups. Cell division numbers (above) and groups of cell divisions for cell sorting (below) are indicated. (D) CFSE staining did not influence overall growth rates of chondrocytes after 7 and 14 days (n=3 preparations from 1 donor, no statistical difference). (E) Surface marker expression, exemplarily shown here for CD90 on day 1 and day 7, was

indistinguishable between CFSE-stained and unstained cells. (F) Micromass pellets generated from unstained and CFSE treated chondrocytes showed similar Safranin-O staining. Scale bar: 100 µm. (G) CFSE staining did not influence GAG/DNA ratios of chondrogenic pellets (n=3 preparations from 1 donor, no statistical difference).

To assess potential effects of CFSE staining on cell functions, we assessed the growth, de-differentiation, and re-differentiation of CFSE-labeled and unstained cells. Results showed that labeled and unstained chondrocyte populations had identic overall growth rates (Fig. 1D) and exhibited the same changes in cell surface marker expression pattern, exemplarily shown here for CD90 at different time points (Fig. 1E). Moreover the re-differentiation potential of CFSE-labeled and unstained cells in chondrogenic pellet cultures was similar as revealed by Safranin-O staining of histological sections and GAG/DNA ratios (Fig. 1F,G).

Surface marker and gene expression changes are linked to cell divisions

The changes in expression of the cell surface markers CD54, CD49c, CD90 and CD166, all known to indicate the progressive de-differentiation of chondrocytes (Diaz-Romero et al., 2005), were measured in combination with CFSE staining to see whether there is a connection between phenotypic alterations and individual cells divisions. Overall CD166 expression was low in freshly isolated chondrocytes, but quickly increased from day 0 to day 7 of *in vitro* culture (Fig. 2A). When relating CD166 expression to cell divisions on day 7, we found that positivity for this marker was increasing with the number of individual cell doublings (Fig. 2B). Whereas undivided cells stayed mostly CD166-, a significantly higher percentage of cells with 6 or more divisions were CD166+ (Fig. 2C). CD54 expression decreased with culture time (Fig. 2D) and also with cell divisions (Fig. 2E). In contrast to slowly dividing cells that retained CD54 expression, almost all rapidly dividing cells were CD54- on day 7, indicating a negative correlation between CD54 and cell divisions (Fig. 2F).

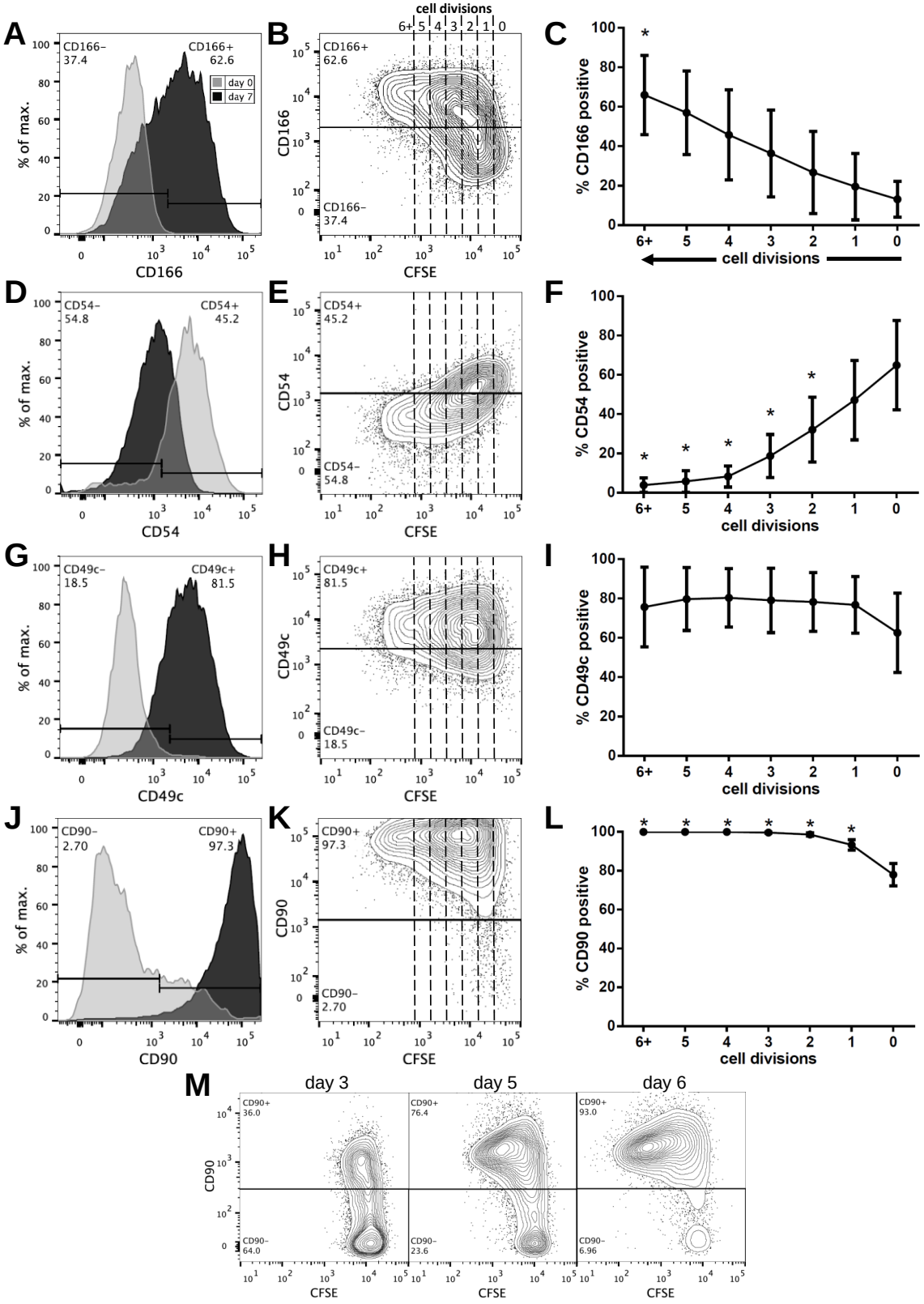

Figure 2: **Changes in cell surface marker expression are linked to cell divisions.** Chondrocytes were assessed for expression of cell surface markers CD49c, CD54, CD90 and CD166 by flow cytometry. (A,D,G,J) Surface marker expression measured on days 0 and 7, confirming changes during culture. Gates indicate positive and negative cell fraction on day 7. (B,E,H,K) CFSE and surface marker expression on day 7, revealing changes of expression with increasing number of cell divisions, except for CD49c. (C,F,I,L) Fraction of cells that for the indicated number of divisions was positive for surface marker expression, which confirmed a link between cell doublings and phenotypic changes (n=4 donors, * significantly different from 0 cell divisions). (M) CFSE and CD90 expression on days 3, 5 and 6, shows progressive CD90 acquisition and proliferation of only CD90+ cells.

Primary chondrocytes quickly became positive for CD49c (Fig. 2G), but the number of CD49c+ cells was high and similar across all numbers of cell doublings, indicating an independence of CD49c expression from cell divisions (Fig. 2H,I). The expression of CD90 completely shifted from day 0, when the vast majority of cells were negative, to day 7 with almost only positive cells (Fig. 2J). Only some of the very slowly dividing or non-dividing chondrocytes remained CD90-, but all moderately to fast dividing cells were CD90+ (Fig. 2K,L). Interestingly and in contrast to the gradual increase of CD166 with cell divisions, when relating CD90 expression to cell doublings, two populations separating over time could be distinguished. During the first days, cultured primary chondrocytes shifted from CD90- to CD90+ and only CD90+ cells started to proliferate, as indicated by diminishing CFSE staining solely in this population. As a result the proportion of non-proliferating CD90- chondrocytes quickly decreased (Fig. 2M).

We next measured the expression of cartilage specific genes in relation to cell divisions, by sorting chondrocytes after 6 days of culture into 4 different groups. Groups were defined according to the number of cells divisions calculated from the remaining CFSE fluorescence, taking into account a partial overlapping of subpopulations (Fig. 1C, 3A). Whereas the expression of collagen type I increased with cell divisions, collagen type II continuously decreased with individual doublings. Hence the ratio of collagen type II to collagen type I was negatively correlated with cell divisions, leading to a more than 400-fold difference between the slowest and the fastest dividing cells after only 7 days (Fig. 3B). A similar result was seen for the ratio of aggrecan to versican which also decreased with cell doublings, indicating that within a pool of cells de-differentiation was fastest progressing in cells that had divided more often (Fig. 3C). Moreover the cartilage transcription factor SOX9 was slightly higher expressed in chondrocytes that were dividing slower (Fig. 3D). For all

genes measured, the whole population showed an expression that was an average of the different groups.

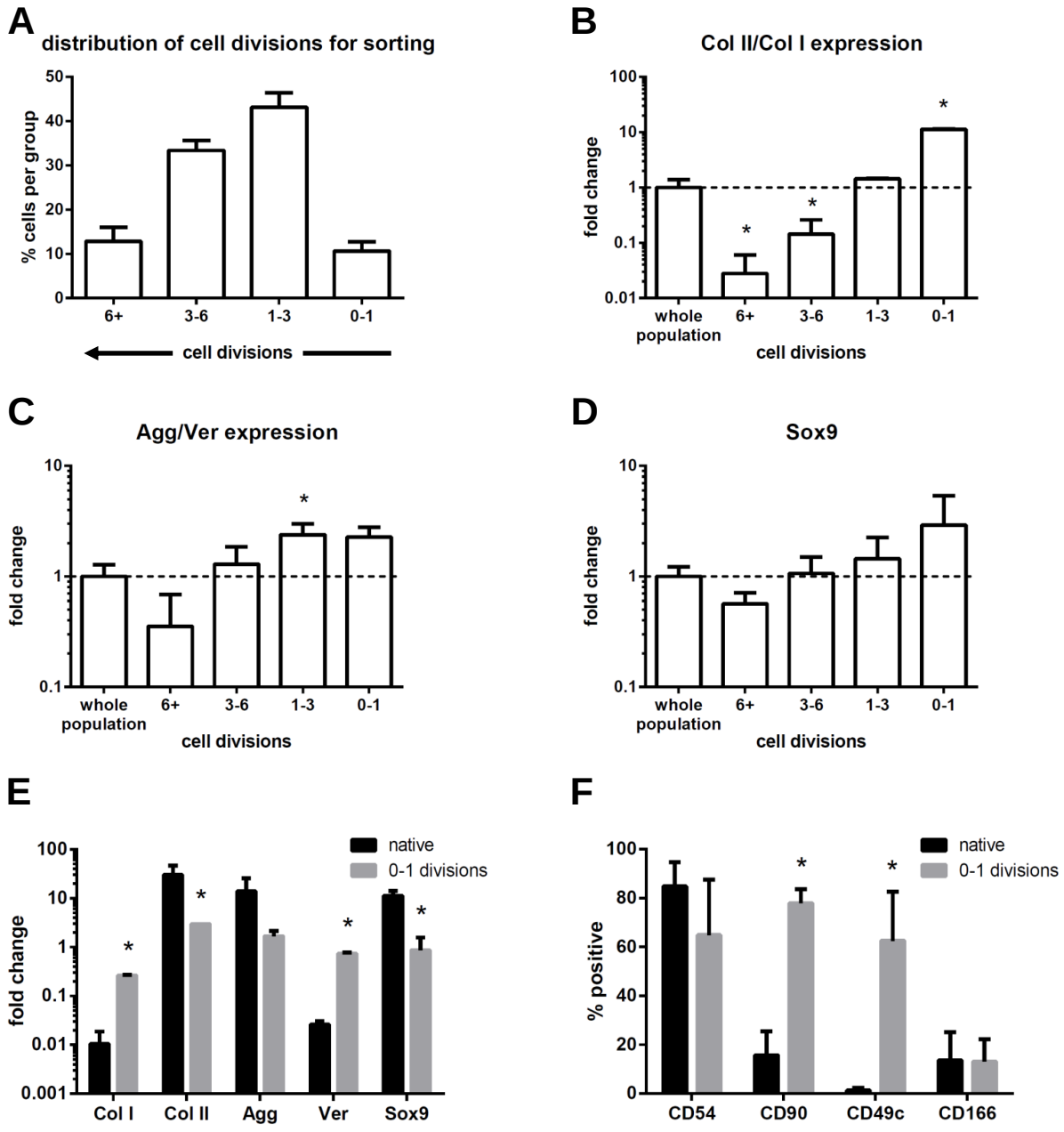

Figure 3: **Alteration of expression of cartilage-specific genes progresses with cell divisions.** (A) Distribution of chondrocytes sorted into each of the 4 groups according to the number of prior cell divisions after 6 days of culture. (B) Fold change of gene expression ratio of collagen type II to collagen type I, relative to the whole population. The ratio strongly decreases with an increasing number of cell divisions. (C) Fold change of gene expression ratio of aggrecan to versican. (D) Fold change of gene expression of SOX9 (n=3 donors, * significantly different from whole population). (E, F) Gene and surface marker expression of native chondrocytes immediately after isolation and chondrocytes that did not divide during culture, suggesting that the culture environment contributes to de-differentiation also in the absence of proliferation (n=3 donors, * significantly different from native chondrocytes).

In order to assess how the de-differentiation of chondrocytes was linked to cell divisions in relation to other factors, we compared the gene and surface marker

expression of cells obtained immediately after isolation and of cells that had undergone 0 to 1 divisions during culture (Fig. 3E, F). The expression of all tested genes had changed towards de-differentiation also in the absence of proliferation, indicating that cell divisions only partially increased the progress of phenotypic changes. Interestingly, the changes of the cell surface markers CD90 and CD49c seemed to be influenced by the *in vitro* culture of cells whereas CD54 and CD166 expression were similar for native and non-dividing cells.

Coupling of chondrocyte de-differentiation to divisions does not depend on the culture environment

Next we wanted to test whether the observed connection between cell divisions and de-differentiation were influenced by the cell culture environment. The use of 3D scaffolds in perfused bioreactors and of growth factors permitted to provide different growth stimuli. CFSE profiles showed that in the presence of growth factors the number of cell divisions in 3D bioreactors was almost identical to those on 2D plastic. On the other hand cells grown on 2D dishes without growth factors were dividing slower on average, and a smaller percentage of cells from this group had achieved 5 or more divisions after 7 days (Fig. 4A). The expression of CD49c, CD90 and CD166 was almost indistinguishable between different culture conditions and followed the same trend of progressive change with cell divisions (Fig. 4B,D,E). On the other hand the expression of CD54 in 2D was very variable and remained on average higher with cell divisions in the absence of growth factors than in their presence (Fig. 4C).

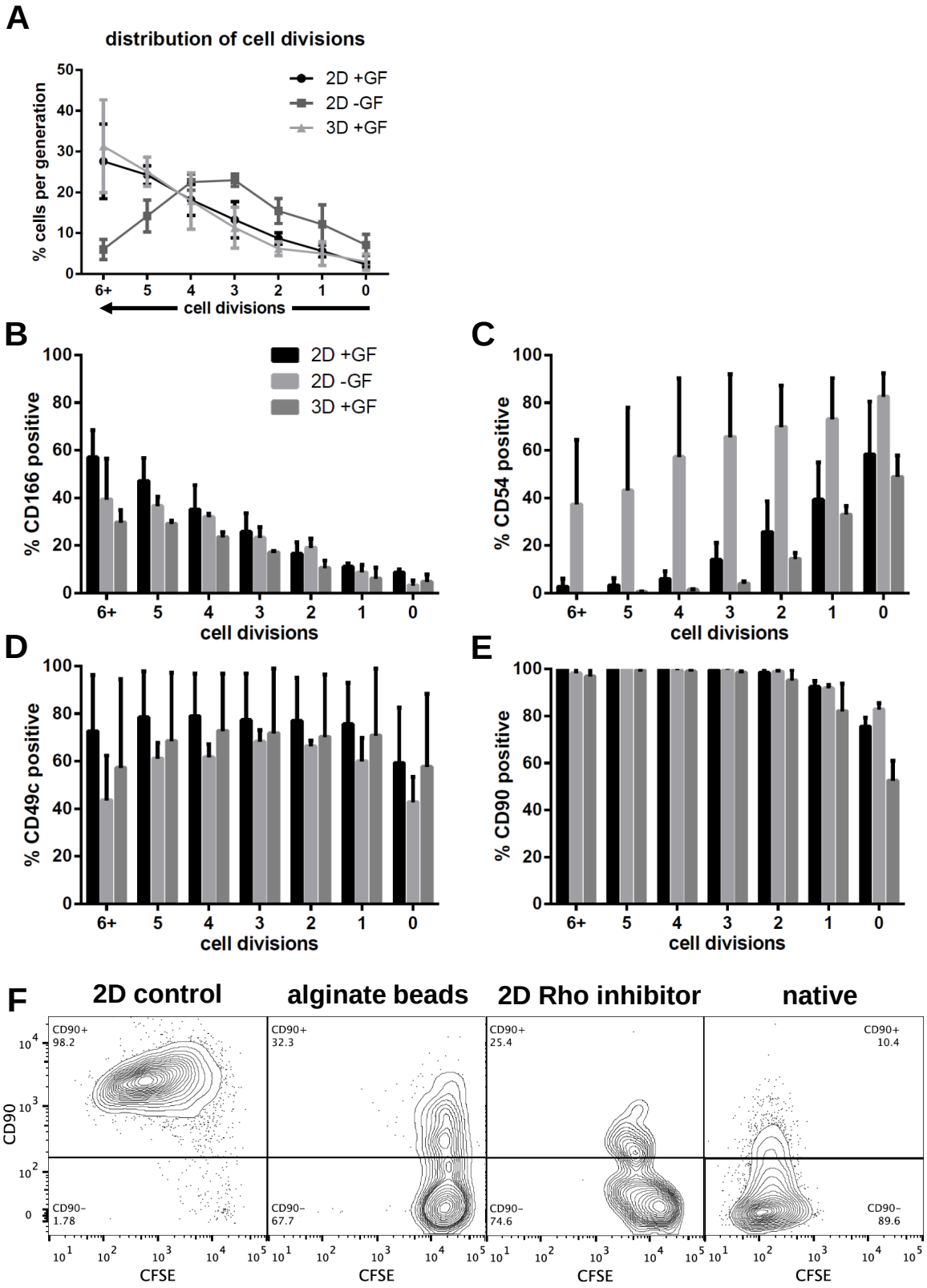

Figure 4: **Division-linked changes are largely independent of the culture environment.** (A) Distribution of chondrocyte cell divisions after 7 days of culture on perfused 3D scaffolds or on 2D dishes, both with growth factors, or on 2D dishes without growth factors. Similar growth rates were found in 3D and 2D with growth factors, but a lower number of doublings occurred in 2D without growth factors. (B, C, D, E) Progression of surface marker expression of chondrocytes grown in 3D or 2D with growth factors, or 2D without growth factors, follows the same trend with cell divisions (n=3 donors, no statistical differences between groups for the same number of divisions). (F) CFSE and CD90 expression on day 7 of chondrocytes cultured on 2D, in alginate beads, or in presence of a Rho GTPase inhibitor, all with growth factors, and of native chondrocytes, highlighting that in the absence of cell spreading, cells showed very limited proliferation and de-differentiation.

To investigate if the cell morphology could affect the relationship between cell divisions and phenotypical changes, cells were encapsulated in alginate beads or a Rho inhibitor was used to restrict stress fiber formation and cell spreading. In both cases, CFSE fluorescence did almost not decrease when compared to the 2D control condition, indicating that cells did not or almost not divide. Moreover these cells remained mostly CD90- during 7 days, which was in contrast to the CD90+ proliferating cells in the control condition. Because the prevention of cell spreading inhibited not only cell divisions but also de-differentiation, these results suggested that both phenomena were strongly coupled. Moreover the de-differentiation progressed slower than for non-dividing cells in the control condition, suggesting that cell spreading was a cause of de-differentiation even in the absence of proliferation (Fig. 4F).

Subpopulations of slowly dividing cells maintain a higher chondrogenic differentiation potential

Chondrocytes sorted after 6 days of culture into 4 groups according to their number of doublings were re-differentiated as micromass pellets to probe their chondrogenic capacity. The best chondrogenesis as assessed by Safranin-O staining and GAG/DNA ratio was found for chondrocytes that were growing slowly and had undergone 1-3 doublings, whereas the fastest proliferating cells with more than 6 divisions only produced fibrous tissue and the group containing non-dividing cells did not undergo proper pellet formation. The whole population had an intermediate re-differentiation potential that was significantly lower than the subpopulation with 1-3 doublings (Fig. 5A,B).

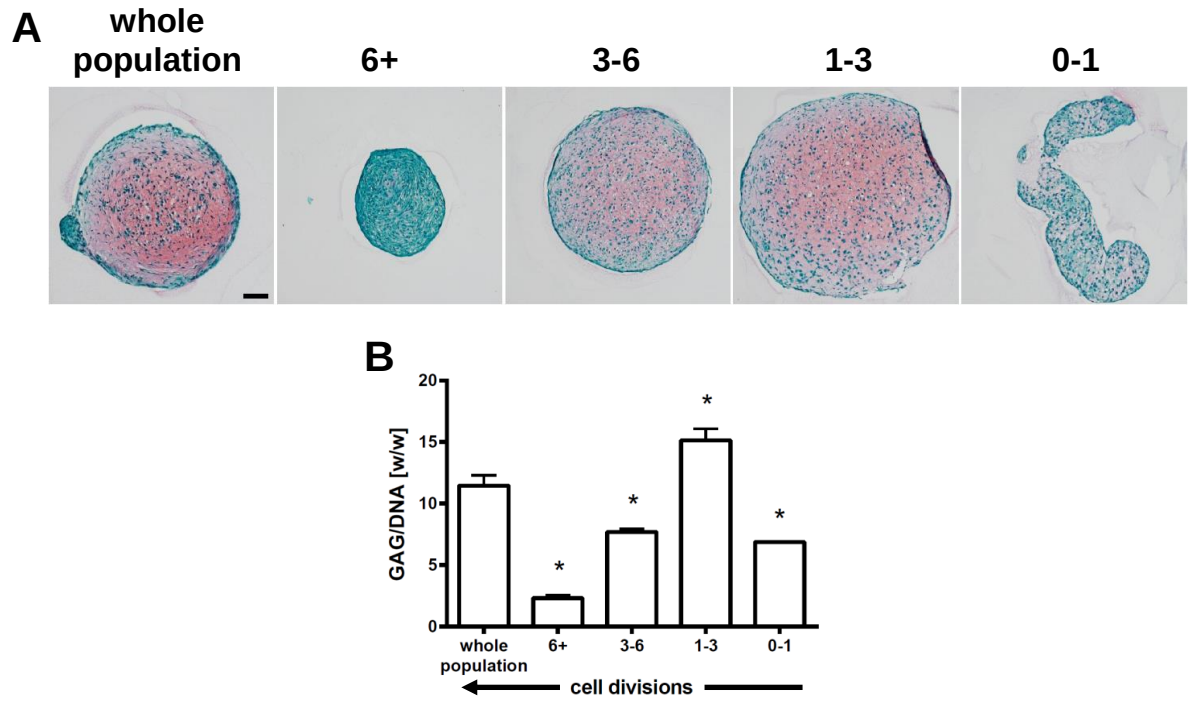

Figure 5: **The highest chondrogenic differentiation potential is found in slowly dividing cells.** (A) Representative Safranin-O staining of chondrogenic micromass pellets from cells sorted according to their number of divisions or the whole population. Scale bar: 100 µm. (B) Biochemical GAG/DNA quantification of chondrogenic pellets, showing the highest ratio for cells that did 1-3 doublings (n=3 preparations from 1 donor, * significantly different from whole population).

To test whether the sorted subpopulations had intrinsically different growth kinetics, sorted cells were further cultured in monolayer. Results revealed that cells that had proliferated fastest during the first 6 days retained the highest doubling rate, meanwhile the slowest dividing cells continued to grow with the least population doublings per day (Fig. 6A). Moreover 3 days after re-plating, cells displayed different morphologies among groups. Cells that had previously undergone 0 to 1 cell division had a roundish to polygonal shape, which was in contrast to fast dividing cells displaying a spindle-like morphology (Fig. 6C). Cells from all groups were then grown until their respective confluence, to assess de-differentiation and chondrogenic potential of subpopulations after having reached a similar number of total population doublings. The gene expression ratio of collagen type II to collagen type I showed that the difference between the fastest and the slowest dividing group was even more pronounced, even though in absolute numbers the ratio was lower than after the first passage for all groups (Fig. 6B). For one donor these cells were re-differentiated and

we found that the chondrocyte subpopulation that was growing slowly, when compared to very slowly/non-dividing or rapidly dividing cells, still had the highest chondrogenic potential (Fig. 6D).

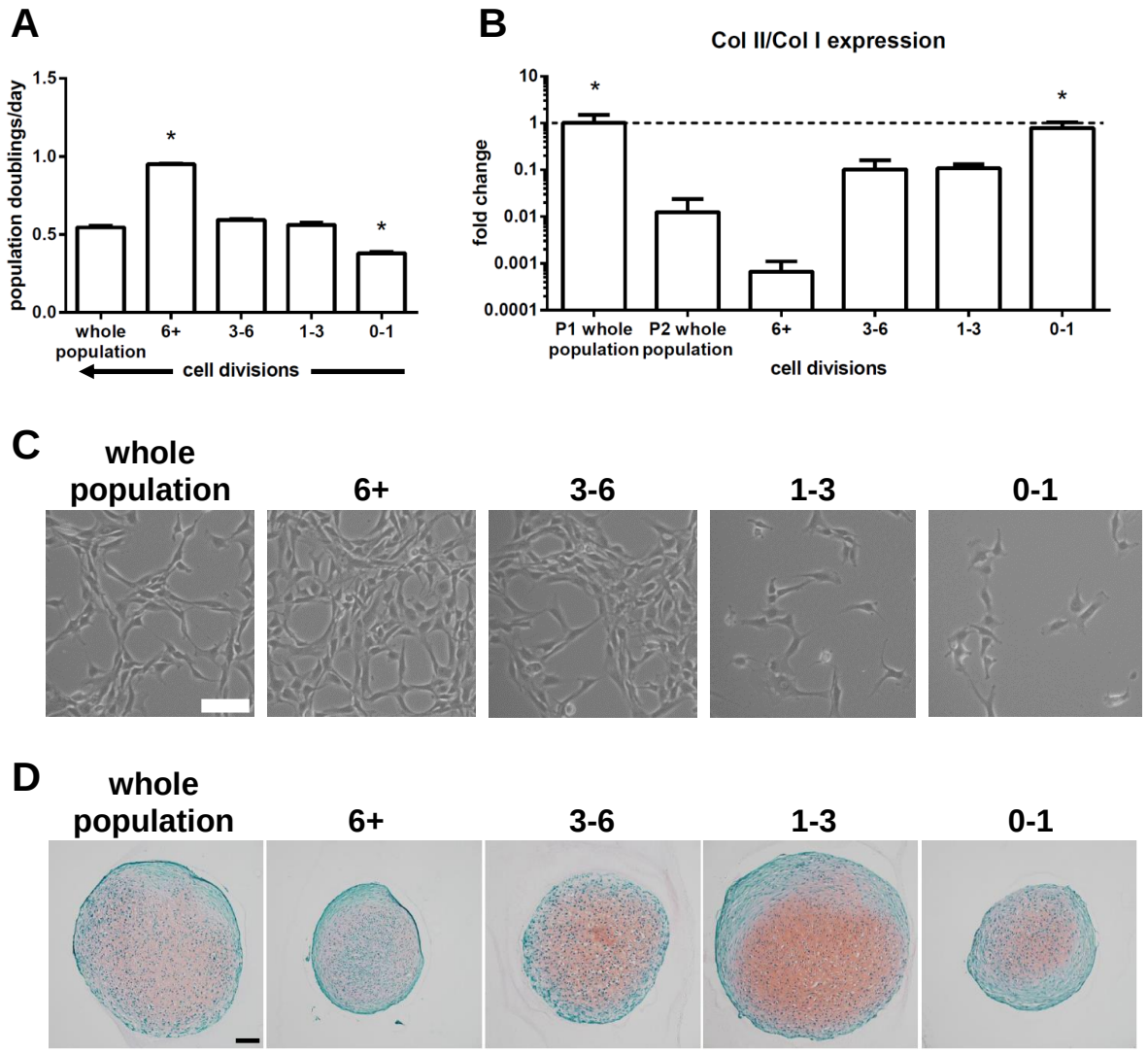

Figure 6: **Differences in growth rate and differentiation potential of subpopulation are maintained during additional culture.** (A) Population doublings per day of sorted cells that were further cultured, indicating that the fastest growing population maintains the highest growth rate (n=3 preparations from 1 donor, * significantly different from whole population). (B) Fold change of gene expression ratio of collagen type II to collagen type I after expansion until a similar number of total doublings. The expression is relative to the whole population P1 after 7 days (n=3 preparations from 1 donor, * significantly different from whole population P2). (C) Phase contrast microscopy of sorted populations. Rapidly proliferating cells have a spindle-like morphology, while slowly dividing and non-dividing cells keep a polygonal to round shape. Scale bar: 100 µm. (D) Safranin-O staining of chondrogenic micromass pellets from cells sorted according to their number of divisions or the whole population and further expanded until a similar number of total doublings was achieved. Scale bar: 100 µm.

DISCUSSION

In this study, we investigated cell divisions and concurrent phenotypic changes during the *in vitro* culture of chondrocytes with the help of cell division tracking. Results showed that chondrocyte subpopulations could be identified based on differential growth rates. When combining cell division tracking with known markers of de-differentiation, we found that changes in surface protein and cartilage gene expression were linked to the number of cell divisions. The observed partial de-differentiation of non-dividing cells suggested that phenotypic changes also occurred independently of proliferation. Different culture environments influenced growth rates, but de-differentiation still progressed with cell divisions. The prevention of cell spreading resulted in a drastic decrease of cell growth and de-differentiation, indicating a strong coupling between both phenomena. Finally we found that the identified chondrocyte subpopulations showed differences in their re-differentiation potential, which persisted even when reaching a similar number of cell divisions, indicating that slower proliferating subpopulations could be enriched for cells with an intrinsically higher chondrogenic capacity.

We identified chondrocyte subpopulations dividing at different rates among the cells from a same cartilage biopsy, confirming here for a whole population the previously reported heterogeneous growth rates of single clones (Barbero et al., 2003; Barbero et al., 2005). The modeling of CFSE fluorescence profiles allowed a quantification of these subpopulations and their precursors. As expected, the calculated precursor frequencies revealed an overgrowth by the fastest proliferating cells, which would lead to results biased towards these cells when assessing only the whole population. Cell division tracking with CFSE has been widely used to monitor the proliferation of various cell types, but was also shown to potentially have detrimental effects on cell behavior (Last'ovicka et al., 2009). Chondrocytes were reported to be slightly

affected by a 20 times higher CFSE concentration (Chawla et al., 2010), but at the concentrations used for this study, CFSE influenced neither their proliferation, nor their re-differentiation potential. Due to the broad initial coefficient of variation of CFSE fluorescence after chondrocyte staining (Chawla et al., 2010), individual peaks of cell divisions could only be visually distinguished when after sorting a gate of uniform fluorescence (Nordon et al., 1999). Nevertheless, even with broader initial fluorescence ranges, division numbers after expansion could be computationally resolved, which was sufficient for sorting subpopulations with only partial overlapping. After approximately 6 to 7 cell divisions CFSE staining became indistinguishable from cell autofluorescence, therefore after 1 week of expansion, precursor frequencies could not be determined and compared among different donors (Hawkins et al., 2007; Parish, 1999). This time frame was however sufficient to encompass the most drastic phenotypic changes (Giovannini et al., 2010). Indeed we found a strong link between the number of cell divisions and the expression of surface markers CD54, CD90 and CD166, which have been shown to characterize de-differentiation of proliferating chondrocytes (Diaz-Romero et al., 2005; Diaz-Romero et al., 2008; Giovannini et al., 2010). Due to partial overlapping subpopulations, the resolution between cells with 0 and 1 division was not sufficient though to conclude whether CD90 (Thy-1) acquisition precedes or follows the first cell division or whether both phenomena are only coincident. The fact that only CD90+ cells were proliferating certainly deserves further investigation. Interestingly, the expression of CD49c (integrin α3) was found to increase over time, independently of cell doublings, which may indicate a reaction to the culture substrate (Elices, 1991). This result together with the observed differences between native cells and cells with 0 to 1 division underlines that even if proliferation and de-differentiation are connected, phenotypical changes are caused and strongly influenced by the cell culture context (Minegishi et al., 2013). The expression of the specific cartilage genes

collagen type II, aggrecan and SOX9 decreased with increasing cell divisions, whereas the expression of collagen type I and versican rose. These changes in gene expression are considered typical for chondrocyte de-differentiation (Barbero et al., 2003) and were reported to depend on time in monolayer culture (Giovannini et al., 2010), but only the use of cell division tracking allowed to show that more specifically the phenotypic alterations progressed with individual cell divisions.

We used different cell culture environments to analyze whether the link between cell divisions and de-differentiation persisted in other conditions. Remarkably, the expansion of chondrocytes on a hyaluronic acid in a perfusion bioreactor seeded scaffold resulted in a very similar cell division pattern than 2D expansion. On the other hand, the omission of growth factors altered cell proliferation rates, yet the trend of increasing de-differentiation with a higher number of cell divisions was conserved for all markers tested, except for CD54. In fact, in the absence of growth factors the latter was maintained in proliferating cells, possibly due to the absence of FGF-2 (Bocelli-Tyndall et al., 2015). Importantly, even if here the connection between cell divisions and phenotypic changes was conserved within every environment, comparison of growth rates among different conditions cannot be used to predict their relative de-differentiation or chondrogenic potential and vice-versa, because of the mentioned role of the cell culture context. For example the addition of growth factors is known to accelerate proliferation and de-differentiation, but at the same time preserve chondrogenic capacity in comparison to expansion without growth factors (Jakob et al., 2001), yet the trend of progressive changes with cell divisions within a same condition was demonstrated here.

The prevention of cell spreading by alginate encapsulation or Rho small GTPase inhibition strongly limited chondrocyte proliferation. At the same time cells remained mostly CD90-, indicating that a differentiated state could be maintained. The finding

that even in these conditions both cell proliferation and phenotypic changes are interdependent indicates the strength of their coupling. Moreover it suggests that cell divisions and de-differentiation are possibly connected through cell morphology and cell spreading via the small GTPase RhoA. Indeed RhoA is not only involved in actin stress fiber formation, but also in cell cycle progression and cell divisions (Croft and Olson, 2006; Wang and Beier, 2005). Moreover RhoA was shown to influence chondrogenic differentiation through the expression of SOX9, the key transcription factor of chondrogenesis (Kumar and Lassar, 2009; Tew and Hardingham, 2006; Wang et al., 2004). A difference in cell morphology was observed after sorting CFSE-labeled chondrocytes according to their number of prior cell divisions and is also possibly due to differences in RhoA activity (Mammoto et al., 2004). The round to polygonal shape observed for non-dividing cells is typically associated with differentiated chondrocytes, whereas the spindle-like shape of faster growing cells is typically seen for expanded and de-differentiated chondrocytes (Kino-oka et al., 2005; von der Mark et al., 1977). Cell tracking or CFSE time-series taking into account cell death and revealing the exact kinetics of phenotypic changes could help to further characterization the connection between cell morphology, divisions and de-differentiation (Etzrodt et al., 2014; Hasbold et al., 1999; Shokhirev and Hoffmann, 2013). The question whether there is a cause-effect relationship between proliferation and de-differentiation namely remains open. Similarly to the hypertrophic differentiation during endochondral ossification in growth plate chondrocytes, molecular switches between proliferation and differentiation could exist (Beier, 2005; Chikuda et al., 2004). On the other hand proliferation and de-differentiation could be simultaneously activated by the culture environment through diverging pathways. If so, the downstream effectors of RhoA could be interesting targets to uncouple both phenomena (Woods and Beier, 2006).

We redifferentiated cells that had proliferated at different rates and observed the highest chondrogenic potential in cells that were slowly dividing. Cells with 0 to 1 divisions showed less cartilaginous matrix production, despite a higher collagen type II to collagen type I ratio, which is generally considered as a good predictor for chondrogenesis (Dell'Accio et al., 2001). Possibly these cells suffered from alterations due to senescence that had occurred already before biopsy collection (Barbero, 2004). The fastest dividing cells had lost most of their potential already after 7 days despite the presence of growth factors known to better preserve chondrogenic capacity (Jakob et al., 2001). The concurrence between high cell proliferation rate and low re-differentiation capacity constitutes thus an important challenge for cartilage tissue engineering applications and underlines the importance of only moderate expansion for clinical applications and of finding ways to specifically increase the proliferation rate of slower dividing cells. Since the number of cell doublings was shown to be of major importance for their chondrogenic potential (Giovannini et al., 2010), chondrocyte subpopulations with divergent growth rates were further cultured until a same number of total doublings was reached. During this additional expansion, the growth rates were still higher for cells that were faster proliferating during primary culture. Although tested for only one donor our results indicate that the differences in chondrogenic capacity persisted, suggesting that the population with moderate growth rate could contain cells that have an intrinsically higher potential. A distinction between different cartilage zones could have helped in better localizing the provenance of these slow cycling cells with high chondrogenic potential (Dowthwaite et al., 2004; Kurth et al., 2011; Williams et al., 2010). We decided here to use only full thickness biopsies because this situation better mimics the cell source in a clinical scenario (Brittberg et al., 1994). Moreover in a previous study, no difference in the proliferation rate between middle and superficial zone chondrocytes was reported (Chawla 2010), indicating that these cells only have the

proliferation rate, but not the origin within a specific region of cartilage in common. In order to better quantify and further analyze these specific cell populations, more primary donors and the use of gene expression arrays will be required (Candela et al., 2014; Isern et al., 2014). Moreover a study of the course of proliferation and de-differentiation of nasal chondrocytes using also additional markers like S100 could reveal if there are mechanistic differences explaining the higher intrinsic chondrogenic potential compared to articular chondrocytes (Diaz-Romero et al., 2014; Pelttari et al., 2014).

Based on the panel of surface markers used here, no clear phenotype of the moderately growing cells with higher chondrogenic potential crystallized, but in order to increase the cartilage forming capacity of the whole population, it could be sufficient to enrich the culture in cells with higher potential by sorting out quickly proliferating and de-differentiating cells, which were found to be CD54-/CD90+/CD166+ after several days in culture. However as long as cell divisions and loss of chondrogenic capacity are strongly coupled and the cell density in tissue engineered constructs positively correlates with cartilage formation, a delicate balance between proliferation and remaining potential must be found to maximize graft quality.

CONCLUSION

Cell proliferation tracking of primary chondrocytes revealed a strong link between characteristic phenotypic changes and individual cell divisions, which persisted in different culture conditions. An increased understanding leading to an uncoupling of this interrelation, would open completely new perspectives for the translation of cartilage tissue engineering. The fact that the highest chondrogenic potential was found in cells that were slowly dividing, even after a same number of total doublings was reached, indicated that this subpopulation could be enriched in cells with an

intrinsically higher chondrogenic capacity. Selection of these cells with superior regenerative properties or elimination of fast growing cells with lower chondrogenic potential could help in the generation of engineered cartilage grafts with a reproducibly high quality.

ACKNOWLEDGEMENTS

We would like to acknowledge the Department of Biomedicine Flow Cytometry Facility for help with flow cytometry and cell sorting. Cartilage samples were kindly provided by Dr. Jeroen Geurts and Dr. Geert Pagenstert. RD would like to thank the Fonds National de la Recherche Luxembourg (4090751) for financial support.

REFERENCES

Barbero, A., Ploegert, S., Heberer, M. and Martin, I. (2003). Plasticity of clonal populations of dedifferentiated adult human articular chondrocytes. *Arthritis Rheum.* **48**, 1315–1325.

Barbero, A., Grogan, S., Schäfer, D., Heberer, M., Mainil-Varlet, P. and Martin, I. (2004). Age related changes in human articular chondrocyte yield, proliferation and post-expansion chondrogenic capacity. *Osteoarthritis Cartilage* **12**, 476–484.

Barbero, A., Palumberi, V., Wagner, B., Sader, R., Grote, M. J. and Martin, I. (2005). Experimental and mathematical study of the influence of growth factors on the growth kinetics of adult human articular chondrocytes. *J. Cell. Physiol.* **204**, 830–838.

Barbero, A., Grogan, S. P., Mainil-Varlet, P. and Martin, I. (2006). Expansion on specific substrates regulates the phenotype and differentiation capacity of human articular chondrocytes. *J. Cell. Biochem.* **98**, 1140–1149.

Barbosa, I., Garcia, S., Barbier-Chassefière, V., Caruelle, J.-P., Martelly, I. and Papy-García, D. (2003). Improved and simple micro assay for sulfated glycosaminoglycans quantification in biological extracts and its use in skin and muscle tissue studies. *Glycobiology* **13**, 647–653.

Beier, F. (2005). Cell-cycle control and the cartilage growth plate. *J. Cell. Physiol.* **202**, 1–8.

Benya, P. D. and Shaffer, J. D. (1982). Dedifferentiated chondrocytes reexpress the differentiated collagen phenotype when cultured in agarose gels. *Cell* **30**, 215–224.

Binette, F., McQuaid, D. P., Haudenschild, D. R., Yaeger, P. C., McPherson, J. M. and Tubo, R. (1998). Expression of a stable articular cartilage phenotype without evidence of hypertrophy by adult human articular chondrocytes in vitro. *J. Orthop. Res. Off. Publ. Orthop. Res. Soc.* **16**, 207–216.

Bocelli-Tyndall, C., Trella, E., Frachet, A., Zajac, P., Pfaff, D., Geurts, J., Heiler, S., Barbero, A., Mumme, M., Resink, T. J., et al. (2015). FGF2 induces RANKL gene expression as well as IL1 regulated MHC class II in human bone marrow-derived mesenchymal progenitor stromal cells. *Ann. Rheum. Dis.* **74**, 260–266.

Brittberg, M., Lindahl, A., Nilsson, A., Ohlsson, C., Isaksson, O. and Peterson, L. (1994). Treatment of Deep Cartilage Defects in the Knee with Autologous Chondrocyte Transplantation. *N. Engl. J. Med.* **331**, 889–895.

Candela, M. E., Yasuhara, R., Iwamoto, M. and Enomoto-Iwamoto, M. (2014). Resident mesenchymal progenitors of articular cartilage. *Matrix Biol.* **39**, 44–49.

Chawla, K., Masuda, K. and Sah, R. L. (2010). Tracking chondrocytes and assessing their proliferation with carboxyfluorescein diacetate succinimidyl ester: effects on cell functions. *Tissue Eng. Part C Methods* **16**, 301–310.

Chikuda, H., Kugimiya, F., Hoshi, K., Ikeda, T., Ogasawara, T., Shimoaka, T., Kawano, H., Kamekura, S., Tsuchida, A., Yokoi, N., et al. (2004). Cyclic GMP-dependent protein kinase II is a molecular switch from proliferation to hypertrophic differentiation of chondrocytes. *Genes Dev.* **18**, 2418–2429.

Croft, D. R. and Olson, M. F. (2006). The Rho GTPase effector ROCK regulates cyclin A, cyclin D1, and p27Kip1 levels by distinct mechanisms. *Mol. Cell. Biol.* **26**, 4612–4627.

De Ceuninck, F., Lesur, C., Pastoureau, P., Caliez, A. and Sabatini, M. (2004). Culture of chondrocytes in alginate beads. *Methods Mol. Med.* **100**, 15–22.

Dell'Accio, F., De Bari, C. and Luyten, F. P. (2001). Molecular markers predictive of the capacity of expanded human articular chondrocytes to form stable cartilage in vivo. *Arthritis Rheum.* **44**, 1608–1619.

Diaz-Romero, J., Gaillard, J. P., Grogan, S. P., Nesic, D., Trub, T. and Mainil-Varlet, P. (2005). Immunophenotypic analysis of human articular chondrocytes: changes in surface markers associated with cell expansion in monolayer culture. *J. Cell. Physiol.* **202**, 731–742.

Diaz-Romero, J., Nesic, D., Grogan, S. P., Heini, P. and Mainil-Varlet, P. (2008). Immunophenotypic changes of human articular chondrocytes during monolayer culture reflect bona fide dedifferentiation rather than amplification of progenitor cells. *J. Cell. Physiol.* **214**, 75–83.

Diaz-Romero, J., Quintin, A., Schoenholzer, E., Pauli, C., Despont, A., Zumstein, M. A., Kohl, S. and Nesic, D. (2014). S100A1 and S100B Expression Patterns Identify Differentiation Status of Human Articular Chondrocytes. *J. Cell. Physiol.* **229**, 1106–1117.

Dowthwaite, G. P., Bishop, J. C., Redman, S. N., Khan, I. M., Rooney, P., Evans, D. J. R., Haughton, L., Bayram, Z., Boyer, S., Thomson, B., et al. (2004). The surface of articular cartilage contains a progenitor cell population. *J. Cell Sci.* **117**, 889–897.

Elices, M. J. (1991). Receptor functions for the integrin VLA-3: fibronectin, collagen, and laminin binding are differentially influenced by Arg-Gly-Asp peptide and by divalent cations. *J. Cell Biol.* **112**, 169–181.

Etzrodt, M., Endele, M. and Schroeder, T. (2014). Quantitative single-cell approaches to stem cell research. *Cell Stem Cell* **15**, 546–558.

Giovannini, S., Diaz-Romero, J., Aigner, T., Mainil-Varlet, P. and Nesic, D. (2010). Population doublings and percentage of S100-positive cells as predictors of in vitro chondrogenicity of expanded human articular chondrocytes. *J. Cell. Physiol.* **222**, 411–420.

Hasbold, J., Gett, A. V., Rush, J. S., Deenick, E., Avery, D., Jun, J. and Hodgkin, P. D. (1999). Quantitative analysis of lymphocyte differentiation and proliferation in vitro using carboxyfluorescein diacetate succinimidyl ester. *Immunol. Cell Biol.* **77**, 516–522.

Hawkins, E. D., Hommel, M., Turner, M. L., Battye, F. L., Markham, J. F. and Hodgkin, P. D. (2007). Measuring lymphocyte proliferation, survival and differentiation using CFSE time-series data. *Nat. Protoc.* **2**, 2057–2067.

Isern, J., García-García, A., Martín, A. M., Arranz, L., Martín-Pérez, D., Torroja, C., Sánchez-Cabo, F. and Méndez-Ferrer, S. (2014). The neural crest is a source of mesenchymal stem cells with specialized hematopoietic stem cell niche function. *eLife* **3**.

Jakob, M., Démarteau, O., Schäfer, D., Hintermann, B., Dick, W., Heberer, M. and Martin, I. (2001). Specific growth factors during the expansion and redifferentiation of adult human articular chondrocytes enhance chondrogenesis and cartilaginous tissue formation in vitro. *J. Cell. Biochem.* **81**, 368–377.

Jakob, M., Démarteau, O., Schäfer, D., Stumm, M., Heberer, M. and Martin, I. (2003). Enzymatic Digestion of Adult Human Articular Cartilage Yields a Small Fraction of the Total Available Cells. *Connect. Tissue Res.* **44**, 173–180.

Kino-oka, M., Maeda, Y., Ota, Y., Yashiki, S., Sugawara, K., Yamamoto, T. and Taya, M. (2005). Process design of chondrocyte cultures with monolayer growth for cell expansion and subsequent three-dimensional growth for production of cultured cartilage. *J. Biosci. Bioeng.* **100**, 67–76.

Kumar, D. and Lassar, A. B. (2009). The transcriptional activity of Sox9 in chondrocytes is regulated by RhoA signaling and actin polymerization. *Mol. Cell. Biol.* **29**, 4262–4273.

Kurth, T. B., Dell'Accio, F., Crouch, V., Augello, A., Sharpe, P. T. and De Bari, C. (2011). Functional mesenchymal stem cell niches in adult mouse knee joint synovium in vivo. *Arthritis Rheum.* **63**, 1289–1300.

Last'ovicka, J., Budinský, V., Spísek, R. and Bartůnková, J. (2009). Assessment of lymphocyte proliferation: CFSE kills dividing cells and modulates expression of activation markers. *Cell. Immunol.* **256**, 79–85.

Mammoto, A., Huang, S., Moore, K., Oh, P. and Ingber, D. E. (2004). Role of RhoA, mDia, and ROCK in cell shape-dependent control of the Skp2-p27kip1 pathway and the G1/S transition. *J. Biol. Chem.* **279**, 26323–26330.

Martin, I., Jakob, M., Schäfer, D., Dick, W., Spagnoli, G. and Heberer, M. (2001). Quantitative analysis of gene expression in human articular cartilage from normal and osteoarthritic joints. *Osteoarthr. Cartil.* **9**, 112–118.

Mhanna, R., Kashyap, A., Palazzolo, G., Vallmajo-Martin, Q., Becher, J., Möller, S., Schnabelrauch, M. and Zenobi-Wong, M. (2014). Chondrocyte culture in three dimensional alginate sulfate hydrogels promotes proliferation while maintaining expression of chondrogenic markers. *Tissue Eng. Part A* **20**, 1454–1464.

Minegishi, Y., Hosokawa, K. and Tsumaki, N. (2013). Time-lapse observation of the dedifferentiation process in mouse chondrocytes using chondrocyte-specific reporters. *Osteoarthr. Cartil.*

Nordon, R. E., Nakamura, M., Ramirez, C. and Odell, R. (1999). Analysis of growth kinetics by division tracking. *Immunol. Cell Biol.* **77**, 523–529.

Parish, C. R. (1999). Fluorescent dyes for lymphocyte migration and proliferation studies. *Immunol. Cell Biol.* **77**, 499–508.

Pelttari, K., Pippenger, B., Mumme, M., Feliciano, S., Scotti, C., Mainil-Varlet, P., Procino, A., von Rechenberg, B., Schwamborn, T., Jakob, M., et al. (2014). Adult human neural crest-derived cells for articular cartilage repair. *Sci. Transl. Med.* **6**, 251ra119.

Santoro, R., Olivares, A. L., Brans, G., Wirz, D., Longinotti, C., Lacroix, D., Martin, I. and Wendt, D. (2010). Bioreactor based engineering of large-scale human cartilage grafts for joint resurfacing. *Biomaterials* **31**, 8946–8952.

Santoro, R., Krause, C., Martin, I. and Wendt, D. (2011). On-line monitoring of oxygen as a non-destructive method to quantify cells in engineered 3D tissue constructs. *J. Tissue Eng. Regen. Med.*

Schrobback, K., Klein, T. J., Schuetz, M., Upton, Z., Leavesley, D. I. and Malda, J. (2011). Adult human articular chondrocytes in a microcarrier-based culture system: expansion and redifferentiation. *J. Orthop. Res.* **29**, 539–546.

Schuh, E., Kramer, J., Rohwedel, J., Notbohm, H., Müller, R., Gutsmann, T. and Rotter, N. (2010). Effect of matrix elasticity on the maintenance of the chondrogenic phenotype. *Tissue Eng. Part A* **16**, 1281–1290.

Schulze-Tanzil, G. (2009). Activation and dedifferentiation of chondrocytes: implications in cartilage injury and repair. *Ann. Anat.* **191**, 325–338.

Schulze-Tanzil, G., Mobasheri, A., de Souza, P., John, T. and Shakibaei, M. (2004). Loss of chondrogenic potential in dedifferentiated chondrocytes correlates with deficient Shc-Erk interaction and apoptosis. *Osteoarthr. Cartil.* **12**, 448–458.

Shokhirev, M. N. and Hoffmann, A. (2013). FlowMax: A Computational Tool for Maximum Likelihood Deconvolution of CFSE Time Courses. *PloS One* **8**, e67620.

Takizawa, H. and Manz, M. G. (2012). In vivo divisional tracking of hematopoietic stem cells. *Ann. N. Y. Acad. Sci.* **1266**, 40–46.

Tew, S. R. and Hardingham, T. E. (2006). Regulation of SOX9 mRNA in human articular chondrocytes involving p38 MAPK activation and mRNA stabilization. *J. Biol. Chem.* **281**, 39471–39479.

von der Mark, K., Gauss, V., von der Mark, H. and Müller, P. (1977). Relationship between cell shape and type of collagen synthesised as chondrocytes lose their cartilage phenotype in culture. *Nature* **267**, 531–532.

Wang, G. and Beier, F. (2005). Rac1/Cdc42 and RhoA GTPases antagonistically regulate chondrocyte proliferation, hypertrophy, and apoptosis. *J. Bone Miner. Res. Off. J. Am. Soc. Bone Miner. Res.* **20**, 1022–1031.

Wang, G., Woods, A., Sabari, S., Pagnotta, L., Stanton, L.-A. and Beier, F. (2004). RhoA/ROCK Signaling Suppresses Hypertrophic Chondrocyte Differentiation. *J. Biol. Chem.* **279**, 13205–13214.

Williams, R., Khan, I. M., Richardson, K., Nelson, L., McCarthy, H. E., Analbelsi, T., Singhrao, S. K., Dowthwaite, G. P., Jones, R. E., Baird, D. M., et al. (2010). Identification and clonal characterisation of a progenitor cell sub-population in normal human articular cartilage. *PloS One* **5**, e13246.

Woods, A. and Beier, F. (2006). RhoA/ROCK signaling regulates chondrogenesis in a context-dependent manner. *J. Biol. Chem.* **281**, 13134–13140.

Chapter II.

Perfused 3D Scaffolds and Hydroxyapatite Substrate Maintain the Osteogenic Potential of Human Bone Marrow-Derived Mesenchymal Stromal Cells during Expansion

Perfused 3D Scaffolds and Hydroxyapatite Substrate Maintain the Osteogenic Potential of Human Bone Marrow-Derived Mesenchymal Stromal Cells during Expansion

Ralph Duhr[1]*, Allison I. Hoch[1,2]*, Nunzia DiMaggio[1], Atanas Todorov[1], Arne Mehrkens[1], David Wendt[1], Ivan Martin[1]

[1] Departments of Surgery and Biomedicine, Institute for Surgical Research and Hospital

Management, University Hospital Basel, Basel, Switzerland

[2] Department of Biomedical Engineering, University of California, Davis, Davis, CA

*These authors contributed equally to this work

Ralph Duhr: Conception and design, collection and/or assembly of data, data analysis and interpretation, manuscript writing

Allison I. Hoch: Conception and design, collection and/or assembly of data, data analysis and interpretation, manuscript writing

Nunzia DiMaggio: Conception and design, data analysis and interpretation

Atanas Todorov: Collection and/or assembly of data

Arne Mehrkens: Collection and/or assembly of data

David Wendt: Conception and design, data analysis and interpretation, final approval of manuscript

Ivan Martin: Conception and design, data analysis and interpretation, final approval of manuscript

ABSTRACT

The expansion of bone-marrow mesenchymal stromal/stem cells (BMSC) on perfused 3D ceramic scaffolds leads to more extensive and more reproducible *in vivo* bone formation than BMSC expanded in monolayer culture on 2D polystyrene (PS). However, several parameters that could largely influence the *in vivo* osteogenic potential completely differ in 3D ceramic and 2D PS culture. We investigated here the effects on the osteogenic potential of i) the 3D scaffold vs 2D surface, ii) the ceramic vs PS substrate material, and iii) the extracellular matrix deposited before implantation. Freshly isolated bone-marrow nucleated cells were expanded on 2D PS dishes for 2 or 3 weeks or in perfusion bioreactors on 3D PS or 3D ceramic scaffolds for 3 weeks. Cells were subsequently retrieved, CD45+ depleted, and re-seeded onto a fresh 3D ceramic scaffold prior to implantation in an ectopic nude mouse model. Other cellular 3D ceramic constructs with an intact niche were directly implanted. After 3 weeks of culture BMSC in 3D PS and 3D ceramic had produced a dense extracellular matrix, but proliferated slightly less than in 2D PS. The colony forming efficiency remained higher in 3D than in 2D after 3 weeks. Whereas the gene expression in 3D PS was more similar to 3D ceramic than to 2D PS, the *in vitro* osteogenic capacity was almost identical in all conditions. *In vivo*, cells expanded in 2D yielded some bone matrix, only if the culture time was not longer than 2 weeks. Cells expanded for 3 weeks on both 3D PS and 3D ceramic scaffolds produced a dense bone matrix. The number of explants containing bone was higher with cells expanded on 3D ceramic compared to 3D PS. However there were no appreciable differences between cells extracted from 3D ceramic and directly implanted constructs. These findings suggest that the bone-forming capacity of BMSC could be maintained by a combination of a 3D environment and a ceramic substrate material, but that a preexisting 3D niche is not required for bone formation. The preservation of BMSC with osteogenic potential during 3D expansion in perfusion bioreactors opens

the perspective for a streamlined production of large-scale bone grafts for clinical use.

INTRODUCTION

Bone marrow-derived mesenchymal stromal/stem cells (BMSC) exhibit remarkable potential for use in cell and tissue therapies due to their proliferation, multilineage differentiation, proangiogenic, tissue homing, and immunomodulation capacities (1,2). In the field of bone regeneration, human BMSC hold promise for the treatment of a breadth of conditions including non-union fractures, osteogenesis imperfecta, and hypophosphatasia (3–7). Therapeutically relevant doses of BMSC are in the range of tens to hundreds of millions of cells, yet a 5 mL bone marrow aspirate only contains roughly 2,500-6,000 BMSC (8). To achieve at least a 1000-fold increase in cell number, BMSC are commonly expanded in monolayer on cell culture plastic formed from processed polystyrene (PS). However, during the requisite duration of expansion in 2D, BMSC demonstrate a substantial decline in progenitor potency (9–11). Specifically, essential properties translating directly toward therapeutic potential such as proliferation, multilineage potential, and colony-forming efficiency (CFE) are abrogated by protracted monolayer culture with serial passages (12,13). To exploit the optimal clinical potential of BMSC, a different expansion protocol that reproducibly maintains the potency of BMSC is therefore imperative.

Recently, several studies demonstrated that expansion in an environment that recapitulates aspects of the native bone marrow niche better preserves the robust therapeutic potential of BMSC (14,15). The 2D cell culture paradigm notably lacks numerous qualities of the complex niche from which bone-marrow derived BMSC are extracted. In particular, *in vivo* BMSC are attached to a 3D environment composed of collagen and inorganic hydroxyapatite, exposed to shearing interstitial fluid movement, and supported by cross-talk with other cell types (13,16,17). We and others have expanded BMSC on 3D ceramic scaffolds in perfusion bioreactors in order to minimize diffusion constraints and stimulate cells in a mechanical and physico-chemical manner that may resemble the native bone milieu (18–23).

However, unlike other approaches that require an initial growth phase of BMSC on 2D plastic, we directly seeded a minimally processed fresh bone marrow aspirate in the bioreactor (12,18,19). We reported that this streamlined system of 3D expansion under continuous perfusion consistently produces tissue constructs, which were osteogenic upon ectopic implantation in nude mice, unlike the counterparts generated from 2D expanded cells (18). We also demonstrated that the BMSC expanded on 3D ceramic scaffolds had enhanced progenitor properties such as higher clonogenicity and superior multilineage differentiation potential. Moreover, more than 700 genes were found to be differentially regulated between BMSC expanded on 2D PS dishes and BMSC expanded on 3D ceramic scaffolds under perfusion (19).

Given that the bioreactor-based culture of BMSC on 3D ceramic inherently encompasses several aspects that are completely different than in 2D PS and could substantially affect the *in vivo* osteogenic potential, we investigated in this study the specific roles of i) the 3D scaffold vs 2D surface, ii) the ceramic vs PS substrate material, and iii) the extracellular matrix deposited before implantation. Our results highlight the importance of certain culture parameters for preserving the bone forming capacity of BMSC during expansion, which allows their further use in clinical applications.

MATERIALS AND METHODS

Bone marrow aspirates

Bone marrow aspirates (20 mL) were obtained from 8 healthy donors (average 32 years old, range 17 – 50 years) after informed consent during orthopedic surgical procedures in accordance with the local ethical committee (University Hospital Basel). Nucleated cells were isolated from aspirates by lysing red blood cells with Ammonium Chloride Solution RBC Lysis Buffer (StemCell Technologies, USA) according to manufacturer protocol. The average colony forming unit-fibroblast (CFU-F) of the fresh marrow aspirates was determined to be 0.0107% ± 0.0067%.

Culture medium and conditions

Complete medium (CM) consisted of α-MEM supplemented with 10% fetal bovine serum (FBS), 10 mM HEPES buffer, 1 mM sodium pyruvate, 10000 U/mL penicillin, and 10000 mg/mL streptomycin (all from GIBCO, Life Technologies, Switzerland). CM was supplemented with 10 nM dexamethasone, 0.1 mM L-ascorbic acid-2-phosphate (both from Sigma, USA), and 5 ng/mL fibroblast growth factor-2 (FGF-2) (R&D, United Kingdom) to enhance BMSC proliferation and osteogenic priming (33,34). All cells were expanded in a humidified incubator under standard culture conditions (37°C, 5% CO_2, 19% O_2).

2D expansion culture

$4x10^4$ cells/cm^2 (2D PS) or $8x10^3$ cells/cm^2(2D PS low) of freshly-isolated bone marrow nucleated cells were seeded on 2D polystyrene Petri dishes (BD Biosciences, USA) to probe the effect of seeding density on BMSC growth (19,25). Cells were expanded for 2 or 3 weeks without passage to examine the impact of culture duration and population doublings. Medium was changed twice per week, with preservation of non-adherent cells (35).

3D expansion culture

Freshly isolated bone marrow nucleated cells were dynamically seeded *via* perfusion on 3D ceramic and 3D polystyrene 8-mm diameter scaffolds to investigate the role of the substrate material. Approximately $1.5x10^7$ cells/scaffold were seeded onto 3D polystyrene (3D PS, 3D Biotek, USA) or 3D ceramic scaffolds (3D Cer, Finceramica, Italy) (20), to have similar seeding densities than for 2D cultures.

3D seeding was performed using a perfusion bioreactor system (U-CUP, Cellec Biotek, Switzerland) as previously described (36). Briefly, seeded cells were perfused for 5 days through the scaffolds at a superficial velocity of 400 mm/s, corresponding to a flow rate of 1.2 mL/min. After the seeding phase, culture medium was refreshed and the expansion phase culture was performed at 100 mm/s, corresponding to 0.28 mL/min, for additional 16 days. Medium was changed twice per week for a total of 3 weeks in culture. Similar to 2D culture, non-adherent cells were re-injected.

Characterization of developed niche on 3D scaffolds

For evaluation of live cells, cellular scaffolds were sterilely retrieved from the bioreactors and placed in a 12-well plate with phosphate buffered saline (PBS, Gibco, Switzerland) to rinse away cellular debris and remnants of FBS. Subsequently, a 10 µM Calcein AM (Invitrogen) solution in PBS was applied for 1 hour in standard culture conditions according to the manufacturer protocol. Scaffolds were rinsed again with PBS to remove stain prior to fluorescent confocal microscopy imaging (LSM 710, Zeiss, Germany). BMSC morphology and matrix deposition on 3D PS and 3D ceramic scaffolds was visualized using scanning electron microscopy (SEM, Nova Nano SEM 230, FEI, USA) following overnight fixation in 4% paraformaldehyde, dehydration, critical point drying, and gold sputtering.

Cell extraction and MACS cell separation

3D expanded cells were extracted by perfusing 0.3% collagenase type II (Worthington, USA) through the scaffolds for 40 min followed by perfusing 0.05% trypsin/0.53 mM EDTA solution (Gibco, Switzerland) for an additional 15 minutes both at 400 mm/s. 2D expanded cells were extracted using the same enzymatic solutions and durations, but applied statically. Extracted cells were CD45+ depleted using human anti-CD45-coated magnetic beads (MACS technology, Miltenyi Biotec, Germany), according to manufacturer protocol. The number of extracted cells was assessed before and after CD45+ depletion using Neubauer counting chambers. The fraction of dead cells following processing, assessed by Trypan blue exclusion (Sigma), was negligible across experimental groups.

Flow cytometry

Before and after CD45+ depletion, expanded cells were stained with mouse anti-human CD90 FITC (BD Pharmigen 555595), mouse anti-human CD73 PE (BD Pharmigen 550257), and mouse anti-human CD45 APC (BD Pharmigen 555485). FITC, PE and APC isotype IgGs were used as controls (BD Biosciences). After washing, cells were suspended in FACS buffer consisting of 0.5% human serum albumin and 0.5 mM EDTA in PBS. Fluorescence was visualized with a LSRFortessa flow cytometer (BD Biosciences) and analyzed using FlowJo software (USA). After CD45+ depletion, cells used for *in vitro* and *in vivo* assays were CD45-/CD73+/CD90+ with a purity of >99.9% in all cases (data not shown).

Colony forming efficiency (CFE)

To determine the fraction of BMSC in the fresh bone marrow aspirate, a colony forming unit-fibroblastic (CFU-F) assay was performed by plating

approximately 2.5x10^5 bone marrow nucleated cells per Petri dish and culturing in CM supplemented with FGF-2. After two weeks, colonies were rinsed with PBS, fixed in 4% formalin, stained with crystal violet solution (Sigma), and counted (37,38). To assess the colony-forming efficiency (CFE) of expanded BMSC following either 3D or 2D expansion, 300 isolated and CD45+ depleted BMSC were plated in a Petri dish, cultured, stained, and analyzed similar to fresh cells. CFE was normalized within each donor to the 3 week expansion on 2D PS at high density seeding condition to adjust for donor-variability. After preliminary experiments had shown negligible losses during seeding and extraction, the number of BMSC population doublings was approximated as follows:

$$doublings = log_2 \frac{extracted\ cells \times \%\ CD45^- CD73^+ CD90^+}{seeded\ cells\ \times\ initial\ CFE}$$

Osteogenic potential

The osteogenic potential of expanded BMSC was assessed by seeding 3 X 10^4 cells/cm^2 in a 12-well plate (TPP, Switzerland) and differentiating cells for 3 weeks using osteogenic media, which consisted of CM supplemented with 100 nM dexamethasone, 10 mM β-glycerophosphate, and 0.05 mM ascorbic acid-2-phosphate (all from Sigma). After 3 weeks, the cellular monolayer was stained with 2% Alizarin Red S (Sigma) solution to visualize mineral deposition. Alizarin Red S quantification was performed by extraction with 10% cetylpyridinium chloride monohydrate (Sigma) for 30 minutes, after which absorbance at 540 nm was measured, as previously described (39).

Ectopic bone formation in a murine subcutaneous tissue site

CD45+ depleted BMSC were reseeded onto 3D ceramic scaffolds overnight at a superficial velocity of 400 mm/s at 2x 10^6 cells/scaffold, corresponding

approximately to the final cell density after expansion and assuring a sufficient number of clonogenic BMSC (12). Alternatively cells were not extracted from 3D ceramic scaffolds after 3 weeks of expansion were left in the bioreactor for another day before implantation (3D Cer direct).

The resulting constructs were cut into quarters and ectopically implanted in the subcutaneous pockets of nude mice (6 weeks old female, CD-1nu/nu, Charles River, Germany), in accordance with in accordance with the guidelines for care and use of laboratory animals the University Hospital Basel, Switzerland. Four randomized constructs were implanted per mouse as previously describe (18). Eight weeks after implantation, constructs were processed by decalcification with EDTA (Sigma) and paraffin embedded. 5 µm thick sections were stained with hematoxylin and eosin (H&E) and analyzed as previously described (12). Briefly, newly formed bone tissue was quantified by the ratio of eosin stained dense matrix and total available pore space, analyzing for each construct 5 full sections spaced at intervals of 600µm spaced full sections per construct.

Statistical analysis

Data are presented as mean ± standard deviation using at least three independent donors that encompassed 3-4 technical replicates per donor. Statistical significance was assessed by one-way ANOVA followed by Tukey's *post hoc* test for multiple comparisons and p-values < 0.05 were considered statistically significant. Categorical data for bone formation are presented as percentage and were analyzed with the 'N-1' chi-squared test (40). Statistical analysis was performed using GraphPad Prism®4 analysis software (GraphPad Software).

RESULTS

3D expansion results in ample matrix deposition and improves colony-forming efficiency

In order to investigate the influences of the 3D or 2D culture environment and of the substrate material, cells obtained from fresh bone marrow aspirates were cultured either as monolayer on 2D PS dishes or in perfused bioreactors on 3D PS and 3D ceramic scaffolds. Expanded cells were then extracted and CD45+ depleted for *in vitro* assessments (**Fig. 1**).

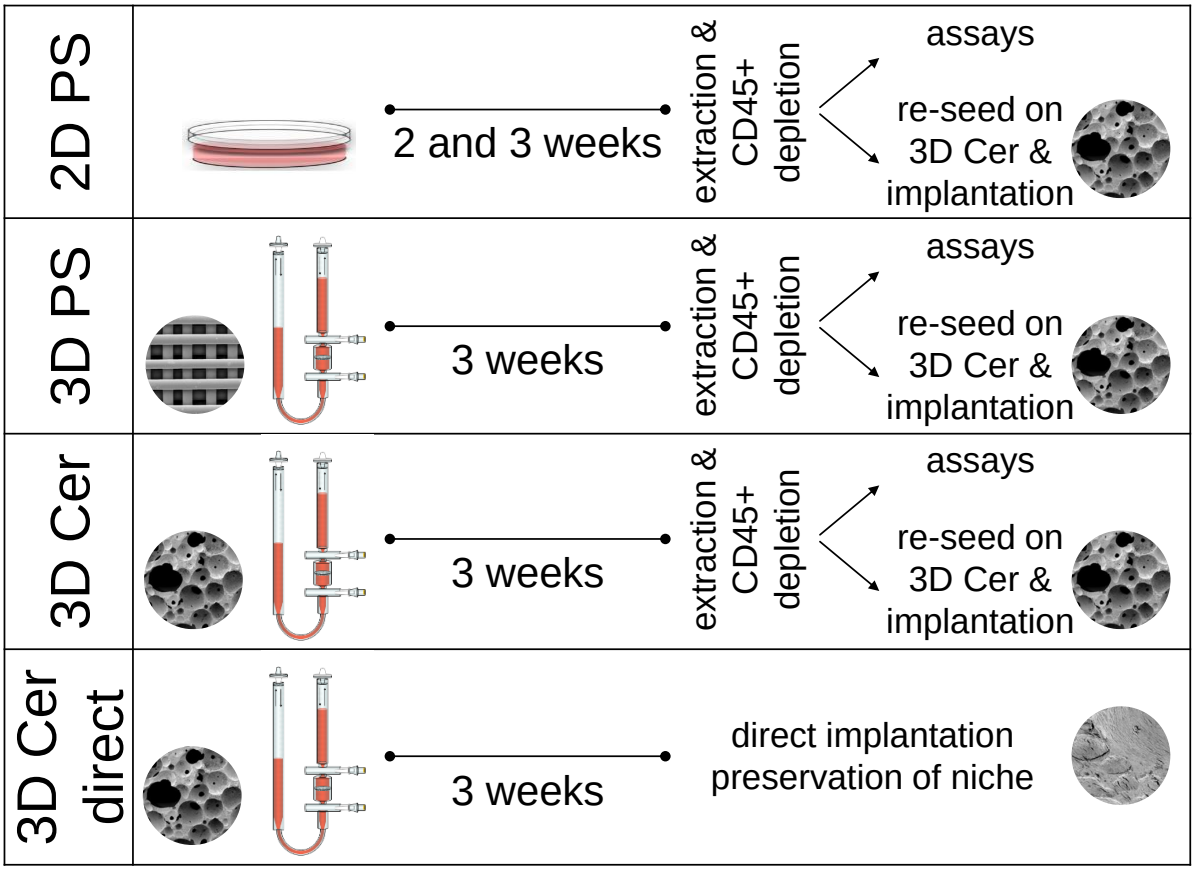

Figure 1: Schematic of the experimental setup illustrating BMSC expansion in different conditions and subsequent *in vitro* or *in vivo* assessment. A fresh bone marrow aspirate was seeded and expanded on 2D polystyrene (2D PS) dishes for 2 weeks (2w) and 3 weeks (3w) or on 3D polystyrene (3D PS) and 3D ceramic (3D Cer) scaffolds for 3 weeks. Cells were extracted and CD45+ depleted, then tested *in vitro* or re-seeded overnight on a fresh 3D ceramic scaffold and implanted *in vivo*. A final group comprised a bone marrow aspirate expanded on 3D ceramic and directly implanted (3D Cer direct). After 8 weeks *in vivo*, constructs were explanted and analyzed.

At the end of bioreactor culture 3D PS and 3D ceramic scaffolds were completely coated with dense extracellular matrix and viable cells were growing on the scaffold and in the pores (**Fig. 2A**). The expansion on both 3D PS and 3D

ceramic scaffolds for 3 weeks resulted in 2 to 3 doublings less than measured for BMSC expanded for the same duration in 2D, indicating an only marginally slower growth rate. On the other hand, in 2D culture the number of population doublings did slightly, but not significantly, increase from 2 to 3 weeks. Different initial seeding densities in 2D did not significantly impact population doublings at neither time point (**Fig. 2B**). The colony-forming efficiency (CFE) of 2D monolayer culture decreased 5 to 6-fold when culture duration was increased from 2 to 3 weeks. In contrast, expansion on both 3D PS and 3D ceramic scaffolds for 3 weeks enhanced CFE approximately 3-fold compared to that of 2D expansion for 3 weeks, but did not overcome the CFE of monolayer expansion for 2 weeks. Similar to population doublings, differential seeding density did not significantly impact CFE (**Fig. 2C**). Since no significant difference was observed between the two seeding densities in 2D, only the higher density was used for the following experiments.

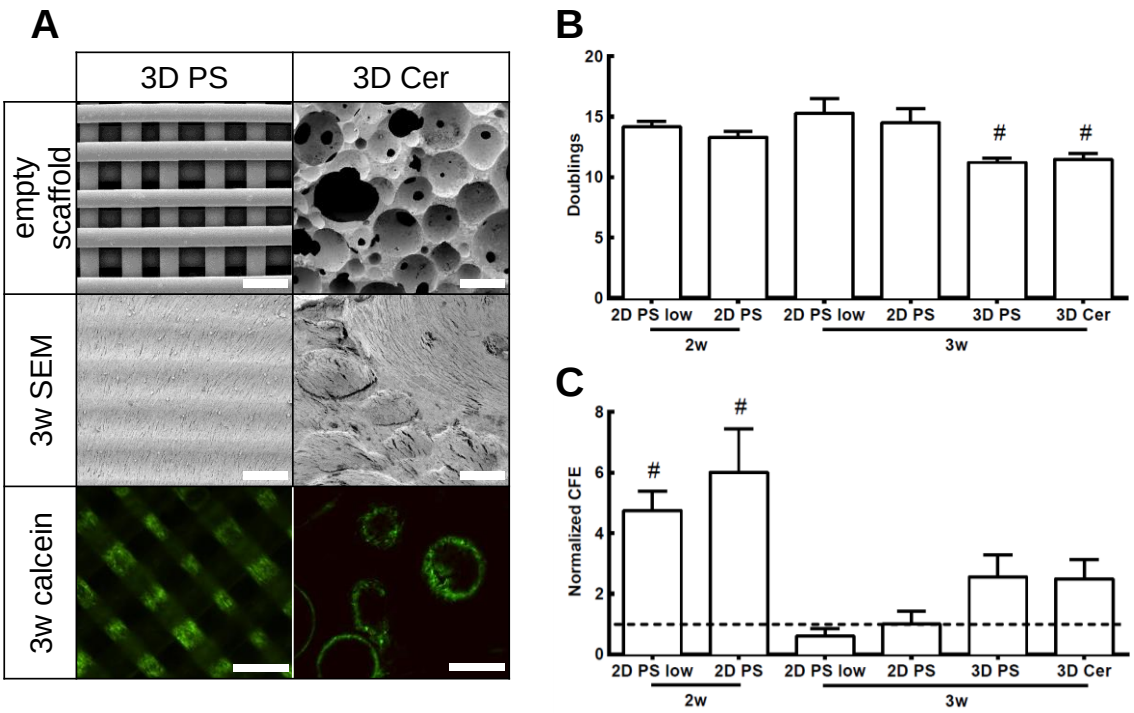

Figure 2: **(A)** Representative SEM images illustrating the formation of extracellular matrix in scaffold pores following 3 week BMSC expansion on 3D PS and 3D ceramic scaffolds. Fluorescent confocal microscopy images of Calcein-AM staining indicating the presence of viable cells in the pores of 3D PS and 3D ceramic scaffolds after 3 weeks. Scale bars are 300 µm. **(B)** Number of BMSC population doublings after 2 weeks and 3 weeks of culture on 2D PS seeded at low or normal density, and 3 weeks on 3D PS and 3D ceramic scaffolds. **(C)** Colony forming efficiency (CFE) of BMSC after expansion, normalized for each donor to the CFE of 3 week expansion on 2D PS at normal density. Chart values represent mean and SD for n ≥ 3 different donors; #p<0.05 vs. 2D PS 3w.

Culture duration and 3D culture environment influence gene expression and in vitro mineralization after expansion

The expression of genes previously shown to be differentially regulated during 2D and 3D expansion was evaluated to identify the specific parameters affecting the cells on a translational level (19). The expression of *AREG, CCL20* and *RUNX2* exhibited an increase from 2 weeks to 3 weeks of expansion on 2D PS, suggesting an influence of culture duration (**Fig. 3A,B,E**). On the other hand the expression of *CXCL5* and *CXCL12* was markedly different between 2D and 3D culture, which indicated an influence of the culture environment on gene expression (**Fig. 3C,D**). The expression of *OSX* was below the limit of detection in all conditions (data not shown), which together with the small differences in RUNX2 expression suggested that none of the expansion conditions primed the cells already during expansion towards the osteogenic lineage. The growth factor VEGF-A was similarly expressed in all groups, implying that the potential for promoting angiogenesis during bone formation was not directly affected by the culture conditions (**Fig. 3F**). When comparing the PS and ceramic 3D scaffolds, we found only negligible differences after expansion for all genes tested.

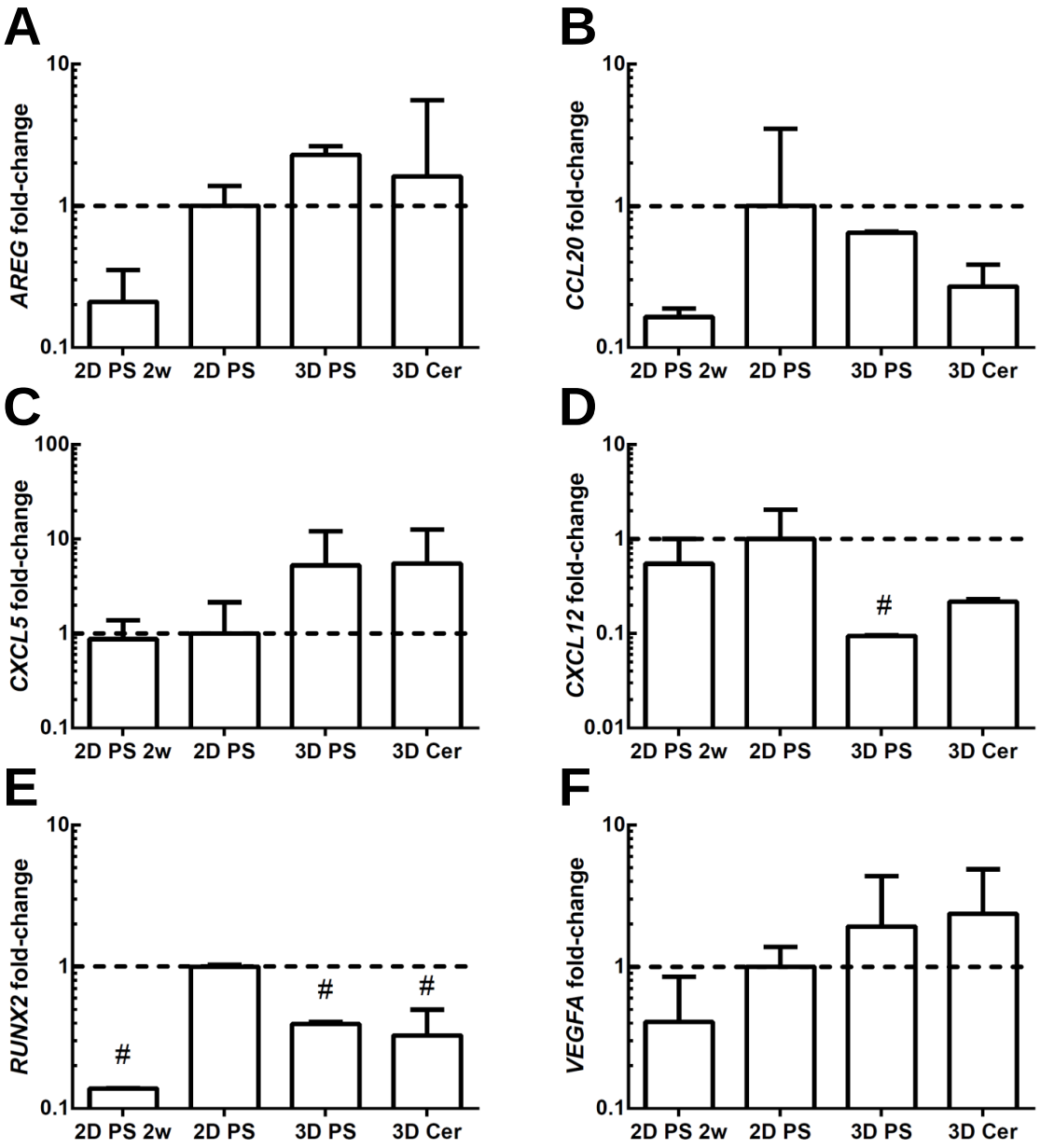

Figure 3: BMSC gene expression after expansion. For each gene, expression was normalized to the one of BMSC expanded for 3 weeks on 2D PS dishes: **(A)** Amphiregulin (*AREG*), **(B)** C-C motif ligand 20 (*CCL20*), **(C)** C-X-C motif chemokine 5 (*CXCL5*), **(D)** C-X-C motif chemokine 12 (*CXCL12*), **(E)** Runt-related transcription factor 2 (*RUNX2*), **(F)** Vascular endothelial growth factor A (*VEGFA*). Chart values represent mean and SD of fold change vs. 2D PS after 3 weeks of expansion for n = 2 different donors; #p<0.05 vs. 2D PS.

Expanded BMSC were also differentiated *in vitro* to estimate their osteogenic potential. Cells from all conditions were able to deposit a mineralized matrix (**Fig. 4A**), however BMSC expanded for 3 weeks in both 2D and 3D regardless of scaffold exhibited slightly but significantly more mineral deposits than cells expanded for 2 weeks in 2D (**Fig. 4B**).

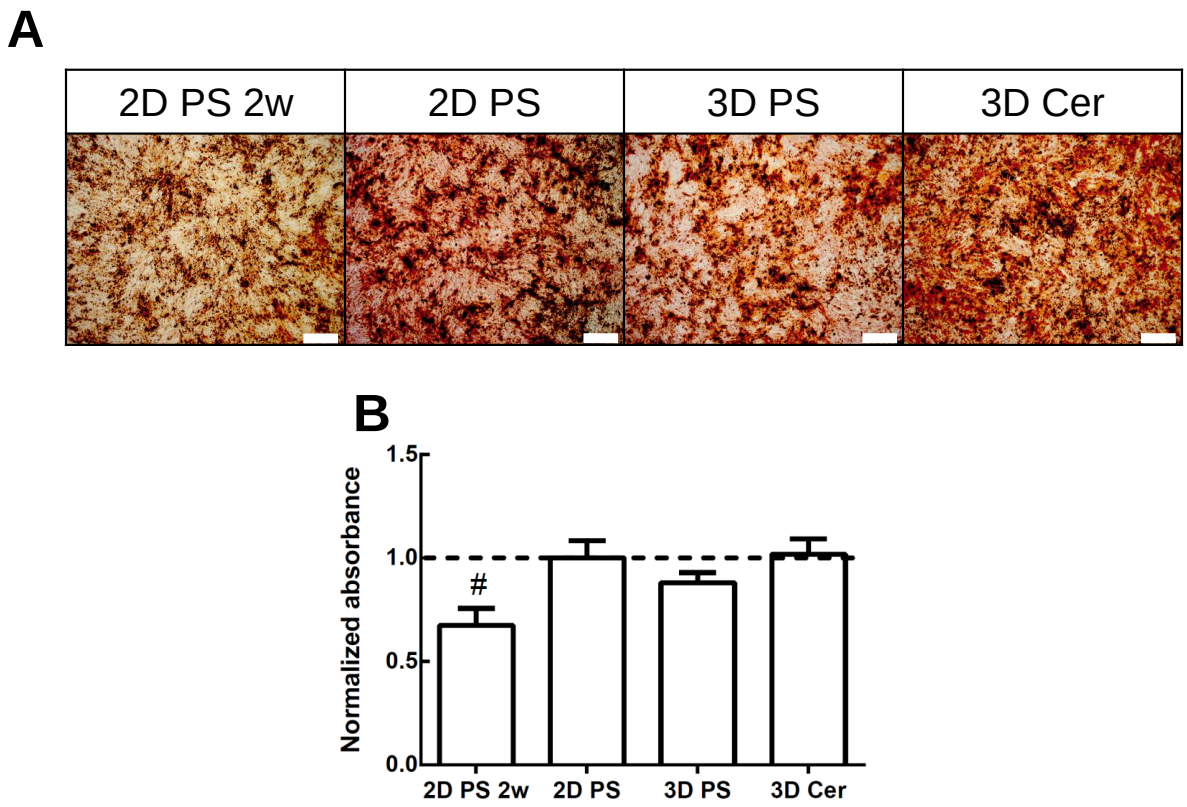

Figure 4: **(A)** Bright field microscopy images of Alizarin Red S staining of mineral deposition from BMSC after expansion and additional 3 weeks of osteogenic differentiation. Scale bars represent 500 µm. **(B)** Quantification of Alizarin Red S, normalized to the absorbance of BMSC expanded for 3 weeks on 2D PS. Chart values represent mean and SD for $n \geq 3$ independent preparations from 1 donor; #$p<0.05$ vs. 2D PS.

3D expansion and ceramic substrate, but not matrix deposition, potentiate bone formation in vivo

The *in vivo* bone formation potential of 2D and 3D expanded BMSC was assessed by either re-seeding of CD45- sorted cells onto a fresh ceramic scaffold and subsequent implantation, or by direct implantation of the cells grown on the ceramic scaffold (**Fig. 1**). H&E staining of explants after 8 weeks revealed bone formation in constructs from all groups except for cells expanded for 3 weeks on 2D PS dishes, as evidenced by intensively stained areas of dense matrix (**Fig. 5A**). Explants derived from acellular 3D ceramic scaffolds did not show any bone formation *via* H&E (data not shown). The percentage of osteogenic explants generated from cells expanded on 3D ceramic scaffolds was substantially higher than for cells grown on 2D dishes for 2 or 3 weeks. BMSC expanded on 3D ceramic

scaffolds also gave rise to more osteogenic constructs than cultured on 3D PS scaffolds. However, no difference was observed in the frequency of constructs with evident bone formation between cells extracted from 3D ceramic and constructs implanted with a conserved extracellular matrix and CD45+ population (**Fig. 5B**). Considering only the osteogenic constructs in each condition, the quantified area of bone formation was variable but on average not significantly different among all groups tested (**Fig. 5C**).

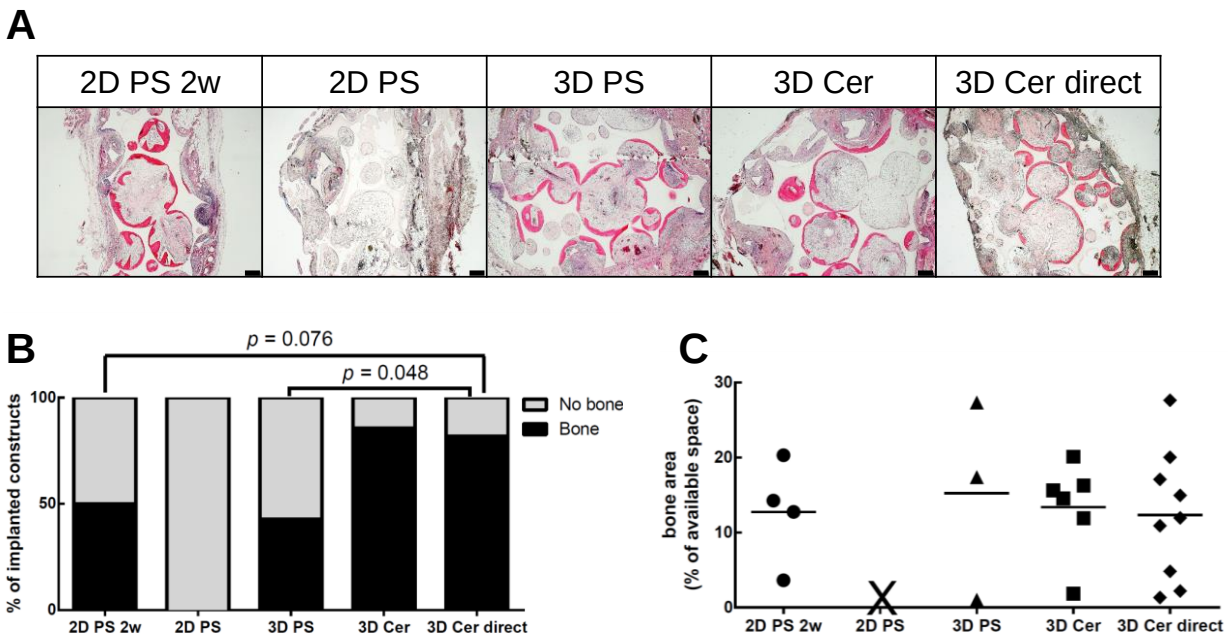

Figure 5: Expanded cells were CD45+ depleted, re-seeded onto a fresh 3D ceramic scaffold and implanted in an ectopic nude mouse model. Alternatively 3D ceramic constructs with an intact extracellular matrix were directly implanted. **(A)** H&E stained histological sections of explants with intensively stained areas of dense matrix, indicating bone formation in constructs from all groups except for cells expanded for 3 weeks on 2D PS dishes. A representative slide is shown for each group. Scale bars are 200 µm. **(B)** Osteogenic constructs as a percentage of total implants. Bone formation was identified by the presence of matrix positive for eosin (2D PS 2w: n=8, 2D PS: n=11, 3D PS: n=7, 3D Cer: n=7, 3D Cer direct: n=11). **(C)** Quantified area of bone formation as a fraction of available pore space and group average (horizontal bar), considering only the osteogenic explants in each condition. For each construct 5 full sections spaced at intervals of 600µm were analyzed. Data points represent averages of constructs.

DISCUSSION

We previously validated the implementation of a streamlined system for the expansion of fresh bone marrow aspirates, which employs 3D ceramic scaffolds in perfusion bioreactors to entirely bypass cell culture on 2D plastic, by demonstrating a more reproducible and more extensive bone formation *in vivo* (18). In the present study, the discrepancy between 2D PS dishes and 3D ceramic scaffolds was bridged via a 3D PS scaffold in order to investigate separately the fundamental roles of the culture dimensionality and the substrate material on the bone formation potential. Results showed that after 3 weeks of culture BMSC in 3D PS and 3D ceramic had proliferated slightly less than in 2D PS, but that their colony forming efficiency (CFE) remained higher. Whereas the gene expression in 3D PS was more similar to 3D ceramic than to 2D PS, the *in vitro* osteogenic capacity was almost identical in all conditions. Considerable differences were found for the osteogenic capacity *in vivo*, where cells expanded in a perfused 3D environment, both on PS and on ceramic scaffolds, were able to produce a dense bone matrix. The number of osteogenic explants was higher when generated from cells cultured on 3D ceramic than from 3D PS, implying that besides the 3D environment also the substrate choice was relevant to maintain a higher bone formation potential. Moreover we observed no differences in bone formation between cells extracted from 3D ceramic and directly implanted constructs, which challenges the necessity of a preformed extracellular matrix for osteogenesis.

Substantial cell expansion is required to achieve a sufficient number of BMSC for clinical applications and in addition to the presence of growth factors other parameters could strongly influence proliferation kinetics (1). Our findings suggested that the 3D culture environment was a more important factor for the doubling rate and the CFE of BMSC than the difference in substrate materials. Population doublings and CFE are likely intertwined and for expanded BMSC the plating density has been

reported to affect CFE (9,24,25). We therefore included additional 2D PS groups with shorter culture periods and lower seeding densities and found important changes in CFE due to culture duration, but not seeding density. The fact that cells in 2D PS dishes approached confluence towards the end of the culture could partially explain the slower growth rate during the 3rd week and could also have affected CFE (9). On the other hand a recent study showed that confluence did not to alter the BMSC phenotype (26).

In our previous transcriptomic analysis of BMSC expanded in plastic dishes or perfused ceramic scaffolds, we reported differences in the expression of more than 700 genes (19). For the genes tested here, we confirmed the disparity between 2D PS and 3D ceramic expansion, but only small differences were detected between 3D PS and 3D ceramic, which was in agreement with prior data showing that perfused bioreactors allow a robust expansion process with reduced variability (19). Interestingly, more pronounced changes were found in the expression profiles from week 2 to week 3 in 2D PS corroborating reports that phenotypical differences of BMSC can arise from the culture environment as well as culture duration (22,27).

Rather than the *in vitro* assessments, the ectopic implantation of scaffolds seeded with 2D or 3D expanded cells revealed dramatic differences in their bone formation capacity. Cells were implanted directly after expansion, without additional osteogenic induction, in order to assess their intrinsic capacity for bone formation (28). Remarkably, we found that a perfused 3D environment was sufficient for the maintenance of osteogenic potential during proliferation, even if the scaffold was made of PS. The ceramic substrate, which is thought to prime BMSC towards the osteogenic lineage (29), further reinforced this effect and lead to a reproducible bone formation. To further elucidate the relative contribution of the environment and the substrate to the maintenance of osteogenic potential, a 2D ceramic material or PS and ceramic 3D scaffolds with exactly identical geometries could be used.

Even if bone formation with cells expanded for 2 weeks in 2D PS was possible, the evident decline of osteogenic potential and CFE during an additional week of culture showed that this environment could not preserve progenitor properties. For the prolonged maintenance of native BMSC such as required by *in vitro* models of bone-marrow (15), perfused 3D ceramic scaffolds could therefore be the more promising system. Interestingly the amount of bone area in osteogenic constructs was variable among the groups tested. Since in all constructs the density of clonogenic BMSC was above the previously found threshold (12), the underlying reasons for the heterogeneous bone area and for the absence of bone formation in part of the constructs from one same group remain unknown. The fact that cell doubling number, RUNX2 expression and *in vitro* mineral deposition did not at all and CFE only partially predict the resultant capacity for bone formation is noteworthy because these assays are frequently used to quantify BMSC progenitor potency (13). Numerous facets of the bone marrow niche, which precisely regulate BMSC phenotype (15,30), are egregiously lacking in 2D culture on plastic. Since bioreactor expansion on 3D scaffolds facilitated extensive extracellular matrix production (18), we investigated whether BMSC extracted from their 3 week developed niche would generate comparable bone *in vivo* to directly implanted scaffolds. However no significant differences were found between these groups, indicating that the osteogenic potential of expanded BMSC does not depend on the presence of a niche at the moment of implantation. This implies that if BMSC are required for cell therapy, they could be expanded on 3D ceramic, subsequently retrieved, and re-implanted without loss of osteogenic potential. On the other hand additional experiments would be required to investigate the effect on BMSC progenitor properties of a niche present during expansion.

With the extended knowledge on the importance of the three-dimensionality and the ceramic material, enhanced strategies can be developed to sufficiently

expand BMSC while maintaining their potential to yield functional grafts for improved treatments of patients. Furthermore rapid-prototyped scaffolds made from polystyrene such as the one used for this study could help to investigate other cell types that have been shown to grow differently in 2D and 3D environments, independently of the influences of an extracellular matrix (31). Besides solely being used for cell expansion, the perfused bioreactors could thereby serve as a model system to study cell phenotypes or interactions among different cell types under more controlled conditions (32).

CONCLUSION

In this work we decoupled two eminent parameters of adherent cell culture, the substrate dimensionality and material, to study their individual effects on the capacity of BMSC to form bone after expansion. We demonstrated that in contrast to 2D plastic the use of a perfused 3D plastic scaffold was sufficient to maintain the *in vivo* osteogenic potential and that this effect could be further reinforced in combination with a ceramic substrate. Furthermore the preexistence of a 3D niche of extracellular matrix in which the expanded cells were embedded was not required for subsequent bone formation. These results underline the importance of a 3D culture environment to preserve the differentiation potential of BMSC. From a clinical perspective, the use of perfusion bioreactors thereby offers the possibility to expand osteogenic cells and to generate robust bone grafts in a reproducible and streamlined process.

ACKNOWLEDGMENTS

The authors would like to acknowledge Evi Bieler from the Centre of Microscopy of the University of Basel for help with the electron microscopy. AIH is grateful for financial support through the Whitaker International Program, administered by the Institute of International Education (IIE), ARCS Foundation, Inc., Northern California Chapter, and an industry/campus-supported fellowship under the Training Program in Biomolecular Technology (T32-GM008799) at the University of California, Davis. RD would like to acknowledge Fonds National de la Recherche, Luxembourg (4090751) for financial support.

REFERENCES

1. Bara JJ, Richards RG, Alini M, Stoddart MJ. Concise review: Bone marrow-derived mesenchymal stem cells change phenotype following in vitro culture: implications for basic research and the clinic. Stem Cells **32**(7), 1713, 2014;

2. Pittenger MF, Mackay AM, Beck SC, Jaiswal RK, Douglas R, Mosca JD, et al. Multilineage potential of adult human mesenchymal stem cells. Science. **284**(5411), 143, 1999;

3. Shekkeris AS, Jaiswal PK, Khan WS. Clinical applications of mesenchymal stem cells in the treatment of fracture non-union and bone defects. Curr. Stem Cell Res. Ther. **7**(2), 127, 2012;

4. Horwitz EM, Gordon PL, Koo WKK, Marx JC, Neel MD, McNall RY, et al. Isolated allogeneic bone marrow-derived mesenchymal cells engraft and stimulate growth in children with osteogenesis imperfecta: Implications for cell therapy of bone. Proc. Natl. Acad. Sci. U. S. A. **99**(13), 8932, 2002;

5. Tadokoro M, Kanai R, Taketani T, Uchio Y, Yamaguchi S, Ohgushi H. New bone formation by allogeneic mesenchymal stem cell transplantation in a patient with perinatal hypophosphatasia. J. Pediatr. **154**(6), 924, 2009;

6. Martin I, Ireland H, Baldomero H, Passweg J. The Survey on Cellular and Engineered Tissue Therapies in Europe in 2012*. Tissue Eng. Part A. **21**(1-2), 1, 2015;

7. Liebergall M, Schroeder J, Mosheiff R, Gazit Z, Yoram Z, Rasooly L, et al. Stem Cell–based Therapy for Prevention of Delayed Fracture Union: A Randomized and Prospective Preliminary Study. Mol. Ther. **21**(8), 1631, 2013;

8. Galotto M, Berisso G, Delfino L, Podesta M, Ottaggio L, Dallorso S, et al. Stromal damage as consequence of high-dose chemo/radiotherapy in bone marrow transplant recipients. Exp. Hematol. **27**(9), 1460, 1999;

9. Banfi A, Muraglia A, Dozin B, Mastrogiacomo M, Cancedda R, Quarto R. Proliferation kinetics and differentiation potential of ex vivo expanded human bone marrow stromal cells: Implications for their use in cell therapy. Exp. Hematol. **28**(6), 707, 2000;

10. Bonab MM, Alimoghaddam K, Talebian F, Ghaffari SH, Ghavamzadeh A, Nikbin B. Aging of mesenchymal stem cell in vitro. BMC Cell Biol. **7**, 14, 2006;

11. Muraglia A, Cancedda R, Quarto R. Clonal mesenchymal progenitors from human bone marrow differentiate in vitro according to a hierarchical model. J. Cell Sci. **113 (Pt 7)**, 1161, 2000;

12. Braccini A, Wendt D, Farhadi J, Schaeren S, Heberer M, Martin I. The osteogenicity of implanted engineered bone constructs is related to the density of clonogenic bone marrow stromal cells. J. Tissue Eng. Regen. Med. **1**(1), 60, 2007;

13. Hoch AI, Leach JK. Concise review: optimizing expansion of bone marrow mesenchymal stem/stromal cells for clinical applications. Stem Cells Transl. Med. **3**(5), 643, 2014;

14. Bhat A, Hoch AI, Decaris ML, Leach JK. Alginate hydrogels containing cell-interactive beads for bone formation. FASEB J. **27**(12), 4844, 2013;

15. Di Maggio N, Piccinini E, Jaworski M, Trumpp A, Wendt DJ, Martin I. Toward modeling the bone marrow niche using scaffold-based 3D culture systems. Biomaterials. **32**(2), 321, 2011;

16. McCoy RJ, O'Brien FJ. Influence of shear stress in perfusion bioreactor cultures for the development of three-dimensional bone tissue constructs: a review. Tissue Eng. Part B Rev. **16**(6), 587, 2010;

17. Eipers PG, Kale S, Taichman RS, Pipia GG, Swords NA, Mann KG, et al. Bone marrow accessory cells regulate human bone precursor cell development. Exp. Hematol. **28**(7), 815, 2000;

18. Braccini A, Wendt D, Jaquiery C, Jakob M, Heberer M, Kenins L, et al. Three-dimensional perfusion culture of human bone marrow cells and generation of osteoinductive grafts. Stem Cells **23**(8), 1066, 2005;

19. Papadimitropoulos A, Piccinini E, Brachat S, Braccini A, Wendt D, Barbero A, et al. Expansion of Human Mesenchymal Stromal Cells from Fresh Bone Marrow in a 3D Scaffold-Based System under Direct Perfusion. PloS One. **9**(7), e102359, 2014;

20. Scaglione S, Braccini A, Wendt D, Jaquiery C, Beltrame F, Quarto R, et al. Engineering of osteoinductive grafts by isolation and expansion of ovine bone marrow stromal cells directly on 3D ceramic scaffolds. Biotechnol. Bioeng. **93**(1), 181, 2006;

21. Zhao F, Grayson WL, Ma T, Irsigler A. Perfusion affects the tissue developmental patterns of human mesenchymal stem cells in 3D scaffolds. J. Cell. Physiol. **219**(2), 421, 2009;

22. Frith JE, Thomson B, Genever PG. Dynamic three-dimensional culture methods enhance mesenchymal stem cell properties and increase therapeutic potential. Tissue Eng. Part C Methods. **16**(4), 735, 2010;

23. Han S, Zhao Y, Xiao Z, Han J, Chen B, Chen L, et al. The three-dimensional collagen scaffold improves the stemness of rat bone marrow mesenchymal stem cells. J. Genet. Genomics Yi Chuan Xue Bao. **39**(12), 633, 2012;

24. Russell KC, Phinney DG, Lacey MR, Barrilleaux BL, Meyertholen KE, O'Connor KC. In vitro high-capacity assay to quantify the clonal heterogeneity in trilineage potential of mesenchymal stem cells reveals a complex hierarchy of lineage commitment. Stem Cells **28**(4), 788, 2010;

25. Sekiya I, Larson BL, Smith JR, Pochampally R, Cui J-G, Prockop DJ. Expansion of human adult stem cells from bone marrow stroma: conditions that maximize the yields of early progenitors and evaluate their quality. Stem Cells **20**(6), 530, 2002;

26. Haack-Sørensen M, Hansen SK, Hansen L, Gaster M, Hyttel P, Ekblond A, et al. Mesenchymal stromal cell phenotype is not influenced by confluence during culture expansion. Stem Cell Rev. **9**(1), 44, 2013;

27. Bruder SP, Jaiswal N, Haynesworth SE. Growth kinetics, self-renewal, and the osteogenic potential of purified human mesenchymal stem cells during extensive subcultivation and following cryopreservation. J. Cell. Biochem. **64**(2), 278, 1997;

28. Jaquiéry C, Schaeren S, Farhadi J, Mainil-Varlet P, Kunz C, Zeilhofer H-F, et al. In Vitro Osteogenic Differentiation and In Vivo Bone-Forming Capacity of Human Isogenic Jaw Periosteal Cells and Bone Marrow Stromal Cells: Ann. Surg. **242**(6), 859, 2005;

29. Krebsbach PH, Kuznetsov SA, Bianco P, Gehron Robey P. Bone Marrow Stromal Cells: Characterization and Clinical Application. Crit. Rev. Oral Biol. Med. **10**(2), 165, 1999;

30. Keung AJ, Kumar S, Schaffer DV. Presentation counts: microenvironmental regulation of stem cells by biophysical and material cues. Annu. Rev. Cell Dev. Biol. **26**, 533, 2010;

31. Tibbitt MW, Anseth KS. Hydrogels as extracellular matrix mimics for 3D cell culture. Biotechnol. Bioeng. **103**(4), 655, 2009;

32. Wendt D, Riboldi SA, Cioffi M, Martin I. Bioreactors in tissue engineering: scientific challenges and clinical perspectives. Adv. Biochem. Eng. Biotechnol. **112**, 1, 2009;

33. Martin I, Muraglia A, Campanile G, Cancedda R, Quarto R. Fibroblast growth factor-2 supports ex vivo expansion and maintenance of osteogenic precursors from human bone marrow. Endocrinology. **138**(10), 4456, 1997;

34. Muraglia A, Martin I, Cancedda R, Quarto R. A nude mouse model for human bone formation in unloaded conditions. Bone. **22**(5 Suppl), 131S, 1998;

35. Di Maggio N, Mehrkens A, Papadimitropoulos A, Schaeren S, Heberer M, Banfi A, et al. Fibroblast growth factor-2 maintains a niche-dependent population of self-renewing highly potent non-adherent mesenchymal progenitors through FGFR2c. Stem Cells **30**(7), 1455, 2012;

36. Wendt D, Marsano A, Jakob M, Heberer M, Martin I. Oscillating perfusion of cell suspensions through three-dimensional scaffolds enhances cell seeding efficiency and uniformity. Biotechnol. Bioeng. **84**, 205, 2003;

37. Bertolo A, Mehr M, Janner-Jametti T, Graumann U, Aebli N, Baur M, et al. An in vitro expansion score for tissue-engineering applications with human bone marrow-derived mesenchymal stem cells. J. Tissue Eng. Regen. Med. 2013;

38. Digirolamo CM, Stokes D, Colter D, Phinney DG, Class R, Prockop DJ. Propagation and senescence of human marrow stromal cells in culture: a simple colony-forming assay identifies samples with the greatest potential to propagate and differentiate. Br. J. Haematol. **107**(2), 275, 1999;

39. Wang W, Xu J, Kirsch T. Annexin-mediated Ca2+ influx regulates growth plate chondrocyte maturation and apoptosis. J. Biol. Chem. **278**(6), 3762, 2003;

40. Campbell I. Chi-squared and Fisher-Irwin tests of two-by-two tables with small sample recommendations. Stat. Med. **26**(19), 3661, 2007;

Chapter III.

Anti-Inflammatory/Tissue Repair Macrophages Enhance the Cartilage-Forming Capacity of Human Bone Marrow-Derived Mesenchymal Stromal Cells

Anti-inflammatory/tissue repair macrophages enhance the cartilage-forming capacity of human bone marrow-derived mesenchymal stromal cells

Sergio B. Sesia[1,2]*, Ralph Duhr[1]*, Carolina Medeiros da Cunha[1], Atanas Todorov[1], Stefan Schaeren[1], Elisabetta Padovan[1], Giulio Spagnoli[1], Ivan Martin[1], Andrea Barbero[1]

[1]Departments of Surgery and of Biomedicine, Basel University Hospital, University of Basel, Basel, Switzerland

[2]Department of Pediatric Surgery, University Children's Hospital of Basel (UKBB), Basel, Switzerland

*These authors contributed equally to this work

Sergio B. Sesia: Conception and design, collection and/or assembly of data, data analysis and interpretation, manuscript writing

Ralph Duhr: Conception and design, collection and/or assembly of data, data analysis and interpretation, manuscript writing

Carolina Medeiros da Cunha: Collection and/or assembly of data

Atanas Todorov: Collection and/or assembly of data

Stefan Schaeren: Collection and/or assembly of data

Elisabetta Padovan: Collection and/or assembly of data, data analysis and interpretation

Giulio Spagnoli: data analysis and interpretation

Ivan Martin: Conception and design, data analysis and interpretation, final approval of manuscript

Andrea Barbero: Conception and design, data analysis and interpretation, manuscript writing, final approval of manuscript

Journal of Cellular Physiology

Anti-Inflammatory/Tissue Repair Macrophages Enhance the Cartilage-Forming Capacity of Human Bone Marrow-Derived Mesenchymal Stromal Cells

SERGIO B. SESIA,[1,2] RALPH DUHR,[1] CAROLINA MEDEIROS DA CUNHA,[1] ATANAS TODOROV,[1] STEFAN SCHAEREN,[1] ELISABETTA PADOVAN,[1] GIULIO SPAGNOLI, IVAN MARTIN,[1]* AND ANDREA BARBERO[1]

[1]*Departments of Surgery and of Biomedicine, University Hospital Basel, University of Basel, Basel, Switzerland*

[2]*Department of Pediatric Surgery, University Children's Hospital of Basel (UKBB), Basel, Switzerland*

Macrophages are key players in healing processes. However, little is known on their capacity to modulate the differentiation potential of mesenchymal stem/stromal cells (MSC). Here we investigated whether macrophages (Mf) with, respectively, pro-inflammatory and tissue-remodeling traits differentially modulate chondrogenesis of bone marrow derived-MSC (BM-MSC). We demonstrated that coculture in collagen scaffolds of BM-MSC with Mf derived from monocytes polarized with M-CSF (M-Mf), but not with GM-CSF (GM-Mf) resulted in significantly higher glycosaminoglycan (GAG) content than what would be expected from an equal number of BM-MSC alone (defined as chondro-induction). Moreover, type II collagen was expressed at significantly higher levels in BM-MSC/M-Mf as compared to BM-MSC/GM-Mf constructs, while type X collagen expression was unaffected. In order to understand the possible cellular mechanism accounting for chondro-induction, developing monoculture and coculture tissues were digested and the properties of the isolated BM-MSC analysed. We observed that as compared to monocultures, in coculture with M-Mf, BM-MSC decreased less markedly in number and exhibited higher clonogenic and chondrogenic capacity. Despite their chondro-inductive effect in vitro, M-Mf did not modulate the cartilage tissue maturation in subcutaneous pockets of nude mice, as evidenced by similar accumulation of type X collagen and calcified tissue. Our results demonstrate that coculture of BM-MSC with M-Mf results in synergistic cartilage tissue formation in vitro. Such effect seems to result from the survival of BM-MSC with high chondrogenic capacity. Studies in an orthotopic in vivo model are necessary to assess the clinical relevance of our findings in the context of cartilage repair.

J. Cell. Physiol. 230: 1258–1269, 2015.

Cartilage has a limited ability for self-repair, due to its avascularity and the low metabolic activity of chondrocytes. As a consequence, untreated articular cartilage defects frequently lead to joint pain, restricted long-term function and the development of osteoarthritis (Messner and Maletius, 1996; Gelber et al., 2000).

A commonly used cartilage repair technique referred to as microfracture consists in drilling holes into the underlying subchondral bone to recruit resident MSC from the marrow. This stimulation leads to the formation of a proteoglycan-rich fibrocartilaginous extra-cellular matrix that fills the defect site. However, likely due to the weaker mechanical properties than hyaline cartilage which is often observed (Knutsen et al., 2007; Saris et al., 2008), clinical outcomes of microfracture at more than 2 years follow-up can be not satisfactory (Kalson et al., 2010). In an attempt to enhance MSC retention, proliferation and differentiation in the cartilage defect site, and ultimately improve the clinical outcome of microfracture, biodegradable scaffolds have been used to cover the blood clot (Chung et al., 2014). In particular, collagen based sponges were reported to positively affect MSC chondrogenesis (Gille et al., 2005).

During microfracture, inflammatory cells are also recruited to the lesioned tissue and therefore may directly influence MSC regenerative properties in situ. In particular, macrophages are key players in healing processes due to their trophic and remodeling functions. Monocytes are recruited at the repair site 48–96 h after injury, where they rapidly differentiate into macrophages (Mf) (Park and Barbul, 2004). In the tissue, Mf clear dead cells, release pro-inflammatory cytokines, and subsequently produce factors that dampen inflammation and stimulate angiogenesis, connective tissue synthesis and cell replication (Park and Barbul, 2004). These distinct functions are exercised by different types of macrophages. Indeed Mf display a high degree of heterogeneity and plasticity and a number of diverse phenotypes under different physiologic and pathologic conditions (Mosser and Edwards, 2008). According to nomenclature and experimental guidelines recently defined

Sergio B. Sesia and Ralph Duhr contributed equally to this work.

The authors declared that they have no conflict of interest.

Contract grant sponsor: The European Union;
Contract grant number: FP7-NMP-2009-SMALL-3–246373.
Contract grant sponsor: Fonds National de la Recherche;
Contract grant number: 4090751.

*Correspondence to: Prof. Ivan Martin, ICFS, University Hospital Basel, Hebelstrasse 20, ZLF, Room 405, 4031 Basel, Switzerland.
E-mail: ivan.martin@usb.ch

Manuscript Received: 22 August 2014
Manuscript Accepted: 29 October 2014

Accepted manuscript online in Wiley Online Library (wileyonlinelibrary.com): 21 November 2014.
DOI: 10.1002/jcp.24861

(Murray et al., 2014) Mf are classified into two main subsets: (i) pro-inflammatory and cytotoxic M1 cells; and (ii) anti-inflammatory M2 cells, promoting tissue repair and remodeling (Wynn et al., 2013). In mice, Mf depletion or disruption of Mf transcriptional regulation after skeletal muscle injury was shown to result in incomplete muscle repair and induction of fibrotic scarring (Tidball and Wehling-Henricks, 2007; Ruffell et al., 2009). The importance of Mf in orchestrating early regenerative response to injuries was also recently described by Godwin et al. (2013). In their study, the authors demonstrated that systemic macrophage depletion 24 h after limb amputation in salamander resulted in wound closure but permanent failure of limb regeneration. Regarding more specifically cartilage repair, it has been reported that an enhanced specific recruitment of anti-inflammatory/tissue repair macrophages in microdrilled cartilage defects through the use of chitosan-glycerol phosphate resulted in an improved subchondral repair that led to superior articular cartilage resurfacing (Hoemann et al., 2010). However, the cellular mechanisms responsible for such improved outcome are far from being elucidated and it remains unclear if distinct macrophage populations can directly modulate the tissue forming capacity of the MSC mobilized in the drilled cartilage defect.

We thus investigated in the current study whether Mf modulate the cartilage forming capacity of MSC. In particular, we explored whether functionally different monocyte-derived macrophages can instruct bone marrow-derived MSC (BM-MSC) to become more chondrogenic and the cellular mechanisms possibly accounting for this phenomenon.

Methods

Cell harvest

Bone marrow aspirates (20 ml volumes) were obtained from the posterior iliac crest of nine non osteoarthritic donors (female/male = 2:7, mean age: 33.1 years, range: 20–44 years) after informed consent during orthopedic surgical procedures, in accordance with the local ethical committee of the University Hospital Basel, Switzerland. Human monocytes were isolated from buffy coats from a pool of healthy donors obtained from the Blutspendezentrum beider Basel (Basel, Switzerland) using a Ficoll-Paque density gradient. Human skin fibroblasts were collected from a skin biopsy of the inner thigh of a 27-year-old female donor.

Cell isolation and culture

Nucleated cells were counted with crystal violet and plated in culture flasks at the density of 150,000 cells/cm^2. Adherent Bone Marrow-derived MSC (BM-MSC) were isolated by plastic adhesion and expanded in Dulbecco's modified Eagle's medium (DMEM) containing 4.5 mg/ml D-glucose, 0.1 mM nonessential amino acids, 1 mM sodium pyruvate, 100 mM HEPES buffer, 100 U/ml penicillin, 100 μg/ml streptomycin, and 0.29 mg/ml L-glutamine (basic medium) supplemented with 10% fetal bovine serum (FBS) and 5 ng/ml Fibroblast Growth Factor (FGF)-2 for a total of two passages as described earlier (Frank et al., 2002). Expanded BM-MSC were cytofluorimetrically characterized to be positive for the MSC surface molecules CD90, CD105, CD166, CD44, and negative for the haematopoietic and endothelial cell markers CD45, CD34, CD11a, HLA-DR, CD144.

CD14+ monocytes were isolated from human peripheral blood mononuclear cells (PBMC) using anti-CD14-coated magnetic beads (Miltenyi Biotec GmbH, Bergisch Gladbach, Germany), followed by MACS LS column separation according to the manufacturer's recommendations. CD14+ monocytes, were cultured for 5 days in Roswell Park Memorial Institute medium-1640 (RPMI) containing 10% FBS, 50 μM β-Mercaptoethanol, 1 mM L-alanyl-L-glutamine (GlutaMAX™, Gibco®, Life Technologies, Basel, Switzerland), 1 mM non-essential amino acids, 1 mM sodium pyruvate and 1 mM kanamycin sulphate. Monocyte were cultured for 5 days in culture medium supplemented with either 50 ng/ml granulocyte-macrophage colony-stimulating factor (GM-CSF, Novartis Pharma, Arnhem, The Netherlands) or 50 ng/ml macrophage colony-stimulating factor (M-CSF, R&D Systems, Inc., Minneapolis, MN) to obtain macrophages with pro-inflammatory (GM-Mf) and tissue-remodeling (M-Mf) traits here named according to the in vitro protocol used for their generation (Murray et al., 2014; Xue et al., 2014).

Dermal fibroblasts, isolated by enzymatic digestion of skin biopsies, were expanded for two passages as previously described (Bocelli-Tyndall et al., 2006).

In vitro culture systems

Culture in type I collagen sponge. For monoculture experiments, BM-MSC or macrophages were seeded onto type I collagen sponges (4 mm diameter, 3 mm thick disks, Ultrafoam®, Davol Warwick, RI) at a density of 2×10^5 cells/sponge (0.2 ml). For coculture, BM-MSC were mixed with either GM-Mf, M-Mf or skin fibroblasts in a 1:1 ratio (0.1/0.1 ml) and a total of 2×10^5 cells was seeded on the type I collagen sponges. As a control having an identical number of BM-MSC than in coculture, constructs were generated by seeding only 1×10^5 BM-MSC (0.1 ml). Chondrogenic medium composed of basic medium supplemented with 1.25 mg/ml human serum albumin (Sigma Aldrich, Milan, Italy), 1% ITS-A (Sigma Chemical, St. Louis, MO), 0.1 mM ascorbic acid 2-phosphate, 10 ng/ml TGFβ3 and 10^{-7} M dexamethasone was added 30 min after seeding and exchanged twice a week.

At the indicated time points, constructs were collected and processed for glycosaminoglycan (GAG) and DNA content quantification, qRT-PCR, flow cytometry or histology and immunohistochemistry as described below.

Culture in pellets with macrophage conditioned media

Monocytes were polarized with GM-MSF or M-CSF as described above. After 5 days the culture media were collected and centrifuged at 500 *g* for 5 min to remove cellular debris. The supernatants were stored at −80°C until further use. As a control, RPMI complete medium supplemented with GM-CSF or M-CSF was incubated without cells for 5 days at 37°C, in a humidified incubator and stored at −80°C until further use.

BM-MSC from three different donors were cultured as pellets of 2.5×10^5 cells (Barbero et al., 2004) in a total volume of 250 μl, consisting of 125 μl chondrogenic medium and 125 μl conditioned or control medium, with medium changes twice a week. After 2 weeks, pellets were processed for histology and biochemistry, as described below.

Clonogenic and chondrogenic culture of Instructed BM-MSC

Some collagen constructs were cultured for one week in chondrogenic medium, then digested using sequential treatment with 0.05% Trypsin-EDTA (Invitrogen, Carlsbad, CA) for 10 min and 0.3% collagenase type II (Worthington, NJ) for 1 h. The resulting cell suspensions were processed with anti-CD14-coated magnetic beads (Miltenyi Biotec GmbH) to remove remaining macrophages. The collected BM-MSC from monoculture and coculture (here named *Instructed* BM-MSC) were further cultured to estimate their clonogenicity (colony-forming unit-fibroblast (CFU-F) assay), proliferation rate and chondrogenic capacity. CFU-F assays of BM-MSC and *Instructed*

BM-MSC were performed by plating four cells per cm^2 in tissue culture dishes. After 14 days of culture in basic medium supplemented with 10% FBS, cells were fixed in 4% formalin and stained with 1% methylene blue, and the number of colonies was counted (Braccini et al., 2005). The proliferation capacity was assessed by plating BM-MSC and *Instructed* BM-MSC in flasks at a density of 1.7×10^5 cells/cm^2. After 10 days of culture in basic medium supplemented with 10% FBS, the cells were counted and their proliferation rate was calculated (Francioli et al., 2007). Additionally, expanded BM-MSC and *Instructed* BM-MSC were cultured for 3 weeks in collagen type I sponges as previously described and the resulting cartilaginous tissues were analysed by histology and biochemistry.

In vivo ectopic culture

After 1 week in chondrogenic medium, monoculture and coculture constructs were implanted subcutaneously in the back of nude mice (CD-1 nu/nu, athymic, 6- to 8-week-old females) (Charles River, Sulzfeld, Germany). Constructs from the same experimental group were implanted in different mice, with up to four constructs per mouse. After 8 weeks in vivo, constructs were harvested and analysed by microtomography and histology as described below. All animals in this research were cared for and processed according to the guidelines of the University of Basel (Basel, Switzerland) for the care and use of laboratory animals.

Analytical assays

Biochemistry. All in vitro generated tissues were digested in proteinase K (1 mg/ml proteinase K in 50 mM Tris with 1 mM EDTA, 1 mM iodoacetamide, and 10 mg/ml pepstatin A) for 16 h at 56°C. The GAG content was determined by spectrophotometry using dimethylmethylene blue, with chondroitin sulphate as a standard (Barbosa et al., 2003). In order to quantify the effect of macrophages on the formation of cartilaginous tissue by BM-MSC, the expected total GAG ($GAG_{expected}$) in coculture constructs was calculated as a linear function of the percentage of BM-MSC, based on the GAG content of monoculture BM-MSC constructs ($GAG_{100\%\ BM\text{-}MSC}$) and monoculture macrophage constructs ($GAG_{100\%\ Mf}$), using the following equation:

$$GAG_{expected} = GAG_{100\%Mf} + (GAG_{100\%\ BM-MSC} - GAG_{100\%Mf}) \times \%\,BM - MSC$$

The interaction index was then calculated as the ratio of the GAG measured in the coculture constructs ($GAG_{measured}$) to the $GAG_{expected}$. Interaction index values higher than 1 were considered to indicate *chondro-induction* (Acharya et al., 2012).

The DNA content of pellets was measured using the CyQuant cell proliferation assay kit (Invitrogen), with calf thymus DNA as a standard. The amount of GAG in pellets was then normalized to the DNA content.

Quantitative real-time RT-PCR

RNA of constructs and of cells was extracted using Trizol (Life Technologies, Basel, Switzerland), according to the Manufacturer's protocol. Constructs were first sonicated for 1 min while in Trizol. RNA was treated with DNAseI using the DNA-freeTM Kit (Ambion, Life Technologies) and quantified by spectrofluorometry. cDNA was generated from 3 μg of RNA by using 500 μg/mL random hexamers (Promega Maddison, WI) and 0.5 μl of 200 UI/ml SuperScript III reverse transcriptase (Invitrogen, Life Technologies), in the presence of dNTPs. PCR reactions were performed and monitored using a ABI Prism 7700 Sequence Detection System (Perkin-Elmer/Applied Biosystems, Rotkreuz, Switzerland). After an initial denaturation at 95°C for 10 min, the cDNA products were amplified with 45 PCR cycles, consisting of a denaturation step at 95°C for 15 sec and an extension step at 60°C for 1 min. Primers and probes used for collagen type II and collagen type X were used as previously described (Barbero et al., 2003). Assays on-Demand (Applied Biosystems) were used to measure the expression of IL-4 (Hs00174122_m1), IL-6 (Hs00985639_m1), TNF-α (Hs01113624_g1), IL-10 (Hs00961622_m1), Sox9 (Hs00165814_m1), GAPDH (Hs02758991_g1). For each cDNA sample, the threshold cycle (Ct) value of each target sequence was subtracted to the Ct value of GAPDH, to derive ΔCt. The level of gene expression was calculated as $2^{\Delta Ct}$. Each sample was assessed at least in duplicate for each gene of interest.

Flow cytometry

The surface marker expression of M-Mf and GM-Mf was measured by staining with fluorochrome-conjugated antibodies against CD16, CD32, CD163 or CD204 (BD Pharmingen, San Diego, CA) on a 2-laser FACSCalibur flow cytometer (Becton Dickinson, Franklin Lakes, NJ). Propidium iodide positive cells were excluded from the analysis. Results were analysed by Flow Jo software (Tree Star, Ashland, OR).

To quantify the different cell types in 3D constructs, macrophages directed towards an M-Mf phenotype were labeled with carboxyfluorescein diacetate succinimidyl ester (CFSE) (Life Technologies, Carlsbad, CA). Briefly, cells were washed with PBS and resuspended in PBS at a concentration of 1×10^6 cells/ml. CFSE was added to a final concentration of 1 μM. After 5 min incubation in the dark at room temperature, the reaction was stopped by adding cold DMEM supplemented with 10% FBS. Monoculture and coculture constructs were digested after 7 and 14 days of culture by sequential treatment with trypsin and collagenase II as described above. The cells from at least three constructs per experimental group were pooled and counted manually in a hemocytometer using the trypan blue exclusion method. Cells retrieved from coculture constructs of labeled M-Mf and unlabeled BM-MSC were analysed by flow cytometry using a Fortessa flow cytometer (Becton Dickinson) to follow the differential expression of known BM-MSC and M-Mf surface markers over time. Ten minutes prior to analysis, 4′,6-diamidino-2-phenylindole (DAPI) (Sigma) was added at a final concentration of 2 μg/ml to gate out dead cells. In addition to the CFSE labeling, a combination of CD45 APC and CD73 PE (BD Pharmingen) provided a clear discrimination between BM-MSC (CD45-/CD73 + /CFSE-) and M-Mf (CD45 + /CD73-/CFSE +) during all time points of assessment. The absolute numbers of BM-MSC and M-Mf during coculture in collagen I sponges were calculated from the relative fractions of CD45-/CD73 + /CFSE- and CD45 + /CD73-/CFSE+ populations, respectively

TABLE 1. Characterization of the phenotypes acquired by monocytes following exposure to GM-CSF or M-CSF

Analyses	GM-Mf	M-MF
FACS	$CD16^+$, $CD32^+$, $CD163^-$, $CD204^{low}$	$CD16^-$, $CD32^{low}$, $CD163^+$, $CD204^+$
RT-PCR	$IL\text{-}6^{high}$, $TNF\text{-}\alpha^{high}$, $IL\text{-}4^{low}$, $IL\text{-}10^{low}$	$IL\text{-}6^{low}$, $TNF\text{-}\alpha^{low}$, $IL\text{-}4^{high}$, $IL\text{-}10^{high}$

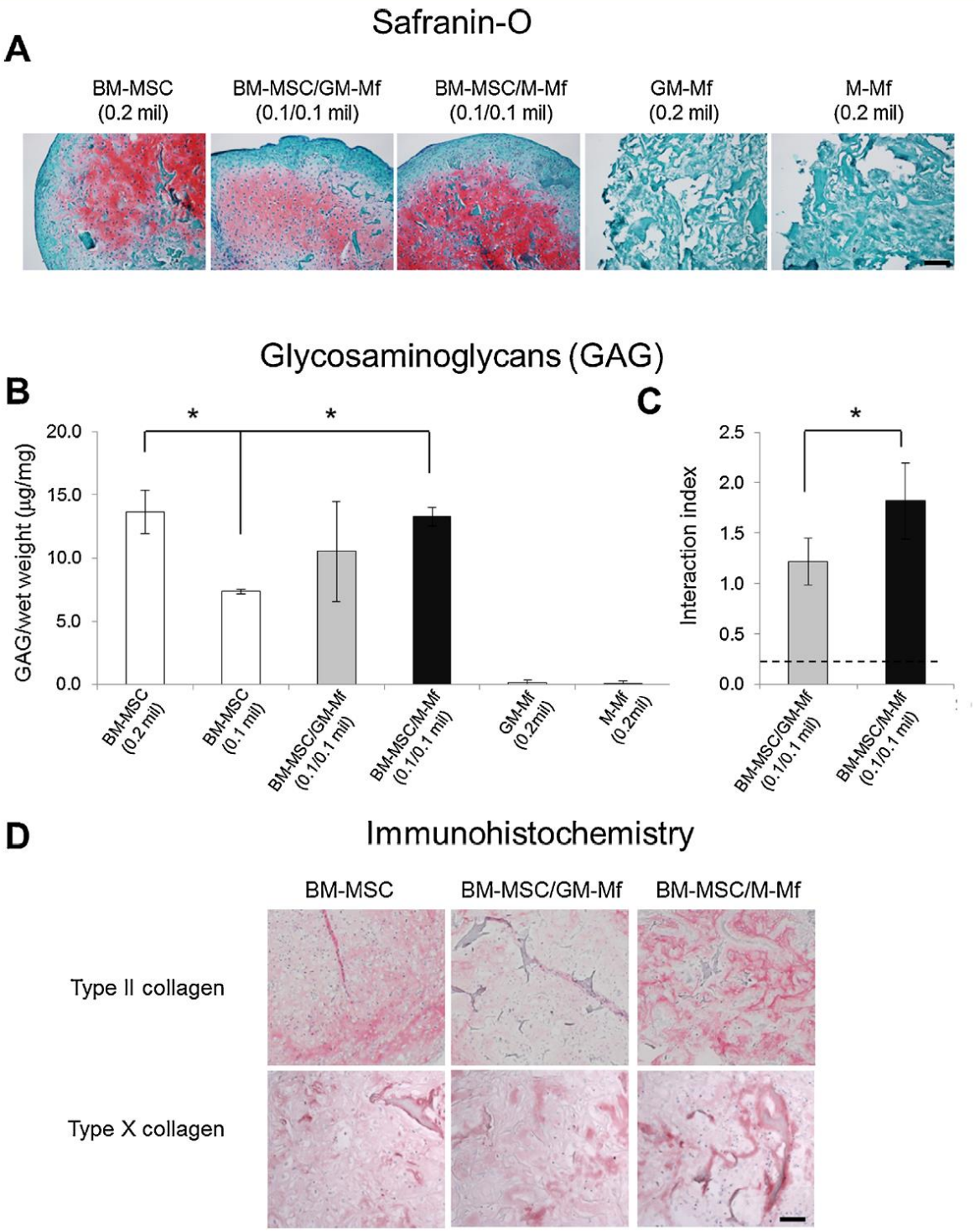

Fig. 1. Interaction between human bone marrow mesenchymal stem/stromal cells (**BM-MSC**) and **GM-Mf** or **M-Mf** macrophages in collagen sponges. **A:** Safranin-O staining of representative tissues generated culturing 2×10^5 (0.2 mil) **BM-MSC, GM-Mf, M-Mf** in collagen sponges alone or in combinations (0.1/0.1 mil) for 3 weeks with chondrogenic medium. Bar = 100 µm. **B:** Glycosaminoglycan (**GAG**) content normalized to the wet weight of monoculture and coculture constructs and corresponding interaction index values (calculated as described in the Materials and Methods Section). Dotted line represents the mean interaction index values calculated in one experiment in which **BM-MSC** were cultured with skin fibroblasts (**C**). Values are mean ± SD of five independent experiments. Asterisks (*) indicate statistically significant differences between the experimental groups. **D:** Type **II** collagen and type **X** collagen immunohistochemical stainings of representative monoculture (**BM-MSC**) and coculture (**BM-MSC/GM-Mf** and **BM-MSC/M-Mf**) constructs. Bar = 100 µm.

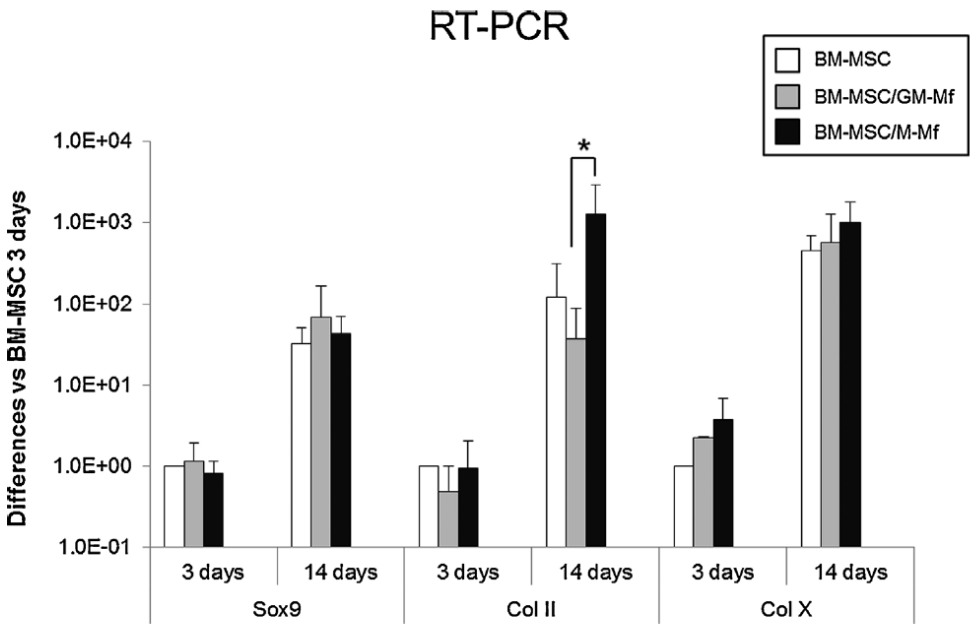

Fig. 2. Real time RT-PCR analyses carried out using specific primers for Sox9, type II collagen (Col II) and type X collagen (Col X) on monoculture (BM-MSC) and coculture (BM-MSC/GM-Mf and BM-MSC/M-Mf) constructs cultured for 3 and 14 days in chondrogenic medium. Levels are normalized to glyceraldehyde 3-phosphate (GAPDH) and expressed as fold differences as compared to cultured BM-MSC constructs at day 3. Values are mean ± SD of three independent experiments. Asterisks (*) indicate statistically significant differences between the experimental groups.

multiplied by the total number of viable cells obtained from hemocytometer counts. The results were normalized by the corresponding cell number that was initially seeded onto the collagen sponge.

Histology and immunohistochemistry

After in vitro and in vivo cultures, the constructs were fixed in 4% formalin, if necessary decalcified with 7% EDTA solution (Sigma) and embedded in paraffin. Sections (5 μm thick) were stained with Safranin-O for sulfated glycosaminoglycans (GAG) (Barbero et al., 2004).

Sections were processed for immuno-histochemistry using antibodies against type II collagen (MPBiomedicals, Illkirch, France), type X collagen (Abcam, Cambridge, UK) or bone sialoprotein (BSP, Immundiagnostik, Bensheim, Germany) as previously described (Scotti et al., 2010).

Microtomography

After explantation, constructs were rinsed with PBS, fixed in 4% formalin, then stored in PBS. Microtomography data were acquired using a Phoenix Nanotom M scanner (General Electric, Fairfield, CT) with 0.5 mm aluminum filtered X-rays (applied voltage 70 kV; current 260 μA). Transmission images were done during a 360° scan rotation with an incremental rotation step size of 0.25°. Reconstruction was made using a modified Feldkamp algorithm at an isotropic voxel size of 2.5 μm. Threshold-based segmentation and 3D measurement analyses (mineral density and volume) were performed using the ImageJ software (Rasband, W.S., U. S. National Institutes of Health, Bethesda, MD) with the BoneJ (Doube et al., 2010) and 3D Shape (Sheets et al., 2013) extensions.

Statistical analysis

In this study, all values are presented as mean and standard deviation of measurements from at least three independent experiments. Statistical analysis was performed using two-tailed unpaired *t*-test or the non-parametric Mann–Whitney *U*-test, after assessing the normality of distribution of the collected data by means of Prism® software (GraphPad Software, La Jolla, CA). One-way analysis of variance (ANOVA), in combination with a Tukey's range post-hoc test, was used when comparing more than two groups. Values of $P < 0.05$ were considered significant.

Results

Phenotypic characterization of monocytes cultured with GM-CSF or M-CSF

Phenotyping by flow cytometry indicated that monocytes differentiated with GM-CSF resulted in Mf with high expression levels of CD16 and CD32, whereas monocytes cultured with M-CSF had high expression levels of CD163 and CD204. RT-PCR results showed that GM-Mf, as compared to M-Mf, expressed higher levels of the inflammatory cytokines IL-6 and TNF-α (9.5- and 10.4-fold, respectively), and lower levels of the anti-inflammatory cytokines IL-4 and IL-10 (54.4- and 7.8-fold, respectively; Table 1). These results confirm the pro-inflammatory M1 traits of the GM-Mf and the anti-inflammatory M2 traits of the M-Mf generated in vitro.

3D culture in type I collagen sponges

Mono- and cocultures of BM-MSC and Mf were performed to determine the respective tissue forming capacities and possible synergistic effects in vitro. For such investigation type I collagen

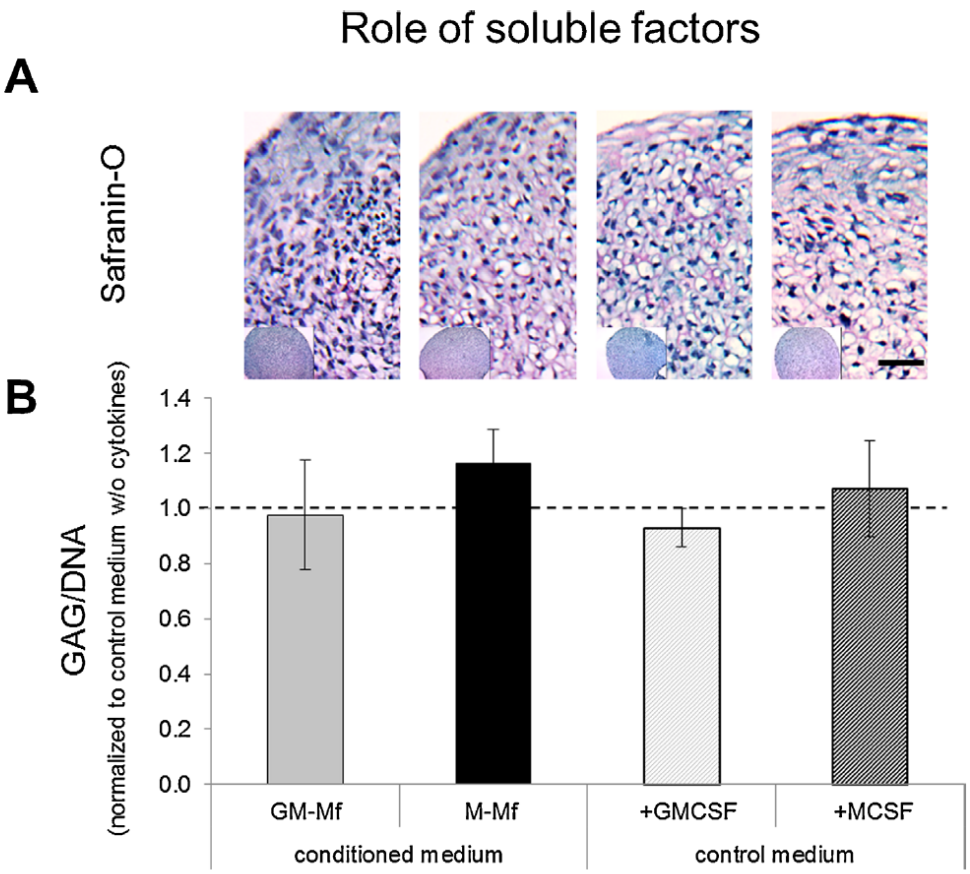

Fig. 3. Effects of soluble factors released by GM-Mf and M-Mf on the chondrogenic capacity of BM-MSC. A: Safranin-O staining of representative pellets generated culturing BM-MSC for 3 weeks with chondrogenic medium supplemented with GM-Mf conditioned medium (GM-Mf), M-Mf conditioned medium (M-Mf), medium containing 50 ng/ml of macrophage colony-stimulating factor (M-CSF) or 50 ng/ml granulocyte-macrophage colony-stimulating factor (GM-CSF). Bar = 100 μm. The inserts are low magnification images of the entire pellets. B: Glycosaminoglycan (GAG) content normalized to DNA amounts in the pellets. Levels are normalized to the GAG contents of BM-MSC pellets cultured in control medium (chondrogenic medium without cytokines). Values are mean ± SD of three independent experiments.

sponges were used in order to enable efficient retention and uniform distribution of the two cell types. BM-MSC cultured for 21 days in chondrogenic medium on type I collagen sponges, alone or in combination with Mf, formed cartilaginous tissues rich in GAG. Intensity and uniformity of Safranin-O staining was similar in the groups BM-MSC (0.2 mil) and BM-MSC/M-Mf, while slightly reduced in the group BM-MSC/GM-Mf. In contrast, tissues generated by GM-Mf or M-Mf in monoculture had fibrotic/necrotic appearances and were negative for Safranin-O staining (Fig. 1A). Biochemical analyses showed that the GAG content of BM-MSC/M-Mf constructs was similar to that of BM-MSC (0.2 mil) constructs, initially containing twice as many BM-MSC, and 1.8-fold ($P < 0.05$) higher than that of BM-MSC (0.1 mil) constructs with the same initial number of BM-MSC. The GAG content of BM-MSC/M-Mf was on average higher than that of BM-MSC/GM-Mf, but the difference was not statistically significant, whereas GM-Mf and M-Mf monoculture constructs had GAG contents close to the limit of detection (Fig. 1B). In order to quantitatively assess the potential *chondro-induction* of macrophages on BM-MSC, the interaction indexes were calculated (see Materials and Methods Section). The interaction index for BM-MSC/M-Mf (1.82 ± 0.38) was significantly higher than one indicating a chondro-inductive effect of M-Mf on BM-MSC. The interaction index for BM-MSC/GM-Mf (1.22 ± 0.24) was instead not significantly higher than one (Fig. 1C). In the experimental setup where macrophages were replaced by skin fibroblasts in the coculture model, the interaction index was drastically lower than in constructs containing macrophages (0.25 ± 0.05). These results highlight the sensitivity of our coculture system and the specificity of the macrophage phenotype for chondro-induction.

Immunohistochemical analyses showed that type II collagen staining intensity was higher in BM-MSC and BM-MSC/M-Mf constructs as compared to BM-MSC/GM-Mf constructs while type X collagen staining intensity was similar in all the groups (Fig. 1D). RT-PCR analyses of constructs from different culture time points indicated that on day 3, Sox9, type II collagen and type X collagen were similarly expressed in BM-MSC monoculture and coculture. Expression levels of Sox9 and type X collagen increased from 3 to 14 days culture to similar extents in the different groups. Instead, the expression levels of type II collagen increased more pronouncedly in the BM-MSC/M-Mf constructs (1,350-fold), as compared to the BM-MSC or BM-MSC/GM-Mf constructs (120- and 77-fold, respectively), so that at the latest time point higher type II collagen expression was detected in BM-MSC/M-Mf constructs (Fig. 2).

Overall our results indicate that only the coculture of BM-MSC with M-Mf resulted in a statistically significant and reproducible chondro-inductive effect. The increasing expression of type X collagen in monoculture and in both

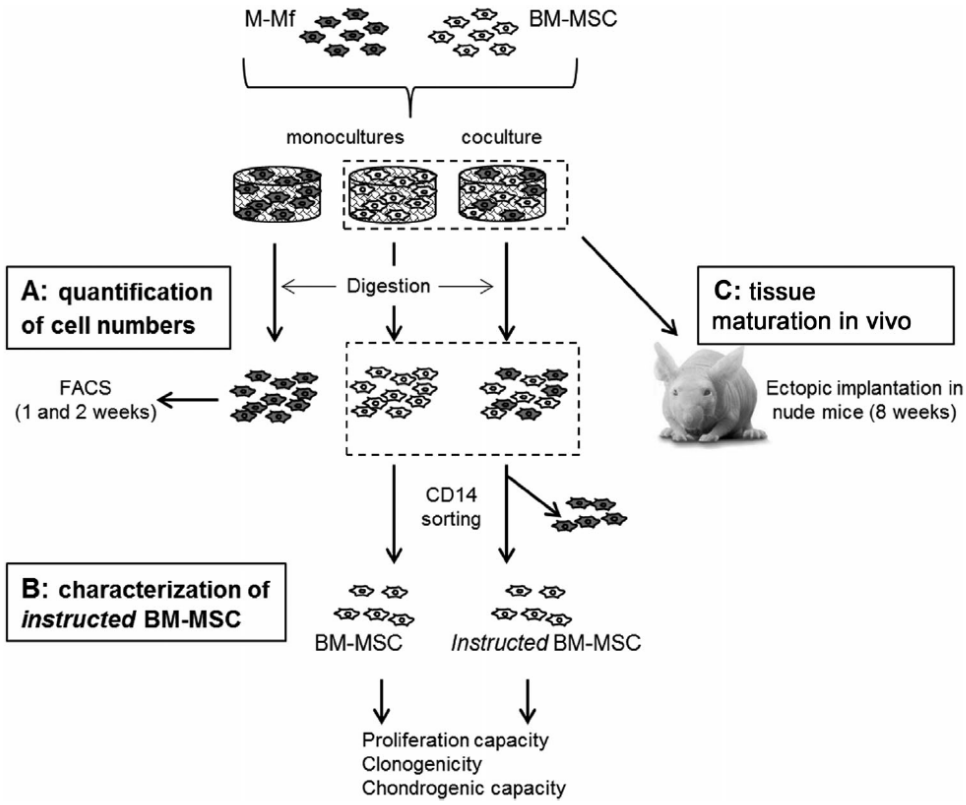

Fig. 4. Design of the experiments performed to investigate the cellular mechanisms leading to *chondro-induction* (A,B) and the maturation of the monoculture and coculture tissues in an ectopic in vivo environment (C). A: Constructs were enzymatically digested and resulting cells were analysed by flow cytometry to quantify the numbers of BM-MSC and M-Mf. B: BM-MSC released from the monoculture or coculture constructs (BM-MSC and *Instructed* BM-MSC respectively) were further cultured in 2D dishes in complete medium or at high density in chondrogenic medium to estimate their proliferation capacity and clonogenicity or chondrogenic capacity respectively. C: Monoculture and coculture constructs were implanted ectopically in nude mice and resulting tissue was analysed to assess cartilage maturation.

coculture groups indicate that macrophages do not modulate the hypertrophic commitment of BM-MSC.

Culture in pellets with macrophage-conditioned media

To address whether soluble factors released by base line M-Mf and GM-Mf could modulate the chondrogenic differentiation of BM-MSC, BM-MSC were cultured as pellets (system typically used to investigate MSC chondrogenesis in response to exogenous soluble factors), in conditioned media from M-Mf and GM-Mf or control media containing recombinant GM-CSF and M-CSF. After 2 weeks of culture, pellets from the different groups displayed similar histological features. The GAG/DNA ratios of pellets cultured in the conditioned media were not significantly different from those in the respective control media (Fig. 3). This finding indicates that the chondrogenesis of BM-MSC was not modulated by factors released by GM-Mf or M-Mf.

Based on the previous results, GM-Mf were not considered further in this study and coculture of BM-MSC and M-Mf in collagen sponges was used to further characterize their interactions according to the layout presented in Figure 4.

Quantification of cell numbers in 3D

In order to assess the differences in relative cell numbers during coculture, BM-MSC and M-Mf were cultured for 7 or 14 days alone or in a 1:1 ratio in 3D collagen sponges. Monoculture and coculture constructs were then digested and the released cells counted and analysed by flow cytometry to distinguish the two cell types based on CD45 and CD73 surface marker expression (Fig. 4A). We observed that the number of BM-MSC in the monoculture constructs markedly decreased (2.3-fold, $P < 0.05$) in the first week and further diminished (1.7-fold, $P > 0.05$) in the second week. In contrast, the number of BM-MSC in the coculture constructs remained almost unchanged in the first week of culture and halved only in the second week of culture. Consequently, the number of BM-MSC present in the first and second week of coculture was respectively twofold ($P < 0.05$) and 1.5-fold ($P > 0.05$) higher as in the monocoltures (Fig. 5A). M-Mf cultured alone were undetectable already after 1 week, whereas they remained present at low amounts (13.7% and 2.2% of the initial number after 1 and 2 weeks, respectively) in the coculture constructs (Fig. 5B).

Clonogenic and chondrogenic capacity of *Instructed* BM-MSC

We then assessed whether short time 3D culture with M-Mf influences the properties of BM-MSC. After 1 week of chondrogenic differentiation, monoculture and coculture constructs were digested and cell suspensions deprived from CD14+ cells, as confirmed by flow cytometry (more than 99% efficiency). BM-MSC previously cultured alone or with M-Mf (here referred to as *Instructed* BM-MSC) were assayed for

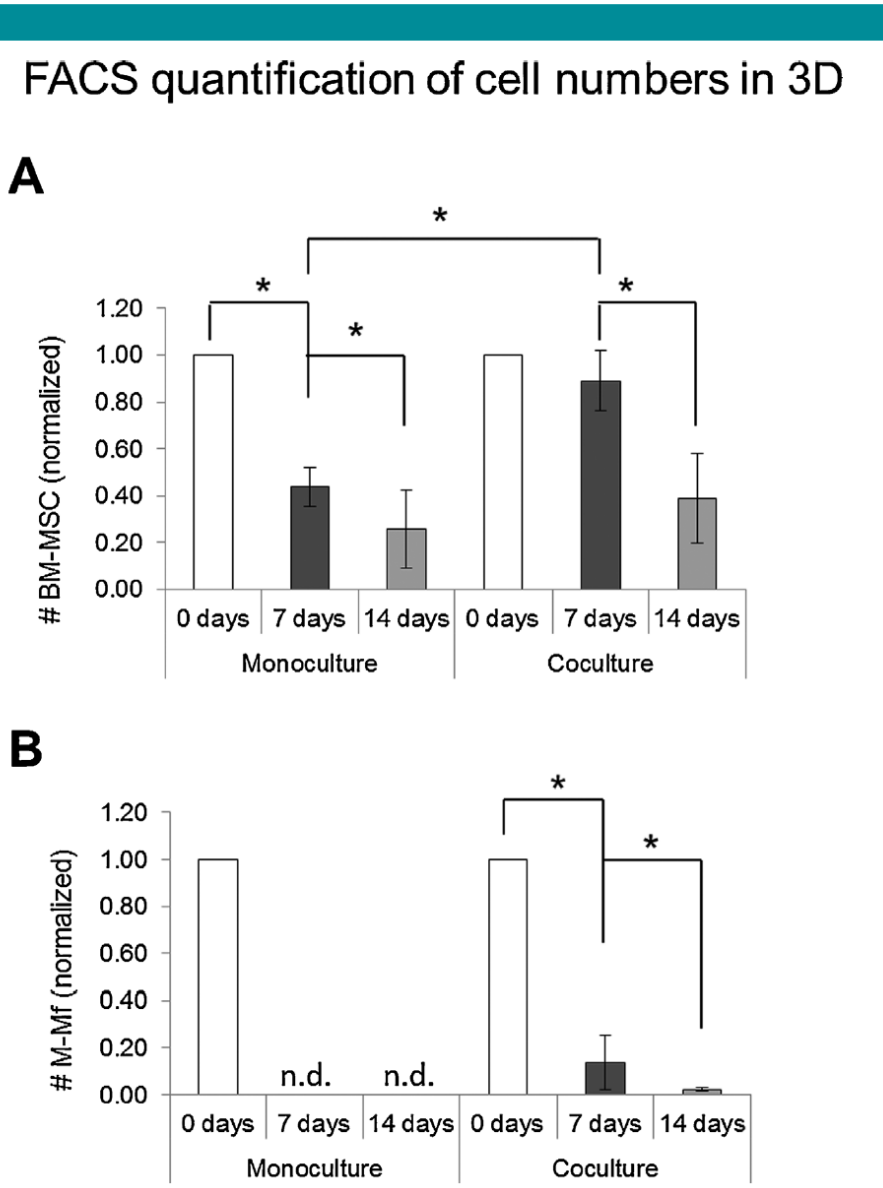

Fig. 5. Modulation of the numbers of BM-MSC and M-Mf during chondrogenic coculture in collagen sponges (see Fig. 4A). Number of BM-MSC (CD45-/CD73+/CFSE- cells) (A) and of M-Mf (CD45+/CD73-/CFSE+ cells) (B) estimated after the digestion of monoculture and coculture constructs at different time points (7 and 14 days). Counts were normalized to the initial number of cells (day 0). Values are mean ± SD of five independent experiments. Asterisks (*) indicate statistically significant differences between the experimental groups. n.d.: under the limit of detection.

proliferation rate, clonogenic potential and chondrogenic capacity (Fig.4B). As compared to BM-MSC, *Instructed* BM-MSC proliferated at a similar rate (2.65 ± 0.22 and 2.71 ± 0.24 doublings in 10 days, $P > 0.05$) but *Instructed* BM-MSC had a 36% higher clonogenicity (CFU-F = 5.9 ± 1.0% vs. 8.2 ± 0.9%, $P < 0.05$; Fig. 6A,B). Tissues generated by *Instructed* BM-MSC after additional 3 weeks of chondrogenic culture in collagen sponges were more intensely and uniformly stained for Safranin-O and contained more GAG as compared to those generated by BM-MSC (39.1 ± 8.2 vs. 24.4 ± 7.1 μg GAG/mg tissue, $P < 0.05$ and 39.1 ± 8.2 vs. 26.1 ± 4.4 μg GAG/μg DNA, $P < 0.05$) (Fig. 6C,D).

Collectively, these results indicate that coculture of BM-MSC with M-Mf in collagen sponges results in enhanced survival of the BM-MSC subpopulation and maintenance of higher clonogenic and chondrogenic capacities.

In vivo tissue maturation

We further explored the capacity of monoculture and coculture tissues to mature in an in vivo environment (Fig. 4C). Since constructs contained considerable numbers of BM-MSC and M-Mf after 1 week of pre-culture, cartilaginous tissues from this time point were selected for ectopic implantation in nude mice. Constructs from both experimental groups underwent a hypertrophic maturation process, as evidenced by the presence of large cells with typical appearance of hypertrophic chondrocytes and the abundant accumulation of type X collagen and BSP in the extracellular matrix (Fig. 7A). Qualitative and quantitative analysis of microtomography reconstructions showed non-statistically significant differences in the volume of calcified tissue, predominantly derived from mineralized hypertrophic cartilage (Fig. 7B,C).

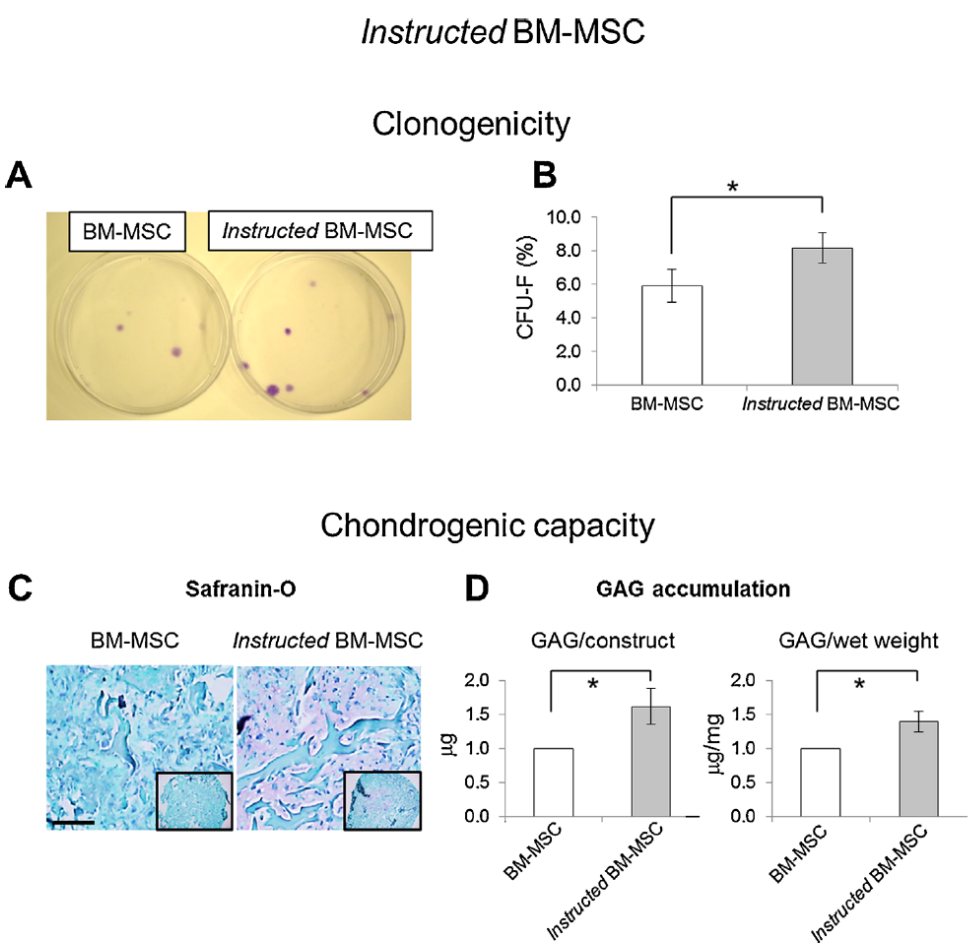

Fig. 6. Characterization of BM-MSC isolated from monoculture (BM-MSC) and coculture (*Instructed* BM-MSC) at day 7 (see Fig. 4B). A: Representative methylene blue staining of colonies derived from culturing BM-MSC and *Instructed*-BMSC at low density (4 cells/cm^2). B: Quantification of the number of colonies (CFU-F). Counts are expressed as percentage of the initial number of seeded cells. Values are mean ± SD of three independent experiments. Asterisks (*) indicate statistically significant differences between the experimental groups. C: Safranin-O staining of representative tissues generated by BM-MSC or *Instructed* BM-MSC in collagen sponges with chondrogenic medium for 3 weeks. Bar = 100 µm. The inserts are low magnification images of the constructs. D: Glycosaminoglycan (GAG) content per construct or normalized to wet weigh of the corresponding tissues. Levels are normalized to the BM-MSC group. Values are mean ± SD of three independent experiments. Asterisks (*) indicate statistically significant differences between the experimental groups.

Altogether, these results suggest that M-Mf do not modulate the in vivo maturation of the cartilage templates.

Discussion

In this study we have shown that coculture of BM-MSC with monocytes polarized towards a tissue-repair but not towards an inflammatory phenotype consistently had a synergistic effect on cartilage tissue formation, here defined as chondro-induction, which is not mediated by soluble factors. The direct coculture of M-Mf and BM-MSC supported mutual cell survival. Additionally, BM-MSC instructed by previous coculture with M-Mf better maintained progenitor properties than BM-MSC cultured alone, as shown by increased clonogenic potential and chondrogenic capacity. The hypertrophic maturation was not influenced by the presence of M-Mf, as could be seen from a comparable production of type X collagen for BM-MSC and BM-MSC/M-Mf constructs and a similar extent of cartilage mineralization following ectopic in vivo implantation.

We investigated the interaction between macrophages and BM-MSC in three-dimensional collagen sponges, which have the advantage to provide a more physiological environment than regular culture dishes. Indeed Bartneck et al. (2012) clearly showed how the transcriptome, cytokine release and surface marker expression of monocytes differed if these cells were cultured in 2D surfaces or in 3D meshes.

The choice not to use terminally polarized M1 and M2 macrophages, as upon stimulation with IFN-gamma or IL-4, respectively (Martinez et al., 2006; Murray et al., 2014), was motivated by our intention to mimic the stimulation of macrophages that come in contact with MSC following microfracture where the aforementioned T cell-derived cytokines might not be present.

Our results showing that the interaction index was >1 but highly variable for the coculture of BM-MSC/GM-Mf could be explained by an incompletely differentiated inflammatory phenotype of macrophages generated using solely GM-CSF. In fact these macrophages still expressed the anti-inflammatory cytokines IL-4 and IL-10, even if at low levels. It is also important to consider that during the coculture phase, Mf are exposed to cues from BM-MSC known to affect macrophage properties (Nemeth et al., 2009; Maggini et al., 2010; Ylostalo

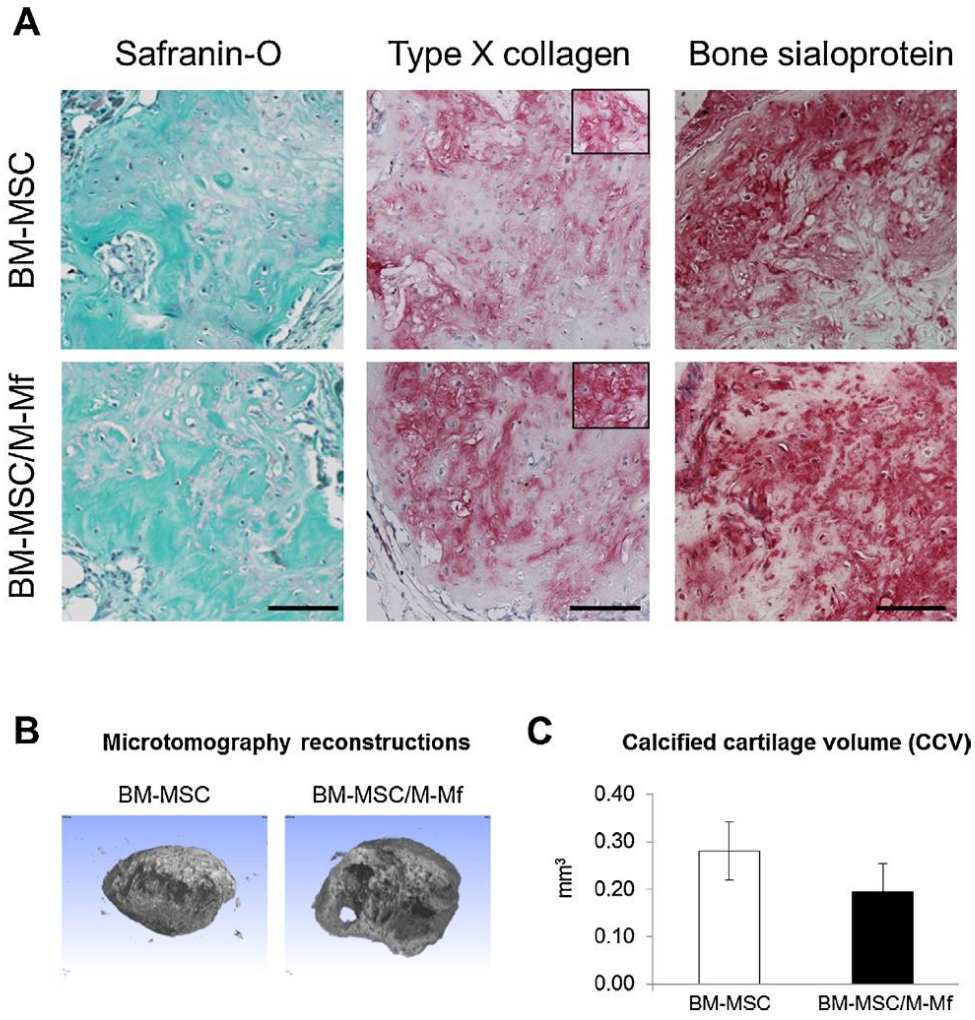

Fig. 7. Characterization of the monoculture (BM-MSC) and coculture (BM-MSC/M-Mf) constructs following 8 weeks ectopic in vivo implantation (see Fig. 4C). A: Representative Safranin O staining, type X collagen and bone sialoprotein immunohistochemical staining of explants. Bar = 100 μm. B: Microtomography reconstructions of representative constructs. C: Quantitative histomorphometric data (N = 4) of calcified cartilage volume/construct or normalized to total tissue volume of constructs (N = 4) of explants.

et al., 2012) that thus may have altered the initially acquired polarization status of the still plastic GM-Mf. Further studies are therefore required to establish a possible correspondence between the generated Mf populations and those that are typically recruited in the sites of microfractured cartilage defects.

We showed that Mf conditioned media did not influence the cartilage forming capacity of BM-MSC. However, we cannot exclude that specific factors released by Mf may modulate chondrogenesis of BM-MSC. It is possible that the concentration of soluble factors within the conditioned media used in our experimental conditions was too low to influence BM-MSC function. Contrarily to our results, Fahy et al. (2014) recently showed that conditioned medium from M1- or M2-polarized Mf differentially modulate the expression of the chondrogenic genes type II collagen and aggrecan. In this study, however, the stimulation with conditioned media was done in chondrogenic BM-MSC (i.e., cells previously cultured for 2 weeks in chondrogenic medium) and for a rather short time (i.e., 3 days). Thus, in contrast to our study, in that experimental model it was not possible to detect possible effects of Mf in the accumulation of cartilage-specific proteins.

Our results suggest that *chondro-induction* is mediated by the M-Mf-driven enhancement of the survival of cartilage-competent BM-MSC. The fact that the BM-MSC number was higher in coculture than in monoculture constructs at day 7 when still few M-Mf were present and unaffected at 14 days when almost all M-Mf were dead, suggests that, even if at low number, M-Mf might be capable to provide survival stimuli for BM-MSC. In our study, GM-Mf were not tested for their possible capacity to modulate BM-MSC number, but considering the absence of *chondro-induction* in BM-MSC/GM-Mf we expect that these pro-inflammatory macrophages are not able to provide surviving signals to BM-MSC. Our assumption is indeed corroborated by the results of Freytes et al. (2013). In their study, the authors showed that after 3 days of coculture of BM-MSC with pro- or anti-inflammatory macrophages, the fraction of CD73+ mesenchymal cells was higher in the second group. Interestingly, Freytes at al. also reported a slightly higher number of CD14+ cells in the BM-

MSC/M2 group, again confirming that coculture of BM-MSC with anti-inflammatory macrophages supported mutual cell survival.

The possibility that the few surviving M-Mf in the coculture tissues could directly contribute to cartilage formation by differentiating into chondrocytic cells is remote. Few studies reported that specific monocyte populations can acquire some chondrocyte-like traits when exposed to chondrogenic factors in 2D (Kuwana et al., 2003; Pufe et al., 2008; Raghunath et al., 2010), but the capacity of these cells to directly form a cartilage tissue has never been reported. It is therefore likely that the observed *chondro-induction* in BM-MSC/M-Mf coculture is mediated by enhanced chondrogenic properties acquired by BM-MSC, upon contact with M-Mf. This hypothesis is consistent with the higher clonogenic and cartilage forming capacity demonstrated for *Instructed*-BM-MSC.

Although future studies are required to investigate the underlying instructive signal(s), the strong and robust *chondro-induction* observed when BM-MSC were cocultured with Mf but not when BM-MSC were exposed to factors released by macrophages suggests the key role of short distance interactions. These may consist in cell communication with extracellular matrix molecules, which would provide a direct signaling via integrins (Djouad et al., 2007; Varas et al., 2007) or would bind to growth factors and cytokines, thus modulating their presentation to cells. Among the large variety of cytokines produced in BM-MSC/M-Mf coculture, IL-6 and IL-10, previously reported to modulate stemness and chondrogenic differentiation of BM-MSC (Pricola et al., 2009; Jung et al., 2013), may be involved in BM-MSC instruction.

To our knowledge, this is the first study demonstrating that coculture with macrophages can positively modulate chondrogenesis of BM-MSC. This information is complementary to convincing evidences on the positive effects of macrophages on the osteogenic differentiation of BM-MSC (Guihard et al., 2012; Nicolaidou et al., 2012; Pirraco et al., 2013).

Considering that chondrogenically differentiated BM-MSC are normally proceeding toward the hypertrophic differentiation (Pelttari et al., 2006), we investigated whether M-Mf might influence further cartilage maturation in an ectopic environment. Indeed it was shown that the number of infiltrating monocytes at the site of non-stabilised bone fractures in mice positively affected callus formation and callus remodeling (Xing et al., 2010). Under our experimental conditions, M-Mf did not modulate the in vivo evolution of the cartilaginous tissues, possibly because of their limited number in the grafts after 1 week of pre-culture. Alternatively the presence of different subpopulations of macrophages could be required to modulate cartilage maturation.

In conclusion, macrophages with anti-inflammatory and tissue repair phenotype had a chondro-inductive effect when cocultured with BM-MSC while Mf with a pro-inflammatory phenotype did not provide chondro-inductive signals. Such effect was not mediated by soluble factors alone and seems to result from the survival of BM-MSC with high chondrogenic capacity. Our results suggest that inflammatory/tissue repair Mf can improve osteochondral repair of microfractured joints not only indirectly by improving the regeneration of subchondral bone as previously reported by Hoemann et al. (2010) but also directly by enhancing the chondrogenic capacity of recruited MSC. Our findings therefore emphasise the importance of developing scaffolds capable of promoting the recruitment/polarization of anti-inflammatory and tissue-repair macrophages to enhance cartilage repair concomitantly with bone marrow stimulation. An orthotopic animal model comprising long term follow-ups (longer that those used in the study of Hoemann et al. (2010) are required to investigate whether such paradigm would lead to durable hyaline cartilage regeneration or will have to be combined with strategies enabling the stabilisation of the phenotype of the newly formed cartilage.

Acknowledgements

We are grateful to Francine Wolf for her help in the histological analyses. We would like to acknowledge the European Union (OPHIS; #FP7-NMP-2009-SMALL-3-246373) and the Fonds National de la Recherche, Luxembourg (# 4090751) for financial support.

Literature Cited

Acharya C, Adesida A, Zajac P, Mumme M, Riesle J, Martin I, Barbero A. 2012. Enhanced chondrocyte proliferation and mesenchymal stromal cells chondrogenesis in coculture pellets mediate improved cartilage formation. J Cell Physiol 227:88–97.

Barbero A, Grogan S, Schafer D, Heberer M, Mainil-Varlet P, Martin I. 2004. Age related changes in human articular chondrocyte yield, proliferation and post-expansion chondrogenic capacity. Osteoarthritis Cartilage 12:476–484.

Barbero A, Ploegert S, Heberer M, Martin I. 2003. Plasticity of clonal populations of dedifferentiated adult human articular chondrocytes. Arthritis Rheum 48:1315–1325.

Barbosa I, Garcia S, Barbier-Chassefiere V, Caruelle JP, Martelly I, Papy-Garcia D. 2003. Improved and simple micro assay for sulfated glycosaminoglycans quantification in biological extracts and its use in skin and muscle tissue studies. Glycobiology 13:647–653.

Bartneck M, Heffels KH, Pan Y, Bovi M, Zwadlo-Klarwasser G, Groll J. 2012. Inducing healing-like human primary macrophage phenotypes by 3D hydrogel coated nanofibres. Biomaterials 33:4136–4146.

Bocelli-Tyndall C, Barbero A, Candrian C, Ceredig R, Tyndall A, Martin I. 2006. Human articular chondrocytes suppress in vitro proliferation of anti-CD3 activated peripheral blood mononuclear cells. J Cell Physiol 209:732–734.

Braccini A, Wendt D, Jaquiery C, Jakob M, Heberer M, Kenins L, Wodnar-Filipowicz A, Quarto R, Martin I. 2005. Three-dimensional perfusion culture of human bone marrow cells and generation of osteoinductive grafts. Stem Cells 23:1066–1072.

Chung JY, Lee DH, Kim TH, Kwack KS, Yoon KH, Min BH. 2014. Cartilage extra-cellular matrix biomembrane for the enhancement of microfractured defects. Knee Surg Sports Traumatol Arthrosc 22:1249–1259.

Djouad F, Delorme B, Maurice M, Bony C, Apparailly F, Louis-Plence P, Canovas F, Charbord P, Noel D, Jorgensen C. 2007. Microenvironmental changes during differentiation of mesenchymal stem cells towards chondrocytes. Arthritis Res Ther 9:R33.

Doube M, Klosowski MM, Arganda-Carreras I, Cordelieres FP, Dougherty RP, Jackson JS, Schmid B, Hutchinson JR, Shefelbine SJ. 2010. BoneJ: Free and extensible bone image analysis in ImageJ. Bone 47:1076–1079.

Fahy N, de Vries-van Melle, Lehmann ML, Wei J, Grotenhuis W, Farrell N, van der Kraan E, Murphy PM, Bastiaansen-Jenniskens JM, van Osch YM. 2014. Human osteoarthritic synovium impacts chondrogenic differentiation of mesenchymal stem cells via macrophage polarisation state. Osteoarthritis Cartilage 22:1167–1175.

Francioli SE, Martin I, Sie CP, Hagg R, Tommasini R, Candrian C, Heberer M, Barbero A. 2007. Growth factors for clinical-scale expansion of human articular chondrocytes: Relevance for automated bioreactor systems. Tissue Eng 13:1227–1234.

Frank O, Heim M, Jakob M, Barbero A, Schafer D, Bendik I, Dick W, Heberer M, Martin I. 2002. Real-time quantitative RT-PCR analysis of human bone marrow stromal cells during osteogenic differentiation in vitro. J Cell Biochem 85:737–746.

Freytes DO, Kang JW, Marcos-Campos I, Vunjak-Novakovic G. 2013. Macrophages modulate the viability and growth of human mesenchymal stem cells. J Cell Biochem 114:220–229.

Gelber AC, Hochberg MC, Mead LA, Wang NY, Wigley FM, Klag MJ. 2000. Joint injury in young adults and risk for subsequent knee and hip osteoarthritis. Ann Intern Med 133:321–328.

Gille J, Meisner U, Ehlers EM, Muller A, Russlies M, Behrens P. 2005. Migration pattern, morphology and viability of cells suspended in or sealed with fibrin glue: A histomorphologic study. Tissue Cell 37:339–348.

Godwin JW, Pinto AR, Rosenthal NA. 2013. Macrophages are required for adult salamander limb regeneration. Proc Natl Acad Sci USA 110:9415–9420.

Guihard P, Danger Y, Brounais B, David E, Brion R, Delecrin J, Richards CD, Chevalier S, Redini F, Heymann D, Gascan H, Blanchard F. 2012. Induction of osteogenesis in mesenchymal stem cells by activated monocytes/macrophages depends on oncostatin M signaling. Stem Cells 30:762–772.

Hoemann CD, Chen G, Marchand C, Tran-Khanh N, Thibault M, Chevrier A, Sun J, Shive MS, Fernandes MJ, Poubelle PE, Centola M, El-Gabalawy H. 2010. Scaffold-guided subchondral bone repair: Implication of neutrophils and alternatively activated arginase-1+ macrophages. Am J Sports Med 38:1845–1856.

Jung YK, Kim GW, Park HR, Lee EJ, Choi JY, Beier F, Han SW. 2013. Role of interleukin-10 in endochondral bone formation in mice: Anabolic effect via the bone morphogenetic protein/Smad pathway. Arthritis Rheum 65:3153–3164.

Kalson NS, Gikas PD, Briggs TW. 2010. Current strategies for knee cartilage repair. Int J Clin Pract 64:1444–1452.

Knutsen G, Drogset JO, Engebretsen L, Grontvedt T, Isaksen V, Ludvigsen TC, Roberts S, Solheim E, Strand T, Johansen O. 2007. A randomized trial comparing autologous chondrocyte implantation with microfracture. Findings at five years. J Bone Joint Surg Am 89:2105–2112.

Kuwana M, Okazaki Y, Kodama H, Izumi K, Yasuoka H, Ogawa Y, Kawakami Y, Ikeda Y. 2003. Human circulating CD14+ monocytes as a source of progenitors that exhibit mesenchymal cell differentiation. J Leukoc Biol 74:833–845.

Maggini J, Mirkin G, Bognanni I, Holmberg J, Piazzon IM, Nepomnaschy I, Costa H, Canones C, Raiden S, Vermeulen M, Geffner JR. 2010. Mouse bone marrow-derived mesenchymal stromal cells turn activated macrophages into a regulatory-like profile. PLoS ONE 5:9252.

Martinez FO, Gordon S, Locati M, Mantovani A. 2006. Transcriptional profiling of the human monocyte-to-macrophage differentiation and polarization: New molecules and patterns of gene expression. J Immunol 177:7303–7311.

Messner K, Maletius W. 1996. The long-term prognosis for severe damage to weight-bearing cartilage in the knee: A 14-year clinical and radiographic follow-up in 28 young athletes. Acta Orthop Scand 67:165–168.
Mosser DM, Edwards JP. 2008. Exploring the full spectrum of macrophage activation. Nat Rev Immunol 8:958–969.
Murray PJ, Allen JE, Biswas SK, Fisher EA, Gilroy DW, Goerdt S, Gordon S, Hamilton JA, Ivashkiv LB, Lawrence T, Locati M, Mantovani A, Martinez FO, Mege JL, Mosser DM, Natoli G, Saeij JP, Schultze JL, Shirey KA, Sica A, Suttles J, Udalova I, van Ginderachter JA, Vogel SN, Wynn TA. 2014. Macrophage activation and polarization: Nomenclature and experimental guidelines. Immunity 41:14–20.
Nemeth K, Leelahavanichkul A, Yuen PS, Mayer B, Parmelee A, Doi K, Robey PG, Leelahavanichkul K, Koller BH, Brown JM, Hu X, Jelinek I, Star RA, Mezey E. 2009. Bone marrow stromal cells attenuate sepsis via prostaglandin E(2)-dependent reprogramming of host macrophages to increase their interleukin-10 production. Nat Med 15:42–49.
Nicolaidou V, Wong MM, Redpath AN, Ersek A, Baban DF, Williams LM, Cope AP, Horwood NJ. 2012. Monocytes induce STAT3 activation in human mesenchymal stem cells to promote osteoblast formation. PLoS ONE 7:39871.
Park JE, Barbul A. 2004. Understanding the role of immune regulation in wound healing. Am J Surg 187:11S–16S.
Pelttari K, Winter A, Steck E, Goetzke K, Hennig T, Ochs BG, Aigner T, Richter W. 2006. Premature induction of hypertrophy during in vitro chondrogenesis of human mesenchymal stem cells correlates with calcification and vascular invasion after ectopic transplantation in SCID mice. Arthritis Rheum 54:3254–3266.
Pirraco RP, Reis RL, Marques AP. 2013. Effect of monocytes/macrophages on the early osteogenic differentiation of hBMSCs. J Tissue Eng Regen Med 7:392–400.
Pricola KL, Kuhn NZ, Haleem-Smith H, Song Y, Tuan RS. 2009. Interleukin-6 maintains bone marrow-derived mesenchymal stem cell stemness by an ERK1/2-dependent mechanism. J Cell Biochem 108:577–588.
Pufe T, Petersen W, Fandrich F, Varoga D, Wruck CJ, Mentlein R, Helfenstein A, Hoseas D, Dressel S, Tillmann B, Ruhnke M. 2008. Programmable cells of monocytic origin (PCMO): A source of peripheral blood stem cells that generate collagen type II-producing chondrocytes. J Orthop Res 26:304–313.
Raghunath J, Sutherland J, Salih V, Mordan N, Butler PE, Seifalian AM. 2010. Chondrogenic potential of blood-acquired mesenchymal progenitor cells. J Plast Reconstr Aesthet Surg 63:841–847.
Ruffell D, Mourkioti F, Gambardella A, Kirstetter P, Lopez RG, Rosenthal N, Nerlov C. 2009. A CREB-C/EBPbeta cascade induces M2 macrophage-specific gene expression and promotes muscle injury repair. Proc Natl Acad Sci USA 106:17475–17480.
Saris DB, Vanlauwe J, Victor J, Haspl M, Bohnsack M, Fortems Y, Vandekerckhove B, Almqvist KF, Claes T, Handelberg F, Lagae K, van der Bauwhede J, Vandenneucker H, Yang KG, Jelic M, Verdonk R, Veulemans N, Bellemans J, Luyten FP. 2008. Characterized chondrocyte implantation results in better structural repair when treating symptomatic cartilage defects of the knee in a randomized controlled trial versus microfracture. Am J Sports Med 36:235–246.
Scotti C, Tonnarelli B, Papadimitropoulos A, Scherberich A, Schaeren S, Schauerte A, Lopez-Rios J, Zeller R, Barbero A, Martin I. 2010. Recapitulation of endochondral bone formation using human adult mesenchymal stem cells as a paradigm for developmental engineering. Proc Natl Acad Sci USA 107:7251–7256.
Sheets KG, Jun B, Zhou Y, Zhu M, Petasis NA, Gordon WC, Bazan NG. 2013. Microglial ramification and redistribution concomitant with the attenuation of choroidal neovascularization by neuroprotectin D1. Mol Vis 19:1747–1759.
Tidball JG, Wehling-Henricks M. 2007. Macrophages promote muscle membrane repair and muscle fibre growth and regeneration during modified muscle loading in mice in vivo. J Physiol 578:327–336.
Varas L, Ohlsson LB, Honeth G, Olsson A, Bengtsson T, Wiberg C, Bockermann R, Jarnum S, Richter J, Pennington D, Johnstone B, Lundgren-Akerlund E, Kjellman C. 2007. Alpha10 integrin expression is up-regulated on fibroblast growth factor-2-treated mesenchymal stem cells with improved chondrogenic differentiation potential. Stem Cells Dev 16:965–978.
Wynn TA, Chawla A, Pollard JW. 2013. Macrophage biology in development, homeostasis and disease. Nature 496:445–455.
Xing Z, Lu C, Hu D, Yu YY, Wang X, Colnot C, Nakamura M, Wu Y, Miclau T, Marcucio RS. 2010. Multiple roles for CCR2 during fracture healing. Dis Model Mech 3:451–458.
Xue J, Schmidt SV, Sander J, Draffehn A, Krebs W, Quester I, De ND Gohel, Emde M, Schmidleithner L, Ganesan H, Nino-Castro A, Mallmann MR, Labzin L, Theis H, Kraut M, Beyer M, Latz E, Freeman TC, Ulas T, Schultze JL. 2014. Transcriptome-based network analysis reveals a spectrum model of human macrophage activation. Immunity 40:274–288.
Ylostalo JH, Bartosh TJ, Coble K, Prockop DJ. 2012. Human mesenchymal stem/stromal cells cultured as spheroids are self-activated to produce prostaglandin E2 that directs stimulated macrophages into an anti-inflammatory phenotype. Stem Cells 30:2283–2296.

Chapter IV.
Chondrogenic Differentiation and Collagen Synthesis of Human Chondrocytes in the Absence of Ascorbic Acid

Chondrogenic Differentiation and Collagen Synthesis of Human Chondrocytes in the Absence of Ascorbic Acid

Ralph Duhr[1*], M. Adelaide Asnaghi[1*], Helen Quasnichka[2], David Wendt[1], Wa'el Kafienah[2], Ivan Martin[1]

[1]Departments of Surgery and of Biomedicine, University Hospital Basel, University of Basel, Basel, Switzerland

[2] School of Cellular and Molecular Medicine, University of Bristol, Bristol, United Kingdom

*both authors contributed equally

Ralph Duhr: Conception and design, collection and/or assembly of data, data analysis and interpretation, manuscript writing

M. Adelaide Asnaghi: Conception and design, financial support, collection and/or assembly of data, data analysis and interpretation, manuscript writing

Helen Quasnichka: Collection and/or assembly of data, data analysis and interpretation

Wa'el Kafienah: Data analysis and interpretation, final approval of manuscript

David Wendt: Conception and design, data analysis and interpretation, final approval of manuscript

Ivan Martin: Conception and design, data analysis and interpretation, final approval of manuscript

ABSTRACT

The introduction of automation for the manufacturing of engineered cartilage will be crucial to standardize production methods and to maximize prospective scale-up and cost-effectiveness in the long-term. However, the limited stability of some bioactive supplements currently used in cartilage engineering, such as growth factors and vitamins, requires specific components to be stored at different temperatures and poses significant challenges to the automation of liquid handling. Ascorbic acid is generally considered to be a critical supplement for cartilage tissue engineering because of its role in collagen hydroxylation. Due to its instability, ascorbic acid is typically added from frozen aliquots at each medium change, preventing straightforward automation. The aim of this study was to investigate the effect of ascorbic acid on the gene expression and extracellular matrix production of human nasal chondrocytes, with special regard to collagen synthesis and hydroxylation, in order to define appropriate requirements for automation strategies. Results showed that cartilage gene expression, pellet formation, and glycosaminoglycans deposition were indistinguishable whether chondrocytes were cultured with or without ascorbic acid. Not adding ascorbic acid caused a 35% reduction of type II collagen in the matrix, whereas hydroxylation of total collagen was not significantly affected. Chondrocytes did not exhibit impaired secretion of collagens and the extracellular matrix showed a similar organization and structure of collagen fibrils in the presence and absence of ascorbic acid. In conclusion, ascorbic acid did not influence chondrogenesis except for a limited effect on collagen deposition, and could thus be omitted to simplify automated manufacturing.

INTRODUCTION

Engineered cartilage grafts have been reported in preclinical and clinical studies to be a promising treatment for the biological resurfacing of acute and chronic joint lesions (1–3). For their widespread implementation as therapeutic option, the high manufacturing expenses generally associated with cartilage tissue engineering need to be considerably decreased (4,5). In this regard, bioreactors have been suggested as suitable means allowing cost reduction by automation, standardization, and scalability (6–8). However, the straightforward automation of bioreactors for cartilage tissue engineering is considerably hindered by the complex liquid handling and storage conditions imposed by unstable compounds currently used in most chondrogenic culture medium formulations.

Ascorbic acid (AA) is a bioactive supplement, which can be rapidly oxidized to dehydroascorbic acid and further irreversibly degraded by oxidation or hydrolysis, resulting in short-time availability (9–11). Several AA derivatives with protective groups against degradation have been developed, such as the more stable but equally bioactive ascorbic acid-2-phosphate (AA2P) (12). Still, the latter is typically added from frozen aliquots at every medium exchange, which drastically complicates bioprocess automation due to the required additional freezing compartment as well as the thawing and supplementation machinery and procedures.

Besides being a notable antioxidant, AA is involved in the synthesis of collagens, amongst others type II collagen, a key protein of hyaline cartilage (13). In particular AA serves as a co-factor for the enzymes prolyl hydroxylase and lysyl hydroxlase, which are responsible for the hydroxylation of proline and lysine residues of the collagen propeptide. This hydroxylation is essential for the cross-linking of alpha peptides and collagen triple helix stability (14–16). Moreover AA is thought to induce chondrogenesis via an upregulation of collagen expression and is therefore added in

most protocols for chondrogenic differentiation (17–19). Nevertheless, it was shown that other available molecules could replace AA as a cofactor and antioxidant in cell-free systems, guinea pigs and for other prolyl-4-hydroxylase domain–containing enzymes (14,15,20–22). Additionally, the recycling of AA from dehydroascorbic acid after uptake via glucose transporter 1 was reported for chondrocytes (23,24).

The possibilities for substitution and recycling suggest that the addition of AA might not be strictly necessary for the generation of a hyaline cartilage-like extracellular matrix. We therefore hypothesized that chondrocytes can synthesize collagens with hydroxylated proline residues and produce a cartilaginous extracellular matrix rich in GAG in the absence of AA. With a better knowledge of the AA requirement of chondrocytes during *in vitro* cartilage graft manufacturing, efficient supplementation schemes can be implemented that simplify the necessary automation, while ensuring adequate product quality.

MATERIALS AND METHODS

Ascorbic acid measurements

AA2P was quantified in medium stored at 4 or 37°C for up to 14 days and in spent medium from pellet cultures using the ferric reducing ascorbate assay kit (FRASC; BioVision, Switzerland), according to the manufacturer's instructions with an additional step to be able to measure the 2-phosphate form. Briefly, to transform AA2P into measurable AA, samples were first incubated with 1 unit/100 µl of alkaline phosphatase (Sigma, Switzerland) for 10 min at 37°C. This step was omitted when measuring the medium concentration of AA molecules without a 2-phosphate group. Ascorbate oxidase or water was then added to generate the AA depleted background or the total oxidant group, respectively. After addition of the ascorbic acid reaction mix, absorbance at 593 nm was measured and the concentration of AA2P or AA was calculated from the difference of the total oxidant and the AA depleted group with the help of an AA standard curve.

Cell isolation and culture

Samples of human cartilage were collected from the nasal septum of 10 patients undergoing rhinoplasty (Mean age 37 years, range 21 – 63 years), after informed consent and in accordance with the local ethical commission (University Hospital Basel). Overlaying perichondrium was carefully removed and cartilage biopsies were digested using 0.15% collagenase II (Worthington, UK) during 22 h at 37°C as previously described (25). After digestion, cells were plated in tissue culture flasks at a density of $1x10^4$ cells/cm^2 and cultured in complete medium (CM) consisting of Dulbecco's modified Eagle's medium containing 4.5 mg/ml D-glucose and 0.1 mM nonessential amino acids (DMEM, Gibco, Life Technologies, Switzerland), 10% fetal bovine serum (FBS), 1 mM sodium pyruvate, 100 mM HEPES buffer, 100 U/ml penicillin, 100 µg/ml streptomycin, and 0.29 mg/ml L-glutamine (all from Gibco),

supplemented with 1 ng/ml transforming growth factor beta 1 and 5 ng/ml fibroblast growth factor 2 (both from R&D Systems, UK) at 37°C and 5% CO_2 in a humidified incubator (Thermo Scientific Heraeus, USA) (26). When approaching 80% confluence, cells were detached using 0.05% trypsin-EDTA (Gibco), resuspended in FBS containing 10% dimethyl sulfoxide, filled in cryovials (Sarstedt, Germany) and stored in liquid nitrogen tanks until further use.

Chondrogenic re-differentiation

Chondrocytes from frozen aliquots were expanded until passage 2 and re-differentiated by culturing $5x10^5$ cells for 2 weeks as micromass pellets, formed by centrifugation at 300x*g* in conical 1.5-ml tubes (Sarstedt), in chondrogenic serum-free medium (SFM) consisting of DMEM containing 1 mM sodium pyruvate, 100 mM HEPES buffer, 100 U/ml penicillin, 100 µg/ml streptomycin, and 0.29 mg/ml L-glutamine, 1.25 mg/ml human serum albumin, 100 nM dexamethasone (Sigma), and 10 ng/ml TGF-β1 (R&D Systems), with addition of ITS+1 (10 µg/ml insulin, 5.5 µg/ml transferrin, 5 ng/ml selenium, 0.5 mg/ml bovine serum albumin, 4.7 µg/ml linoleic acid; Sigma, Switzerland), with or without 100 µM ascorbic acid 2-phosphate (Sigma) (+ AA2P / - AA2P). Chondrogenic culture medium was changed twice weekly (27). No chondrogenic induction was provided in one group, culturing pellets in the absence of ITS+1 (- AA2P - ITS). For an additional experimental group AA2P was supplemented every day after quantification to maintain a constant concentration of 100 µM (daily AA2P).

Histology and immunohistochemistry

Micromass pellets were fixed overnight in 4% formalin and embedded in paraffin. 5 µm thick sections were stained with Safranin-O for sulfated glycosaminoglycans (GAG) with hematoxylin as nuclear counterstaining (27). Immunohistochemistry

against type I and type II collagen (both from MPBiomedicals, France) was performed using the Vectastain ABC kit (Vector Labs, USA) and counterstaining with hematoxylin as previously described (28). Terminal deoxynucleotidyl transferase dUTP nick end labeling with an Alexa Fluor 647 dye (Click-iT TUNEL assay; Molecular Probes, Switzerland) was performed on formalin-fixed paraffin-embedded sections, according to the manufacturer's instructions. A positive control with DNA strand breaks was generated by 30 min incubation at room temperature with 1 unit of DNase I (Molecular Probes). Immunofluorescence staining against type II collagen was performed on OCT (CellPath, UK) embedded 10 µm thick cryosections using a mouse type II collagen primary antibody (MPBiomedicals) and a goat anti-mouse Alexa Fluor 546 secondary antibody (Invitrogen), with DAPI as a nuclear counterstain.

Quantitative RT-PCR

mRNA of chondrocytes was extracted using Quick-RNA Miniprep (Zymo Research, USA), according to the manufacturer's protocol. DNaseI (Zymo Research) was used to remove trace DNA. Isolated RNA was quantified using a NanoDrop spectrophotometer (ThermoFischer Scientific). Reverse transcription into cDNA was done from 3 µg of RNA by using 500 µg/ml random hexamers (Promega, Switzerland) and 0.5 µl of 200 UI/ml SuperScript III reverse transcriptase (Invitrogen), in the presence of dNTPs. Quantitative real-time PCR was carried out on an ABI Prism 7700 Sequence Detection System (Perkin-Elmer/Applied Biosystems, Switzerland). After initial denaturation at 95°C for 10 min, cDNA was amplified for 40 cycles, each consisting of a denaturation step at 95°C for 15 s and an annealing/extension step at 60°C for 60 s. Primers and probes for aggrecan, versican, collagen type I, collagen type II and GAPDH were used with TaqMan Gene Expression Master Mix (Applied Biosystems) as previously described (29). Assay on-

Demand (Applied Biosystems) was used to measure the expression of SOX9 (Hs00165814_m1). The threshold cycle (Ct) value of the reference gene GAPDH was subtracted from the Ct value of the gene of interest to derive ΔCt. The relative gene expression of each group normalized to the cells after expansion was calculated as $2^{-\Delta\Delta Ct}$. Each sample was assessed at least in duplicate for each gene of interest.

Biochemical analyses

Micromass pellets were digested in proteinase K (1 mg/ml proteinase K in 50 mM Tris with 1 mM EDTA, 1 mM iodoacetamide, and 10 mg/ml pepstatin A) for 16 h at 56°C. The glycosaminoglycan content of pellets was determined by spectrophotometry using dimethylmethylene blue, with chondroitin sulphate as a standard (30). The DNA content of pellets was measured using the CyQuant cell proliferation assay kit (Invitrogen), with calf thymus DNA as a standard. The amount of GAG in pellets was then normalized to the DNA content (27).

For hydroxyproline quantification, samples were processed as previously described (18,31). Briefly, proteinase K digested samples were mixed with equal amounts of 12M HCl and hydrolysed at 120°C for 24h. Specimens were then transferred into 96-well plates and left to dry before addition of acetate-citrate buffered chloramine T and incubation for 20 min at room temperature. Dimethylaminobenzaldehyde was added and the plates heated for 20 min to 60°C. Absorbance was then measured at 550nm. Concentrations were calculated with the help of a hydroxyproline (Sigma) standard curve.

Collagen quantification

Pellets were solubilized by an initial digestion in 25 µl of 2 mg/ml TPCK-treated bovine pancreatic trypsin (in 50 mM Tris HCl pH 7.5, 1 mM EDTA, 1mM iodoacatamide, 20 µg/ml Pepstatin A), for 15 h at 37 °C. A further 25 µl of freshly prepared trypsin solution was added, and digests were incubated for 2 h at 65 °C,

with intermittent vortexing. Digests were then boiled for 15 min to destroy remaining enzyme activity. The quantity of type II collagen was determined using an inhibition ELISA with a mouse IgG monoclonal antibody to denatured type II collagen (32). Type I collagen was measured by inhibition ELISA using a rabbit anti-peptide antibody to type I collagen (33).

Scanning electron microscopy

For scanning electron microscopy (SEM), pellets were fixed for 2 days in 0.1 M cacodylate-buffered 2% glutaraldehyde at pH 7.2 at 25°C, then glued onto a Teflon disc with a rapidly curing epoxy glue (Araldite; Huntsman, UK). Next the specimens were placed in a cryostat microtome to trim off the outermost, approximately 150 µm thick cartilage layer parallel to the support surface to assess the central part of the samples. In a next step, proteoglycans were extracted in 100 mM Soerensen's phosphate buffer (pH 7.2) containing 1 mg/ml bovine hyaluronidase (type I, Sigma), 1 mg/ml trypsin (type I, Sigma) and 0.01% NaN_3 at 37°C for 3 days. After dehydration in graded ethanol series and critical point drying, samples were sputter-coated with 3–5 nm platinum and examined by SEM (Hitachi S-4800 FEG, Japan), operated at 1.5–5 kV accelerating voltage in immersion mode (34,35).

Statistical analysis

Data are presented as mean and standard deviation of independent experiments with cells from at least 2 different donors. For each analysis at least 3 replicate micromass pellets were used per condition. Statistical analysis was performed with Prism software (GraphPad Software, USA) using one-way ANOVA followed by Tukey’s post hoc test for multiple comparisons. Values of $p < 0.05$ were considered statistically significant.

RESULTS

AA2P stability

In order to test the availability of AA in chondrogenic medium formulations, the stability of AA2P was assessed in stored medium with or without fetal bovine serum. Whereas in serum-free conditions the concentration of AA2P was constant over 2 weeks, both at 4°C and 37°C, the presence of serum lead to rapid AA2P degradation. AA2P appeared to be particularly unstable when stored in serum containing medium at 37°C, dropping to less than 10% of the initial concentration within 24 hours (Fig. 1A). Since AA2P was stable only in the absence of serum, we performed all following cell culture experiments in serum-free conditions. When culturing micromass pellets, the concentration of AA2P decreased by almost 50% during the first 24 hours of culture and further declined to less than 25% by day 3 (Fig. 1B). A higher, relatively constant concentration of 100.6 ± 26.6 µM AA2P could be maintained by daily supplementation of AA2P. Interestingly, the concentration of AA deprived of the protective 2-phosphate group was below the limit of detection in stored and pellet culture medium at all time points, indicating immediate further degradation or consumption (not shown).

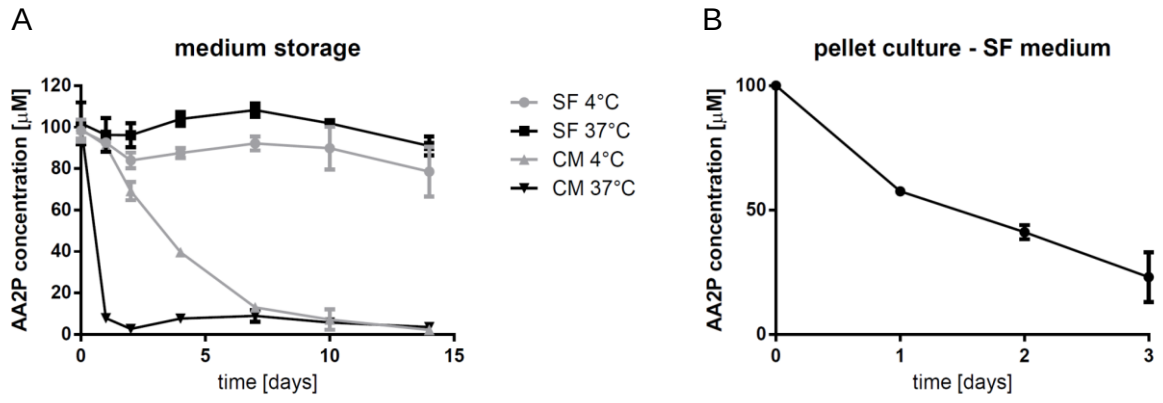

Figure 1: **Availability of ascorbic acid 2-phosphate in stored medium and micromass pellet culture.** (A) Concentration of ascorbic acid 2-phosphate (AA2P) in serum-free medium (SF) or 10% fetal bovine serum-containing medium (CM) stored at 4°C or 37°C for up to 14 days, showing a fast degradation in the presence of serum. (B) Concentration of AA2P in spent serum-free medium of micromass pellet culture, revealing progressive rapid decrease over 3 days.

Cell viability in pellet culture

Since AA is a potent antioxidant that prevents oxidative stress in cells, the effect of its absence on cell viability was tested in chondrocyte pellet culture. Terminal deoxynucleotidyl transferase dUTP nick end labeling (TUNEL) revealed only few events of DNA fragmentation across all conditions, indicating that the vast majority of cells were alive even in the absence of AA2P (Fig. 2A). The quantification of DNA showed very similar quantities in the pellets from all conditions, suggesting that no significant decrease in cell mass occurred when cells were cultured without AA2P and that no additional protection was provided when the antioxidant was present at a higher concentration (Fig. 2B).

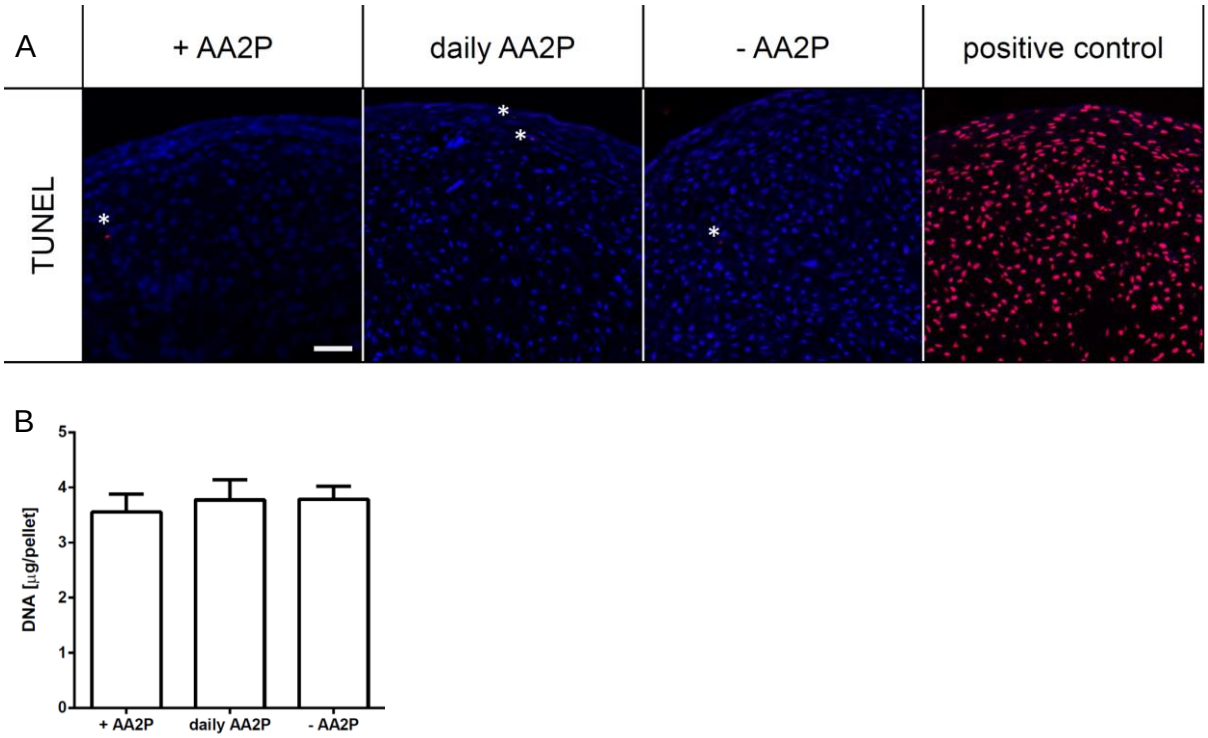

Figure 2: **Cell viability and cell mass.** (A) Terminal deoxynucleotidyl transferase dUTP nick end labeling (TUNEL; red, indicated by asterisk *) and DAPI nuclear counterstain (blue) of histological sections of micromass pellets after 2 weeks of chondrogenic culture in the presence or absence of AA. The few TUNEL-positive DNA strand breaks indicate rare events of cell necrosis or apoptosis in all culture conditions. Scale bar 50 µm. (B) DNA quantification of micromass pellets cultured with or without AA, indicating similar cell masses.

Gene expression and glycosaminoglycan deposition

Nasal chondrocytes showed an upregulation in the expression of collagen type II, aggrecan and Sox9, which was similar when comparing chondrocytes cultured in chondrogenic medium with or without AA2P (Fig. 3A). This finding indicated that the induction of chondrogenesis did not depend on the presence of AA2P in the culture medium. Histological sections of micromass pellets revealed a cartilaginous extracellular matrix with a similar cellularity and distribution of glycosaminoglycans (GAG) in the presence and in the absence of AA2P, as displayed by uniform Safranin-O staining. In the case where ITS was not supplemented, pellets were much smaller and had little extracellular matrix that was not positively stained for GAG (Fig. 3C). These findings were further substantiated by the quantification of the amount of GAG per DNA. Compared to the standard condition with supplementation of AA2P at each medium change, neither the absence of AA2P nor the maintenance of a higher AA2P concentration resulted in significant changes in the GAG/DNA ratio. On the other hand, the omission of ITS drastically reduced the production of GAG (Fig. 3B).

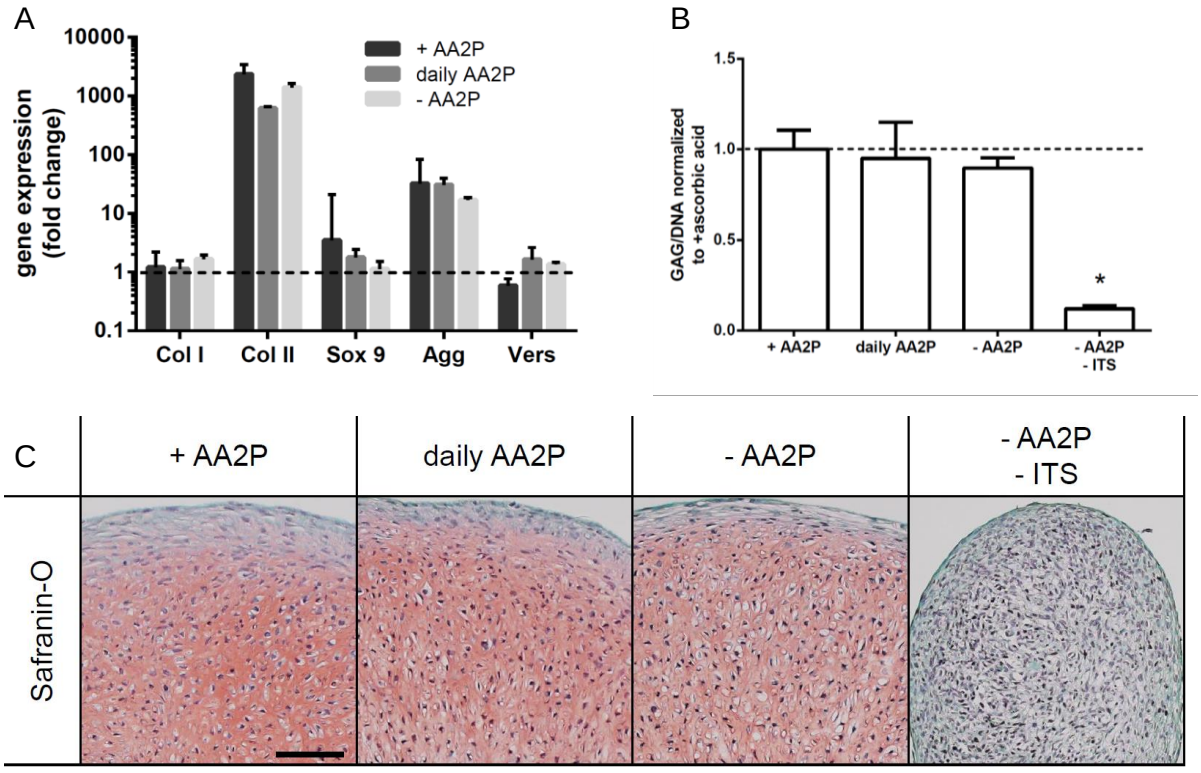

Figure 3: **Gene expression and glycosaminoglycan production.** (A) Gene expression after 2 weeks of chondrogenic differentiation with or without ascorbic acid as fold increase relative to expanded cells, showing similar upregulation of collagen type II, aggrecan and SOX9. (B) GAG/DNA ratios of micromass pellets normalized to the condition with ascorbic acid of the same donor. GAG production was similar in all conditions except for the pellets cultured without ITS (* $p < 0.05$). (C) Safranin-O staining of histological sections of micromass pellets revealing the production of an extracellular matrix rich in glycosaminoglycans, except for pellets cultured without ITS. Scale bar 200 µm.

Distribution of collagens and quantification of collagens and hydroxyproline

As AA is a cofactor in the hydroxylation of proline during collagen synthesis, we tested the effects of its absence on collagen deposition and hydroxylation. Immunohistochemistry revealed that chondrogenic pellets contained collagens type I and type II independently of the addition of AA2P, but not in the absence of ITS. Whereas collagen type I was distributed mainly on the edge of the pellets, collagen type II was abundantly present in the extracellular matrix of the whole pellet, except for a thin outer rim (Fig. 4).

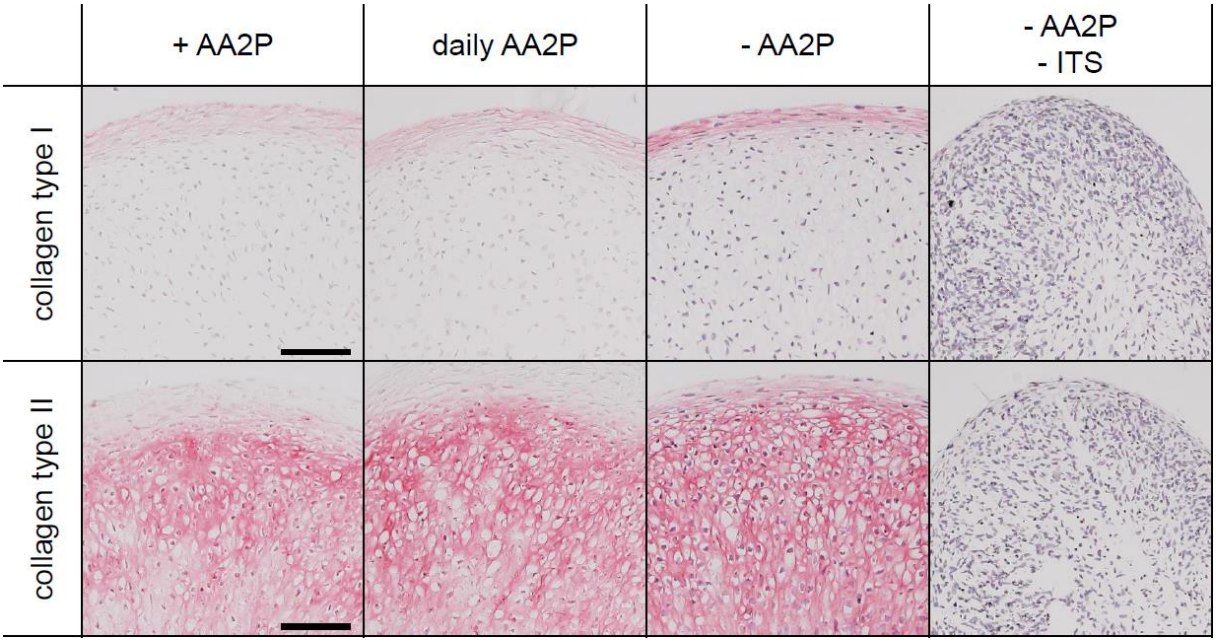

Figure 4: **Collagen type I and collagen type II distribution.** Histological sections of micromass pellets stained by immunohistochemistry against collagen type I or collagen type II. Matrix positive for collagen type I was found on the edge of the pellets, whereas collagen type II was located in the whole pellet except for a thin external rim. None of the collagens was found is pellets cultured without ITS. Scale bar 200 µm.

Quantification of collagens type I and type II by specific immunoassays confirmed deposition of both proteins in the absence of ascorbic acid. Relative to the addition of

AA2P, the amounts of collagens type I and type II secreted in cultures without AA2P were reduced by 50% and 34%, respectively. Daily AA2P did not lead to a substantial change in collagens quantity, while pellets maintained without ITS contained almost no collagen type I and significantly reduced levels of collagen type II (Fig. 5 A,B). The post-translational hydroxylation of collagens was confirmed by quantification of hydroxyproline in pellets from all groups, although the amount per pellet was reduced in the absence of AA2P compared to the groups with AA2P and daily AA2P addition (Fig. 5 C). The ratio of hydroxyproline/collagen was not significantly reduced in the absence of AA2P and the maintenance of a higher concentration of AA2P did not lead to an increased percentage of hydroxylation compared to supplementation only during medium exchange. In the group without ITS, only background levels of hydroxyproline were measured. As a result, the reduced amounts of collagens detected were also underhydroxylated (Fig. 5D).

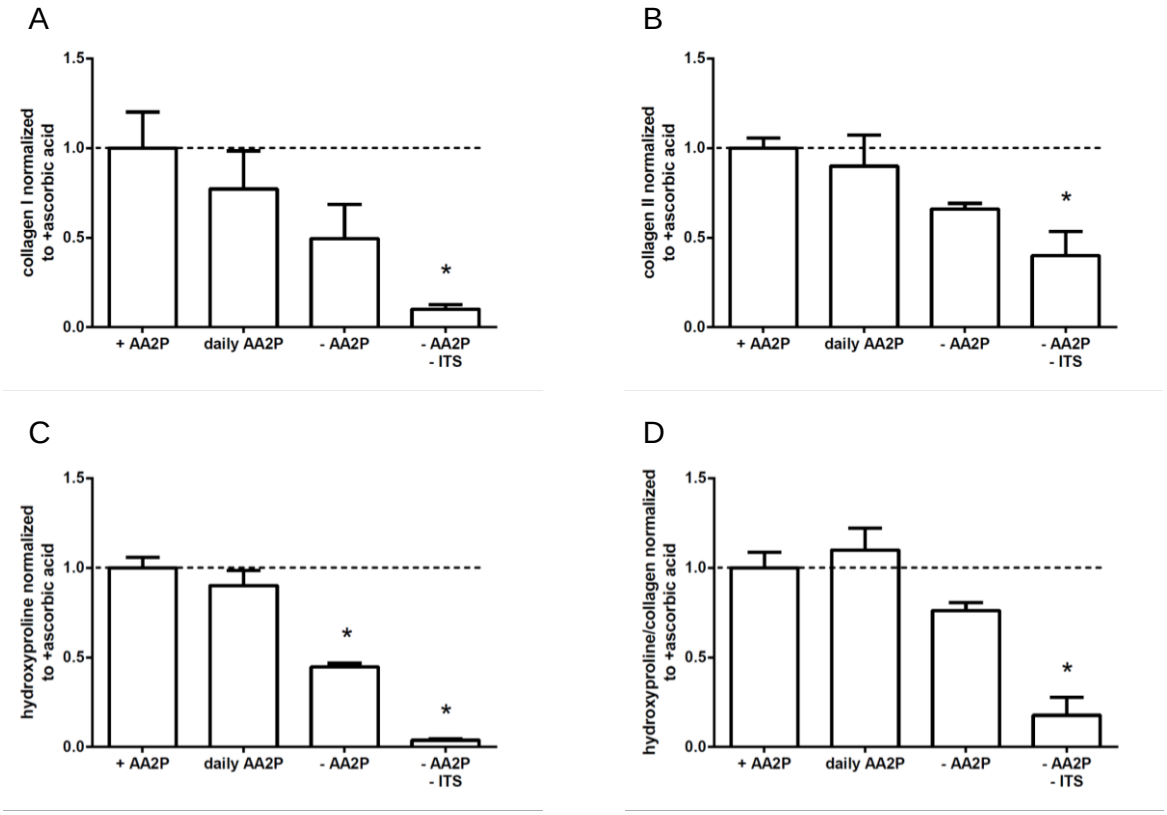

Figure 5: **Collagen type I, collagen type II, and hydroxyproline quantification.** (A) Quantification of collagen type I. (B) Quantification of collagen type II. (C) Quantification of hydroxyproline. (D) Ratio of hydroxyproline to collagen. All normalized to the value of the condition with ascorbic acid of the same donor (* $p < 0.05$). Results show that collagens type I and type II were produced in the absence of ascorbic acid and had a similar ratio of hydroxylation/collagen.

Collagen secretion

Since the slight reduction of collagen amounts in spite of similar gene expression could have resulted from impaired secretion in the absence of AA2P, we used high magnification immunofluorescence to assess whether collagen type II accumulated intracellularly. Images showed that collagen type II was evenly distributed in the extracellular matrix and no aggregation of type II collagen close to the nucleus was observed, independently of the presence or absence of AA2P. In case of the omission of ITS, no collagen type II was detected, which confirmed the results found by immunohistochemistry (Fig. 6).

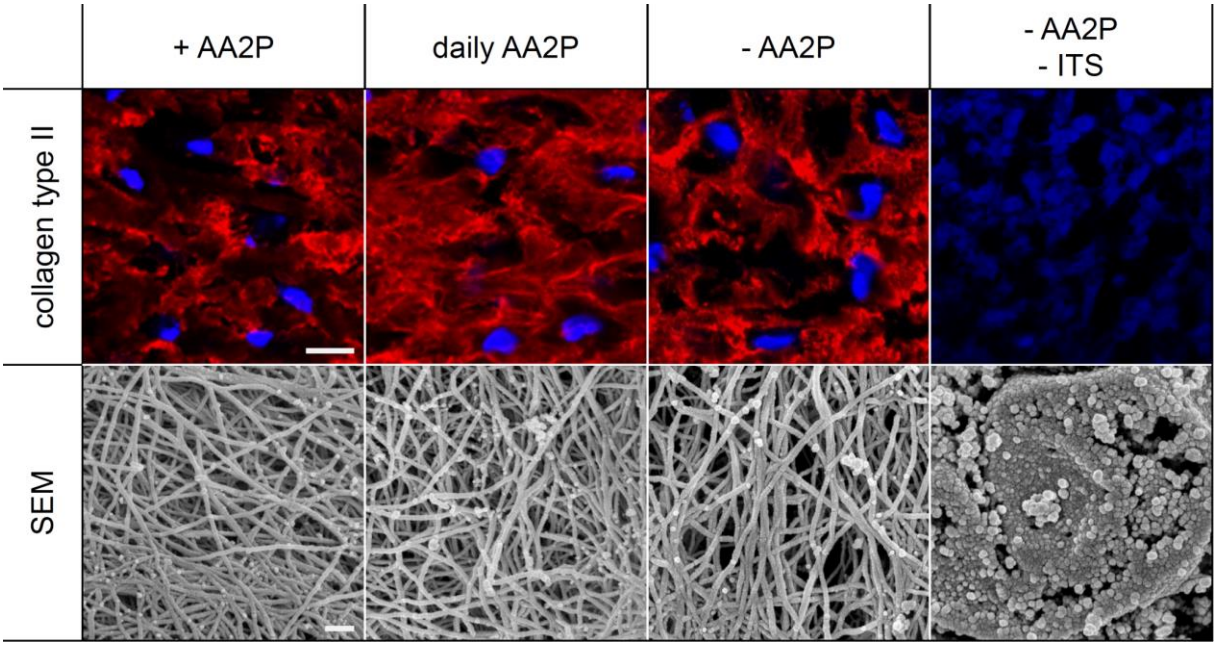

Figure 6: **Collagen type II immunofluorescence and scanning electron.** (A) Cryosections of micromass pellets stained by immunofluorescence against collagen type I (red) and DAPI nuclear counterstain (blue). Scale bar 10 µm. (B) Scanning electron microscopy of micromass pellets after digestion of glycoproteins showing collagen fibril network. Scale bar 200 nm.

Collagen fibril network structure

We investigated next whether the absence of AA2P had an effect on the structure and arrangement of collagen fibrils. High magnification scanning electron microscopy showed no collagen fibrils in the absence of ITS, but a similar fibril distribution, thickness and alignment when chondrocytes were cultured with or without AA2P.

This finding visually confirmed that in the absence of AA2P intact collagen fibers with normal appearance were secreted. Moreover it indicated that the absence of AA2P did not impair the formation of a dense network formed by single collagen fibrils (Fig. 6).

DISCUSSION

The present study showed that AA2P was stable in serum-free culture medium when stored at 4 or 37°C, but it was fast degraded in the presence of serum and rapidly decreased in serum-free pellet culture. The omission of AA2P in chondrogenic pellet culture did not lead to increased cell death. Gene expression, pellet formation, and glycosaminoglycans deposition were indistinguishable whether chondrocytes were cultured with or without AA2P. Type I and type II collagens were produced also in the absence of AA2P, even if to a lower extent. The ratio of hydroxyproline/collagen was unchanged in the absence of ascorbic acid. Chondrocytes did not exhibit impaired secretion of collagens and the extracellular matrix showed a similar organization and structure of collagen fibrils in the presence and absence of AA2P.

AA is known to be an unstable component of cell culture medium due to a fast degradation process catalyzed by iron and copper ions (11). The AA derivative AA2P was shown to be more stable and to have the same bioactivity than AA (12). The increased stability of AA2P with its protective phosphate group strongly depends on the culture conditions and thus needs to be assessed in each case. Our results proved the stability of AA2P in serum-free medium for up to 2 weeks when stored both at 4 and 37°C. However, the stability of AA2P was drastically reduced in serum-containing medium, likely due to the presence of phosphatases (9). AA2P concentration was rapidly reduced also in serum-free medium when culturing chondrocytes in micromass pellets: membrane-bound or secreted phosphatases likely degraded AA2P to AA, which was then further degraded or taken up by the cells (12). In the culture conditions tested, daily addition of AA2P was required to maintain constant concentration of AA2P. Overall, the collected results highlight the need to assess the availability of AA2P in the specific culture conditions/experimental setup, in order to define the most appropriate strategy to ensure the required levels

(e.g., sustained supply through continuous addition, more frequent medium change or larger volumes).

The potent antioxidative effect of AA consists in scavenging reactive oxygen and nitrogen species (36,37). The observed absence of apoptosis and necrosis in micromass cultures, suggests that AA was not required to prevent oxidative stress and that probably the presence of endogenous oxidants such as glutathione sufficed (38). The TUNEL assay was considered to be a more adequate indicator of the actual effects of the absence of AA, rather than the unreliable direct quantification of reactive oxygen species (39,40).

The absence of AA in pellet culture did not affect the expression of cartilage specific genes, which is in contrast to earlier studies claiming AA-induced upregulation of collagen synthesis on a translational level (41–43). Moreover, the extracellular matrix formed without AA was dense and rich in proteoglycans. In humans and guinea pigs, dietary AA deficiency leads to severe defects in connective tissues, known as scurvy, attributed to an impaired collagen synthesis due to insufficient proline hydroxylation (15). In the present study we found that chondrocytes could produce collagen type I and type II proteins in the absence of AA. The secreted amounts were only slightly reduced compared to the culture with AA and considerably higher than without chondrogenic induction. Quantification by immunoassay allowed a specific detection independent of the hydroxylation of the collagen proteins, which was also shown to be more precise than histological grading (32,33). The quantity of hydroxyproline per pellet was inferior in the absence of AA, confirming that AA had an effect on proline hydroxylation (44). However the amount of hydroxyproline per collagen was only marginally less in the absence of collagen, indicating that the enzyme proline hydroxylase was largely functional. Altogether these findings are in agreement with studies challenging the essentiality of AA as a co-factor for prolyl hydroxylase in

certain conditions. In fact, mutant mice lacking the final enzyme for AA synthesis were recently shown to have a normal collagen production and the absence of AA had no direct effect on collagen hydroxylation in guinea pigs (45,46). Probably other molecules present in the medium such as glutathione or cysteine can compensate for the lack of a co-factor, even if at a lower activity (14). Alternatively AA could be recycled over long durations, which could also explain why proper collagen production without ascorbic acid supplementation was observed in vivo (23,24). The discrepancy with previous studies showing a strong effect of AA on gene expression, collagen synthesis and hydroxylation might derive from the use of different culture conditions and need further investigation (17,18,41–43,47,48). The above-mentioned substitute molecules could be absent in certain medium preparations or certain cell types may be incapable of AA recycling. Interestingly, no increase in collagen deposition or hydroxylation per collagen was observed when maintaining a constant concentration of ascorbic acid: this data indicate that the applied regime of medium exchanges was sufficient to reach saturation of AA-dependent mechanisms in our specific setting. The differences in the quantity of collagen deposition between groups, despite a similar gene expression and similar hydroxyproline/collagen could have resulted from a slower secretion. In fact an accumulation in the endoplasmic reticulum has been reported for insufficiently hydroxylated collagens, which could be the case here as a consequence of the lower activity of alternative co-factors (49,50). However, intracellular collagen accumulation indication of impaired secretion could not be detected using high magnification immunofluorescence (50).

The unique biomechanical features of articular cartilage largely depend on its highly organized molecular and structural composition (13). The secreted collagens displayed here similar fibrils organization and structure in all chondrogenic pellets, regardless of AA supplementation. Together with the similar hydroxylation profiles,

this suggested that the engineered extracellular matrix could have similar biomechanical features, even if produced in the absence of ascorbic acid (51).

Altogether, the absence of AA was shown here to result in a very similar cartilaginous extracellular matrix, but with reduced quantities of collagens. On the other hand the omission or a temporarily discontinued supply of AA in chondrogenic medium could help in simplifying the automation of bioreactors, which will be required to drastically lower the manufacturing expenses. In order to promote the clinical translation of tissue engineering in the long-term, a delicate balance between sufficient product quality and acceptable cost-efficiency needs to be reached (4,7). Since the extracellular matrix of engineered cartilage grafts will anyway have to further mature and will be remodeled after implantation, where AA is available at physiologic concentrations, the omission of AA2P could be considered.

CONCLUSION

In this study we demonstrated that ascorbic acid is not essential for the synthesis of collagen type I and type II with hydroxylated proline residues. Moreover the pellet culture of human nasal chondrocytes with or without ascorbic acid 2-phosphate resulted in similar cell viability, gene expression, cartilaginous extracellular matrix production and collagen fibril organization. Overall, the collected data support the possibility of omitting ascorbic acid from chondrogenic medium in certain conditions. Together with the increased knowledge on ascorbic acid 2-phosphate stability in serum-containing and serum-free medium under different conditions, these results will help to define an efficient strategy for medium storage and ascorbic acid supplementation that ensures adequate quality of in vitro engineered cartilage grafts.

ACKNOWLEDGEMENTS

The authors would like to acknowledge Evi Bieler from the Centre of Microscopy of the University of Basel for help with the electron microscopy. Nasal cartilage samples were kindly provided by Dr. Martin Haug. This project has received funding from the European Union's Seventh Program for research, technological development, and demonstration under grant agreement No. 278807 (BIO-COMET). RD would like to thank the Fonds National de la Recherche Luxembourg (4090751) for financial support.

REFERENCES

1. Fulco I, Miot S, Haug MD, Barbero A, Wixmerten A, Feliciano S, et al. Engineered autologous cartilage tissue for nasal reconstruction after tumour resection: an observational first-in-human trial. Lancet **384**(9940), 337, 2014;

2. Miot S, Gianni-Barrera R, Pelttari K, Acharya C, Mainil-Varlet P, Juelke H, et al. In vitro and in vivo validation of human and goat chondrocyte labeling by green fluorescent protein lentivirus transduction. Tissue Eng. Part C Methods. **16**(1), 11, 2010;

3. Pelttari K, Pippenger B, Mumme M, Feliciano S, Scotti C, Mainil-Varlet P, et al. Adult human neural crest-derived cells for articular cartilage repair. Sci. Transl. Med. **6**(251), 251ra119, 2014;

4. Asnaghi MA, Smith T, Martin I, Wendt D. Bioreactors: Enabling Technologies for Research and Manufacturing. In: Blitterswijk CAV, Boer JD, editors. Tissue Engineering, Second Edition. Oxford: Academic Press; p. 393–425, 2014;

5. Martin I, Simmons PJ, Williams DF. Manufacturing challenges in regenerative medicine. Sci. Transl. Med. **6**(232), 232fs16, 2014;

6. Martin I, Wendt D, Heberer M. The role of bioreactors in tissue engineering. Trends Biotechnol. **22**(2), 80, 2004;

7. Martin I, Smith T, Wendt D. Bioreactor-based roadmap for the translation of tissue engineering strategies into clinical products. Trends Biotechnol. **27**(9), 495, 2009;

8. Santoro R, Olivares AL, Brans G, Wirz D, Longinotti C, Lacroix D, et al. Bioreactor based engineering of large-scale human cartilage grafts for joint resurfacing. Biomaterials. **31**(34), 8946, 2010;

9. Chepda T, Cadau M, Girin P, Frey J, Chamson A. Monitoring of ascorbate at a constant rate in cell culture: effect on cell growth. In Vitro Cell. Dev. Biol. Anim. **37**(1), 26, 2001;

10. Kurano S, Kurano N, Leist C, Fiechter A. Utilization and stability of vitamins in serum-containing and serum-free media in CHO cell culture. Cytotechnology. **4**(3), 243, 1990;

11. Fisher AEO, Naughton DP. Iron supplements: the quick fix with long-term consequences. Nutr. J. **3**, 2, 2004;

12. Takamizawa S, Maehata Y, Imai K, Senoo H, Sato S, Hata R-I. Effects of ascorbic acid and ascorbic acid 2-phosphate, a long-acting vitamin C derivative, on the proliferation and differentiation of human osteoblast-like cells. Cell Biol. Int. **28**(4), 255, 2004;

13. Buckwalter JA, Mankin HJ. Articular cartilage: tissue design and chondrocyte-matrix interactions. Instr. Course Lect. **47**, 477, 1998;

14. Barnes MJ, Kodicek E. Biological hydroxylations and ascorbic acid with special regard to collagen metabolism. Vitam. Horm. **30**, 1, 1972;

15. Englard S, Seifter S. The biochemical functions of ascorbic acid. Annu. Rev. Nutr. **6**, 365, 1986;

16. Kavitha O, Thampan RV. Factors influencing collagen biosynthesis. J. Cell. Biochem. **104**(4), 1150, 2008;

17. Ibold Y, Lübke C, Pelz S, Augst H, Kaps C, Ringe J, et al. Effect of different ascorbate supplementations on in vitro cartilage formation in porcine high-density pellet cultures. Tissue Cell. **41**(4), 249, 2009;

18. Cigan AD, Nims RJ, Albro MB, Esau JD, Dreyer MP, Vunjak-Novakovic G, et al. Insulin, Ascorbate, and Glucose Have a Much Greater Influence Than Transferrin and Selenous Acid on the In Vitro Growth of Engineered Cartilage in Chondrogenic Media. Tissue Eng. Part A. 2013;

19. Altaf FM, Hering TM, Kazmi NH, Yoo JU, Johnstone B. Ascorbate-enhanced chondrogenesis of ATDC5 cells. Eur. Cell. Mater. **12**, 64, 2006;

20. Mårtensson J, Han J, Griffith OW, Meister A. Glutathione ester delays the onset of scurvy in ascorbate-deficient guinea pigs. Proc. Natl. Acad. Sci. U. S. A. **90**(1), 317, 1993;

21. Nytko KJ, Maeda N, Schläfli P, Spielmann P, Wenger RH, Stiehl DP. Vitamin C is dispensable for oxygen sensing in vivo. Blood. **117**(20), 5485, 2011;

22. Flashman E, Davies SL, Yeoh KK, Schofield CJ. Investigating the dependence of the hypoxia-inducible factor hydroxylases (factor inhibiting HIF and prolyl hydroxylase domain 2) on ascorbate and other reducing agents. Biochem. J. **427**(1), 135, 2010;

23. McNulty AL, Stabler TV, Vail TP, McDaniel GE, Kraus VB. Dehydroascorbate transport in human chondrocytes is regulated by hypoxia and is a physiologically relevant source of ascorbic acid in the joint. Arthritis Rheum. **52**(9), 2676, 2005;

24. Qutob S, Dixon SJ, Wilson JX. Insulin stimulates vitamin C recycling and ascorbate accumulation in osteoblastic cells. Endocrinology. **139**(1), 51, 1998;

25. Jakob M, Démarteau O, Schäfer D, Stumm M, Heberer M, Martin I. Enzymatic Digestion of Adult Human Articular Cartilage Yields a Small Fraction of the Total Available Cells. Connect. Tissue Res. **44**, 173, 2003;

26. Jakob M, Démarteau O, Schäfer D, Hintermann B, Dick W, Heberer M, et al. Specific growth factors during the expansion and redifferentiation of adult human articular chondrocytes enhance chondrogenesis and cartilaginous tissue formation in vitro. J. Cell. Biochem. **81**(2), 368, 2001;

27. Barbero A. Age related changes in human articular chondrocyte yield, proliferation and post-expansion chondrogenic capacity. Osteoarthritis Cartilage. **12**, 476, 2004;

28. Scotti C, Tonnarelli B, Papadimitropoulos A, Scherberich A, Schaeren S, Schauerte A, et al. Recapitulation of endochondral bone formation using human adult mesenchymal stem cells as a paradigm for developmental engineering. Proc. Natl. Acad. Sci. U. S. A. **107**(16), 7251, 2010;

29. Martin I, Jakob M, Schäfer D, Dick W, Spagnoli G, Heberer M. Quantitative analysis of gene expression in human articular cartilage from normal and osteoarthritic joints. Osteoarthr. Cartil. **9**(2), 112, 2001;

30. Barbosa I, Garcia S, Barbier-Chassefière V, Caruelle J-P, Martelly I, Papy-García D. Improved and simple micro assay for sulfated glycosaminoglycans quantification in biological extracts and its use in skin and muscle tissue studies. Glycobiology. **13**(9), 647, 2003;

31. Hofman K, Hall B, Cleaver H, Marshall S. High-throughput quantification of hydroxyproline for determination of collagen. Anal. Biochem. **417**(2), 289, 2011;

32. Dickinson SC, Sims TJ, Pittarello L, Soranzo C, Pavesio A, Hollander AP. Quantitative outcome measures of cartilage repair in patients treated by tissue engineering. Tissue Eng. **11**(1-2), 277, 2005;

33. Hollander AP, Heathfield TF, Webber C, Iwata Y, Bourne R, Rorabeck C, et al. Increased damage to type II collagen in osteoarthritic articular cartilage detected by a new immunoassay. J. Clin. Invest. **93**(4), 1722, 1994;

34. Stolz M, Gottardi R, Raiteri R, Miot S, Martin I, Imer R, et al. Early detection of aging cartilage and osteoarthritis in mice and patient samples using atomic force microscopy. Nat. Nanotechnol. **4**(3), 186, 2009;

35. Ströbel S, Loparic M, Wendt D, Schenk AD, Candrian C, Lindberg RLP, et al. Anabolic and catabolic responses of human articular chondrocytes to varying oxygen percentages. Arthritis Res. Ther. **12**(2), R34, 2010;

36. Grasl-Kraupp B, Ruttkay-Nedecky B, Koudelka H, Bukowska K, Bursch W, Schulte-Hermann R. In situ detection of fragmented DNA (TUNEL assay) fails to discriminate among apoptosis, necrosis, and autolytic cell death: a cautionary note. Hepatol. Baltim. Md. **21**(5), 1465, 1995;

37. Fulda S, Gorman AM, Hori O, Samali A, Fulda S, Gorman AM, et al. Cellular Stress Responses: Cell Survival and Cell Death, Cellular Stress Responses: Cell Survival and Cell Death. Int. J. Cell Biol. e214074, 2010;

38. Espinosa-Diez C, Miguel V, Mennerich D, Kietzmann T, Sánchez-Pérez P, Cadenas S, et al. Antioxidant responses and cellular adjustments to oxidative stress. Redox Biol. **6**, 183, 2015;

39. Winterbourn CC. The challenges of using fluorescent probes to detect and quantify specific reactive oxygen species in living cells. Biochim. Biophys. Acta **1840**, 730–738, 2014;

40. Wardman P. Fluorescent and luminescent probes for measurement of oxidative and nitrosative species in cells and tissues: progress, pitfalls, and prospects. Free Radic. Biol. Med. **43**(7), 995, 2007;

41. Murad S, Grove D, Lindberg KA, Reynolds G, Sivarajah A, Pinnell SR. Regulation of collagen synthesis by ascorbic acid. Proc. Natl. Acad. Sci. U. S. A. **78**(5), 2879, 1981;

42. Ronzière MC, Roche S, Gouttenoire J, Démarteau O, Herbage D, Freyria AM. Ascorbate modulation of bovine chondrocyte growth, matrix protein gene expression and synthesis in three-dimensional collagen sponges. Biomaterials. **24**(5), 851, 2003;

43. Temu TM, Wu K-Y, Gruppuso PA, Phornphutkul C. The mechanism of ascorbic acid-induced differentiation of ATDC5 chondrogenic cells. Am. J. Physiol. Endocrinol. Metab. **299**(2), E325, 2010;

44. Myllylä R, Majamaa K, Günzler V, Hanauske-Abel HM, Kivirikko KI. Ascorbate is consumed stoichiometrically in the uncoupled reactions catalyzed by prolyl 4-hydroxylase and lysyl hydroxylase. J. Biol. Chem. **259**(9), 5403, 1984;

45. Parsons KK, Maeda N, Yamauchi M, Banes AJ, Koller BH. Ascorbic acid-independent synthesis of collagen in mice. Am. J. Physiol. Endocrinol. Metab. **290**(6), E1131, 2006;

46. Peterkofsky B. Ascorbate requirement for hydroxylation and secretion of procollagen: relationship to inhibition of collagen synthesis in scurvy. Am. J. Clin. Nutr. **54**(6 Suppl), 1135S, 1991;

47. Tsutsumi K, Fujikawa H, Kajikawa T, Takedachi M, Yamamoto T, Murakami S. Effects of L-ascorbic acid 2-phosphate magnesium salt on the properties of human gingival fibroblasts: Effects of l-ascorbic acid 2-phosphate magnesium salt. J. Periodontal Res. **47**(2), 263, 2012;

48. Omata S, Sonokawa S, Sawae Y, Murakami T. Effects of both vitamin C and mechanical stimulation on improving the mechanical characteristics of regenerated cartilage. Biochem. Biophys. Res. Commun. **424**(4), 724, 2012;

49. Uitto J, Hoffman H, Prockop DJ. Retention of nonhelical procollagen containing cis-hydroxyproline in rough endoplasmic reticulum. Science. **190**(4220), 1202, 1975;

50. Bentovim L, Amarilio R, Zelzer E. HIF1α is a central regulator of collagen hydroxylation and secretion under hypoxia during bone development. Dev. Camb. Engl. **139**(23), 4473, 2012;

51. Berg RA, Prockop DJ. The thermal transition of a non-hydroxylated form of collagen. Evidence for a role for hydroxyproline in stabilizing the triple-helix of collagen. Biochem. Biophys. Res. Commun. **52**(1), 115, 1973;

Conclusions

Engineered tissue grafts have the potential to substantially contribute to the treatment of challenging cartilage and bone lesions. In order to accelerate their clinical translation, engineered products will have to prove a fast restoration with predictable clinical outcome. For this objective, increased quality and reproducibility will be required, which can be accomplished through an extended knowledge and improved control of the cell phenotype during all phases of tissue graft manufacturing. In the previous chapters, I demonstrated that the growth and differentiation of chondrocytes and BMSC can be modulated in order to better maintain and utilize their potential for cartilage and bone tissue engineering.

The relationship between chondrocyte proliferation and concurrent phenotypic changes was poorly understood. In **chapter I**, cell division tracking of primary chondrocytes revealed that the progression of de-differentiation is strongly connected to cell doublings. The cell subpopulation with the highest proliferation rate exhibited the lowest re-differentiation capacity, whereas the highest chondrogenic potential was found here in cells that were slowly dividing. Since over time rapidly proliferating cells will overgrow all other subpopulations, this underlines the importance of only moderate expansion for clinical applications. An uncoupling of the link between proliferation and de-differentiation would open completely new perspectives for cartilage tissue engineering by allowing an extensive cell expansion while maintaining cell differentiation and chondrogenic potential. The existence of a slowly proliferating subpopulation with an intrinsically higher chondrogenic capacity will need to be verified for a much larger number of donors. A prospective selection of these cells with superior regenerative properties or an elimination of fast growing cells with lower chondrogenic potential could help in the generation of engineered cartilage grafts with a reproducibly higher quality.

The bioreactor-based expansion of BMSC on 3D ceramic scaffolds were reported to lead to more extensive bone formation than culture on 2D polystyrene, but the influence of the multiple different culture parameters was unknown. In **chapter II**, the decoupling of the substrate dimensionality from the substrate material provided valuable insights into their individual roles during BMSC culture. In contrast to 2D polystyrene, a perfused 3D polystyrene scaffold was sufficient to maintain the *in vivo* osteogenic potential of BMSC over 3 weeks, which underlines the important effect of

a 3D environment on the cell phenotype. A ceramic scaffold further increased the preservation of osteogenic capacity, proving the impact of the substrate material. Moreover it was demonstrated that the preexistence of a 3D niche of extracellular matrix, in which the expanded cells were embedded, was not required for subsequent bone formation. The direct expansion of BMSC in a 3D ceramic construct offers thus the possibility to conserve bone formation potential and to streamline the manufacturing of large-scale bone grafts. Alternatively, BMSC expanded in 3D scaffolds could be extracted and administered as cell suspensions for osteogenic cell therapies.

Macrophages have been reported to play an important role in healing processes by modulating tissue inflammation and repair, but their influence on the chondrogenic differentiation capacity of BMSC has not been established yet. In **chapter III**, macrophages with a tissue repair phenotype were demonstrated to have a chondro-inductive effect on BMSC with increased collagen type II expression and GAG production, while pro-inflammatory macrophages did not influence chondrogenesis. The observed chondro-induction seemed to be due to the survival of BMSC with high chondrogenic capacity and to be mediated by short distance interactions between the two cell types. *In vivo*, the presence of tissue-repair macrophages did not influence tissue maturation. Altogether, the coculture with tissue-repair macrophages can become an attractive strategy for the sustained chondrogenic differentiation of BMSC *in vitro*.

The small molecule ascorbic acid is involved in collagen synthesis and is therefore a standard supplement in chondrogenic differentiation medium. However the limited stability of ascorbic acid presents a considerable challenge to the automation of liquid handling for cartilage graft manufacturing. The effect of omitting ascorbic acid during chondrogenic differentiation, with special regard to collagen synthesis and hydroxylation, was thus investigated in **chapter IV**. Ascorbic acid was found not to be essential for the production of collagens type I and type II with hydroxylated proline residues. Since cell viability, gene expression, and glycosaminoglycan production were also similar, these results supported the possibility of omitting ascorbic acid in certain conditions. The increased knowledge on ascorbic acid requirements will help to define an efficient strategy for medium storage and ascorbic acid supplementation that facilitates automation, while ensuring the quality of *in vitro* engineered cartilage grafts.

In this thesis, I highlighted four different approaches to gain increased control over the growth and differentiation of chondrocytes and BMSC. To reach the ultimate goal of a sufficiently high quality of engineered tissues for clinical translation, a combination of different actions will be required to direct the cell phenotype throughout all phases of the manufacturing process. During cell isolation, subpopulations promoting or impairing the regenerative potential should already be separated. The increased differentiation potential can then be preserved during proliferation by uncoupling phenotypic changes from cell divisions, possibly through the provision of specific 3D scaffolds. After sufficient expansion, the deposition of extracellular matrix can be enhanced by the coculture with macrophages promoting survival and differentiation. Finally in order to achieve cost-effectiveness through the implementation of automation, manufacturing procedures can be simplified by the omission of certain factors or process steps without compromising product quality (Fig. 1). The increased graft quality achieved through the control of the cell phenotype will thereby result in mature tissues which will need to be further evaluated in clinical trials.

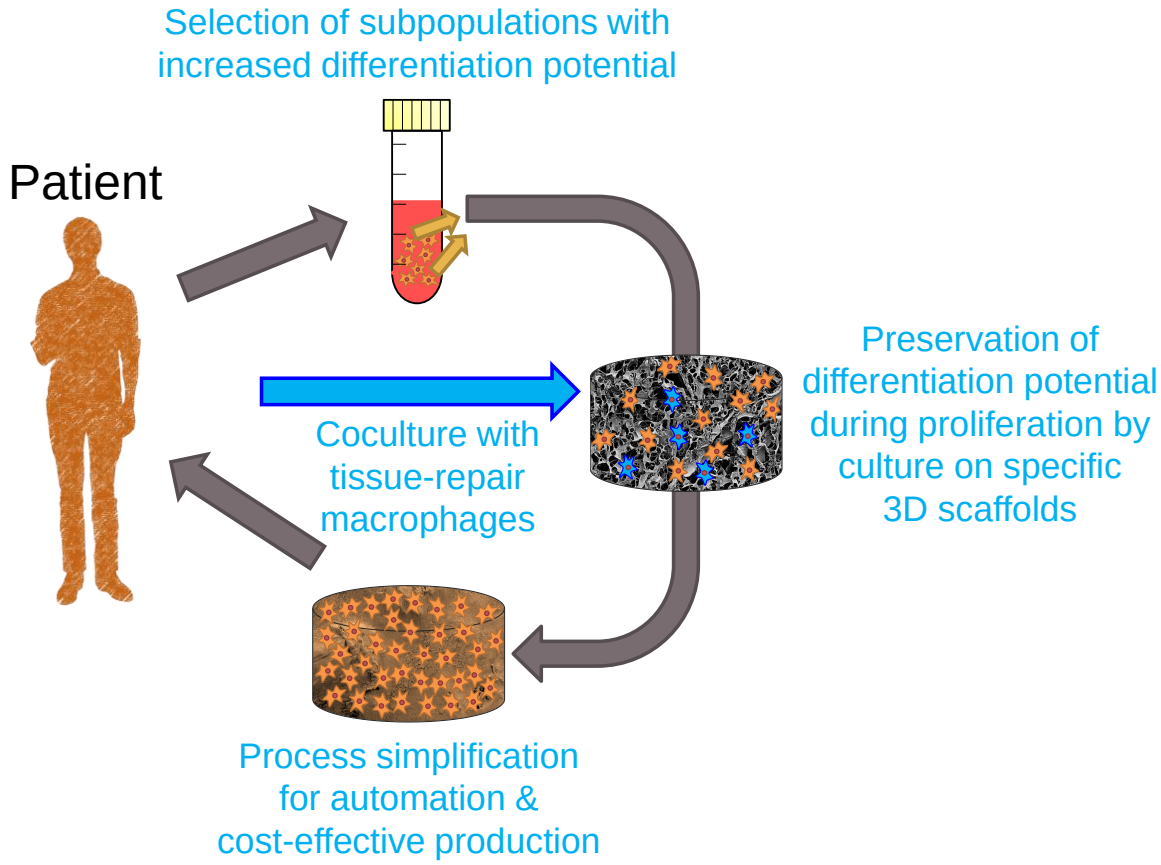

Figure 1: Increased quality of engineered tissues can be achieved by integrating the approaches presented in this work into the tissue engineering paradigm in order to better control the cell phenotype during all stages of the manufacturing process.

Future perspectives

Besides the above mentioned combination of the different approaches to provide a better control over the phenotype of mesenchymal cells, this work can also serve as a starting point for future studies exploring the cellular mechanisms of growth and differentiation of chondrocytes and BMSC, but also of other cell types used for tissue repair. Indeed the achievement of high product quality during graft manufacturing through robust processes controlling cell proliferation and differentiation is a recurring theme in many tissue engineering applications (Martin et al., 2014).

The cell division tracking method employed in **chapter I** has been extensively used to gain mechanistic insights in the field of immunology (Quah and Parish, 2012). In order to further study the coupling between proliferation and de-differentiation of chondrocytes, the technique could be combined with quantitative imaging. Pathways that could be involved in the described interplay include cell spreading, motility and adhesion, maybe through RhoA or CD90 (Barker et al., 2004; Beier and Loeser, 2010; Mammoto et al., 2004). Since no distinctive profile of cell surface protein expression was detected here to select cells with an intrinsically higher potential, testing of additional markers like the previously described CD44 or CD49e could help in better defining or even prospectively isolating these cells (Dowthwaite et al., 2004; Grogan et al., 2007; Williams et al., 2010). Also the combination with S100, another marker reported to indicate cell potency, could give helpful insights (Diaz-Romero et al., 2014). A transcriptomic analysis would probably provide a better understanding of the mechanisms responsible for the maintenance of a higher chondrogenic potential of these cells. The increased knowledge could then again be used to design more robust cartilage manufacturing processes. Moreover other cell types such as BMSC could benefit from the same method of cell division tracking to distinguish subpopulations with possibly diverse differentiation potential (Bara et al., 2014; Tormin et al., 2009).

Considering that the 3D expansion in perfused bioreactors used in **chapter II** is also known to be more robust across different donors (Papadimitropoulos et al., 2014), this process could become the method of choice for the expansion of BMSC with maintained progenitor properties. Such a system could as well be used for the establishment of an artificial bone marrow niche to study hematopoiesis *in vitro* (Di Maggio et al., 2011). The effect of the developing niche made from extracellular

matrix on the maintenance of BMSC functionality during expansion still needs to be explored. Furthermore the ceramic substrate was shown here to preserve the bone formation potential of BMSC, without priming the cells towards an osteogenic phenotype. A better understanding of the interactions between BMSC and ceramic substrates could thus lead to the development of new materials that have superior properties to maintain the cells' progenitor potential. In addition the same technique of bridging the gap between 2D polystyrene and 3D materials by the use of a 3D polystyrene scaffold could be employed to analyze different aspects of substrate dimensionality on other cell types (Baker and Chen, 2012).

The coculture with macrophages resulted in an enhanced chondrogenesis and cell survival of BMSC in **chapter III**. The presence of macrophages was not sufficient though to stabilize the chondrogenic phenotype. Nevertheless this coculture method could be used to improve the formation of a cartilaginous template for bone tissue engineering through an endochondral pathway (Scotti et al., 2010). Moreover these results indicate that the presence of macrophages could be beneficial for the culture and differentiation of other progenitor cell types for regenerative purposes (Brown et al., 2014). In view of a direct application of these results, the administration of compounds promoting the recruitment/polarization of anti-inflammatory and tissue-repair macrophages should be tested in an orthotopic large animal model (Hoemann et al., 2010). Supposedly these macrophages could promote chondrogenesis and also keep cells alive in hostile environments such as after microfracture surgery or after implantation in an osteoarthritic joint site.

Ascorbic acid was shown in **chapter IV** to be an unessential component of chondrogenic medium. The molecules acting as a substitute for ascorbic acid in the role of antioxidant and co-factors of proline hydroxylation deserve further investigation. In addition, this study showed how inefficient process steps can be scrutinized and replaced by a more innovative process design, such as in the case of changing from manual to automated medium exchange procedures. For a faster clinical translation, tissue engineering processes that are inherently robust by their design need to be obtained (Martin et al., 2014). Once a certain robustness and quality have been achieved, a balance then needs to be found between what is technically or biologically feasible and what is cost-efficient for the clinical translation of tissue engineered products (Butler et al., 2000; Wendt et al., 2009).

Ultimately, besides a deeper understanding of the biological processes during the production of engineered tissue and ongoing work in advancing the automation of manufacturing, future research efforts in tissue engineering will have to address the more fundamental mechanisms of regeneration and disease of the human body. In fact, little attention has been given to date to the recipient side where the graft environment is likely to play an important role and could even be instructed to promote regeneration (Tonnarelli et al., 2014). In this context, the function of macrophages during inflammation and regeneration deserves further investigation (Brown et al., 2014). Moreover, the target quality of tissue grafts in terms of biomechanical properties needs to be better defined, by evaluating which features are essential to overcome the disabling condition and to support regeneration (Butler et al., 2000). A continuous and even intensified collaboration between clinicians, biologists and engineers will be required to develop and validate these novel paradigms. In this way, tissue engineering can hold its promise of delivering the most advanced and efficacious treatments for the cure of challenging cartilage and bone lesions.

REFERENCES

Baker, B. M. and Chen, C. S. (2012). Deconstructing the third dimension: how 3D culture microenvironments alter cellular cues. *J. Cell Sci.* **125**, 3015–3024.

Bara, J. J., Richards, R. G., Alini, M. and Stoddart, M. J. (2014). Concise review: Bone marrow-derived mesenchymal stem cells change phenotype following in vitro culture: implications for basic research and the clinic. *Stem Cells Dayt. Ohio* **32**, 1713–1723.

Barker, T. H., Grenett, H. E., MacEwen, M. W., Tilden, S. G., Fuller, G. M., Settleman, J., Woods, A., Murphy-Ullrich, J. and Hagood, J. S. (2004). Thy-1 regulates fibroblast focal adhesions, cytoskeletal organization and migration through modulation of p190 RhoGAP and Rho GTPase activity. *Exp. Cell Res.* **295**, 488–496.

Beier, F. and Loeser, R. F. (2010). Biology and pathology of Rho GTPase, PI-3 kinase-Akt, and MAP kinase signaling pathways in chondrocytes. *J. Cell. Biochem.* **110**, 573–580.

Brown, B. N., Sicari, B. M. and Badylak, S. F. (2014). Rethinking Regenerative Medicine: A Macrophage-Centered Approach. *Front. Immunol.* **5**,.

Butler, D. L., Goldstein, S. A. and Guilak, F. (2000). Functional tissue engineering: the role of biomechanics. *J. Biomech. Eng.* **122**, 570–575.

Diaz-Romero, J., Quintin, A., Schoenholzer, E., Pauli, C., Despont, A., Zumstein, M. A., Kohl, S. and Nesic, D. (2014). S100A1 and S100B Expression Patterns Identify Differentiation Status of Human Articular Chondrocytes. *J. Cell. Physiol.* **229**, 1106–1117.

Di Maggio, N., Piccinini, E., Jaworski, M., Trumpp, A., Wendt, D. J. and Martin, I. (2011). Toward modeling the bone marrow niche using scaffold-based 3D culture systems. *Biomaterials* **32**, 321–329.

Dowthwaite, G. P., Bishop, J. C., Redman, S. N., Khan, I. M., Rooney, P., Evans, D. J. R., Haughton, L., Bayram, Z., Boyer, S., Thomson, B., et al. (2004). The surface of articular cartilage contains a progenitor cell population. *J. Cell Sci.* **117**, 889–897.

Grogan, S. P., Barbero, A., Diaz-Romero, J., Cleton-Jansen, A.-M., Soeder, S., Whiteside, R., Hogendoorn, P. C. W., Farhadi, J., Aigner, T., Martin, I., et al. (2007). Identification of markers to characterize and sort human articular chondrocytes with enhanced in vitro chondrogenic capacity. *Arthritis Rheum.* **56**, 586–595.

Hoemann, C. D., Chen, G., Marchand, C., Tran-Khanh, N., Thibault, M., Chevrier, A., Sun, J., Shive, M. S., Fernandes, M. J. G., Poubelle, P. E., et al. (2010). Scaffold-guided subchondral bone repair: implication of neutrophils and alternatively activated arginase-1+ macrophages. *Am. J. Sports Med.* **38**, 1845–1856.

Mammoto, A., Huang, S., Moore, K., Oh, P. and Ingber, D. E. (2004). Role of RhoA, mDia, and ROCK in cell shape-dependent control of the Skp2-p27kip1 pathway and the G1/S transition. *J. Biol. Chem.* **279**, 26323–26330.

Martin, I., Simmons, P. J. and Williams, D. F. (2014). Manufacturing challenges in regenerative medicine. *Sci. Transl. Med.* **6**, 232fs16.

Papadimitropoulos, A., Piccinini, E., Brachat, S., Braccini, A., Wendt, D., Barbero, A., Jacobi, C. and Martin, I. (2014). Expansion of Human Mesenchymal Stromal Cells from Fresh Bone Marrow in a 3D Scaffold-Based System under Direct Perfusion. *PloS One* **9**, e102359.

Quah, B. J. C. and Parish, C. R. (2012). New and improved methods for measuring lymphocyte proliferation in vitro and in vivo using CFSE-like fluorescent dyes. *J. Immunol. Methods* **379**, 1–14.

Scotti, C., Tonnarelli, B., Papadimitropoulos, A., Scherberich, A., Schaeren, S., Schauerte, A., Lopez-Rios, J., Zeller, R., Barbero, A. and Martin, I. (2010). Recapitulation of endochondral bone formation using human adult mesenchymal stem cells as a paradigm for developmental engineering. *Proc. Natl. Acad. Sci. U. S. A.* **107**, 7251–7256.

Tonnarelli, B., Centola, M., Barbero, A., Zeller, R. and Martin, I. (2014). Re-engineering development to instruct tissue regeneration. *Curr. Top. Dev. Biol.* **108**, 319–338.

Tormin, A., Brune, J. C., Olsson, E., Valcich, J., Neuman, U., Olofsson, T., Jacobsen, S.-E. and Scheding, S. (2009). Characterization of bone marrow-derived mesenchymal stromal cells (MSC) based on gene expression profiling of functionally defined MSC subsets. *Cytotherapy* **11**, 114–128.

Wendt, D., Riboldi, S. A., Cioffi, M. and Martin, I. (2009). Potential and bottlenecks of bioreactors in 3D cell culture and tissue manufacturing. *Adv. Mater. Deerfield Beach Fla* **21**, 3352–3367.

Williams, R., Khan, I. M., Richardson, K., Nelson, L., McCarthy, H. E., Analbelsi, T., Singhrao, S. K., Dowthwaite, G. P., Jones, R. E., Baird, D. M., et al. (2010). Identification and clonal characterisation of a progenitor cell sub-population in normal human articular cartilage. *PloS One* **5**, e13246.